NASA-CR-174597

# Composite
## Structural Program

NASA-CR-174597
19840004189

Rensselaer Polytechnic Institute
Troy, N.Y. 12181

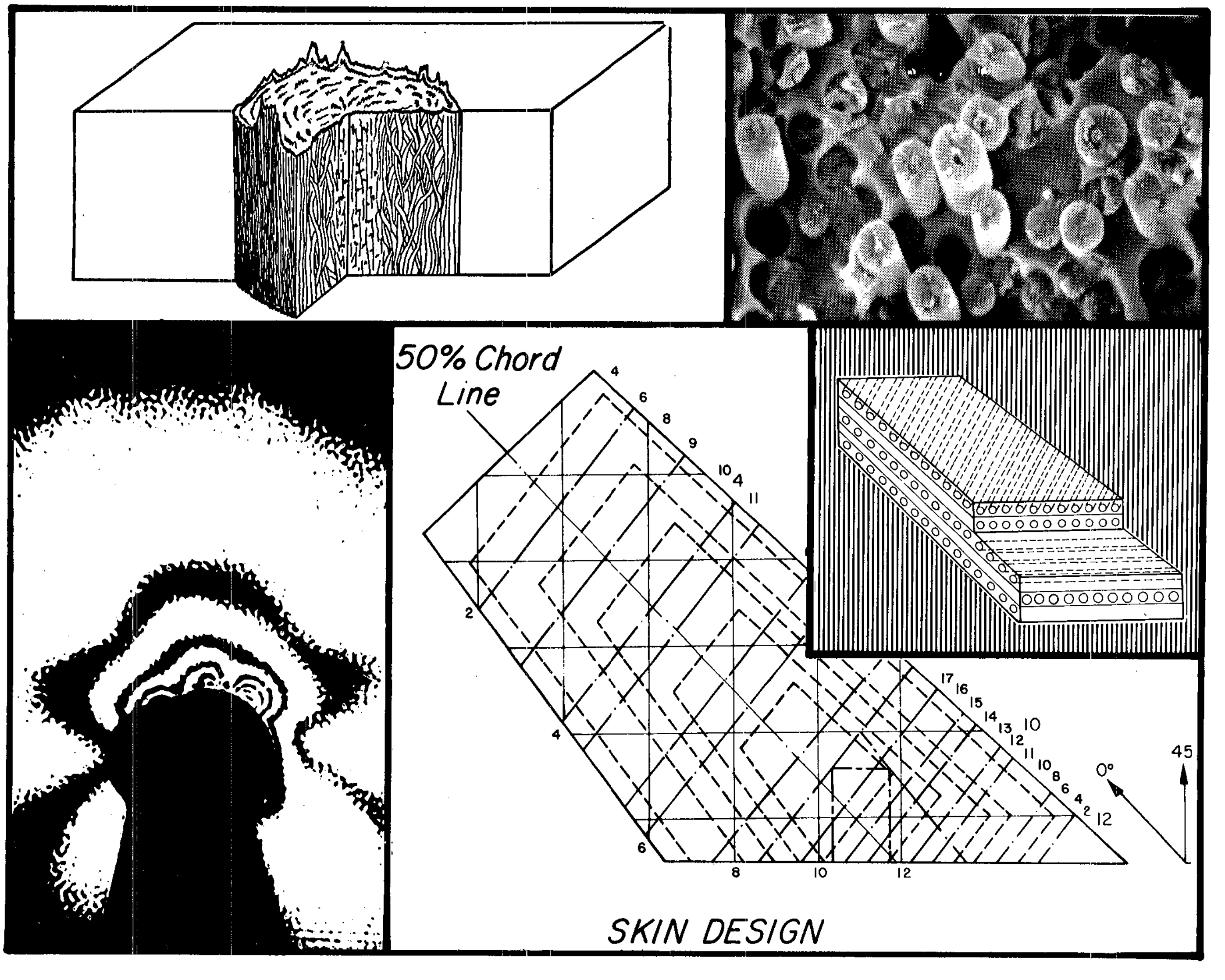






Sponsored by
NASA/AFOSR

Semi-Annual Progress Report

September 30, 1982 through April 30, 1983

# COMPOSITE STRUCTURAL MATERIALS

Air Force Office of Scientific Research

and

National Aeronautics and Space Administration

Grant No. NGL 33-018-003

Co-Principal Investigators:

George S. Ansell
Dean, School of Engineering

Robert G. Loewy
Institute Professor

and

Stephen E. Wiberley
Professor of Chemistry

Rensselaer Polytechnic Institute

Troy, New York 12181

NASA Technical Officer

Michael A. Greenfield
Materials and Structures Division

NASA Headquarters

44th Semi-Annual Report July 1983

N84-12257 #

CONTENTS

LIST OF TABLES

## LIST OF FIGURES

This Page Intentionally Left Blank

# PART I

# INTRODUCTION

# INTRODUCTION

The promise of filamentary composite materials, whose development may be considered as entering its second generation, continues to generate intense interest and applications activity. Such interest and activity are well-founded, since they are based on the possibility of using relatively brittle materials with high modulus, high strength, but low density in composites with good durability and high tolerance to damage and which, when they do fail, do so in a non-catastrophic manner. Fiber reinforced composite materials of this kind offer substantially improved performance and potentially lower costs for aerospace hardware.

Much progress has been achieved since the initial developments in the mid 1960's. Rather limited applications to primary aircraft structure have been made, however, mainly in a material-substitution mode on military aircraft, except for a few experiments currently underway on large passenger airplanes in commercial operation and a few military developments which have not seen service use.

To fulfill the promise of composite materials completely requires a strong technology base. NASA and AFOSR recognize the present state of the art to be such that to fully exploit composites in sophisticated aerospace structures, the technology base must be improved. This, in turn, calls for expanding fundamental knowledge and the means by which it can be successfully applied in design and manufacture.

As technology of composite materials and structures moves toward fuller adoption into aerospace structures, some of the problems of an earlier era are being solved, others which seemed important are being put into perspective as relatively minor, and still others unanticipated or put aside are emerging as of high priority. The purpose of the RPI program as funded by NASA and AFOSR has been to develop critical advanced technology in the areas of physical properties, structural concepts and analysis, manufacturing, reliability and life prediction.

Our approach to accomplishing these goals is through an interdisciplinary program, unusual in at least two important aspects for a university. First, the nature of the research is comprehensive - from fiber and matrix constituent properties research, through the integration of constituents into composite materials and their characterization, the behavior of composites as they are used in generic structural components, their non-destructive and proof testing and, where the state of the art will be advanced by doing so, extending the research effort into simulated service use so that the composite structure's long-term integrity under conditions pertinent to such use can be assessed. Inherent in the RPI program is the motivation which basic research into the <u>structural</u> aspects provides for research at the <u>materials</u> level, and vice versa.

Second, interactions among faculty contributing to program objectives - which is a group wider than that supported under the project - is on a day to day basis, regardless of organizational lines. Program management is largely at the working level, and administrative, scientific and technical decisions are made, for the most part, independent of considerations normally associated with academic departments. Involvement of this kind includes - depending on the flow of the research - faculty, staff and students from chemistry, civil engineering, materials engineering and the department of mechanical engineering, aeronautical engineering and mechanics.

Both of these characteristics of the NASA/AFOSR program of research in composite materials and structures foster the kinds of fundamental advances which are triggered by insights into aspects beyond the narrow confines of an individual discipline. This is a program characteristic often sought in many fields at a university, but seldom achieved.

Overall program emphasis is on basic, long-term research in the following categories: (a) constituent materials, (b) composite materials, (c) generic structural elements, (d) processing science technology and (e) maintaining long-term structural integrity. Emphasis has shifted, and can be expected to continue to shift from one time period to another, among these areas depending on the states of composite materials and structures. Progress in the program will be reported in the following pages under these headings. Those computer software developments are also undertaken which both support Rensselaer projects in composite materials and structures research in the areas listed above and which also represent research with the potential of widely useful results in their own right.

In short, the NASA/AFOSR Composites Aircraft Program is a multi-faceted program planned and managed so that scientists and engineers in a number of pertinent disciplines will interact to achieve its goals. Research in the basic composition, characteristics and processing science of composite materials and their constituents is balanced against the mechanics, conceptual design, fabrication and testing of generic structural elements typical of aerospace vehicles so as to encourage the discovery of unusual solutions to present and future problems. In the following sections, more detailed descriptions of the progress achieved in the various component parts of this comprehensive program are presented.

An evaluative site visit was made to the campus on December 2 and 3, 1982, headed by Project Monitor Michael Greenfield. The site visit team, together with members of the Composite Structural Materials Industrial Technical Committee who attended this meeting, are listed in Table I-1. Discussion subsequent to briefings and laboratory tours, during which progress in the program during the previous six months was addressed, provided considerable guidance for the months

TABLE I-1

PARTICIPANTS IN THE SITE VISIT OF DECEMBER 2 AND 3, 1982

NASA/AFOSR Evaluators

| | |
|---|---|
| Anthony Amos | AFOSR/NA |
| Michael Greenfield | NASA Headquarters |
| Robert Johns | NASA Lewis |
| Norman Johnston | NASA Langley |
| Mark Shuart | NASA Langley |

Industrial Technical Advisory Committee (ITAC)

| | |
|---|---|
| Stanley Harvey | Program Manager, Composites<br>Boeing Commercial Airplane Company |
| I. Grant Hedrick | Presidential Assistant for Corporate Technology<br>Grumman Aerospace Corporation |
| Karl Stenberg | Branch Chief - Design Composites<br>McDonnell Aircraft Company |

ahead. Salient among the points which emerged are that changes in program direction away from those projects involving generic design concepts to the more fundamental materials and structural behavior are likely, as pursued at RPI, to have the more significant impact on the applications of interest to NASA/AFOSR at this juncture in advanced composites developments.

Accordingly, two new program components were planned and set up during the ensuing months, one in the Constituent Materials area, the other in Composite Materials. Both new projects will begin immediately following the current reporting (and budget) period. Professor Bernhard Wunderlich, of the Department of Chemistry, will undertake studies to determine the precise glass transition temperatures of samples from various points within laminates, which will help to establish the uniformity of resin matrices at various positions within cured parts, as such may be influenced by the thickness, or other dimensions of the laminates in question. Professor Ting-Leung Sham will initiate theoretical and experimental investigations of the mechanics of delamination as it occurs at the free edges of loaded laminates.

Progress in these two new areas will be covered in the next semi-annual report. It is expected that projects in generic structural elements, processing science technology and maintaining long-term structural integrity will either wind down or reduce the level of their activities as the new studies pick up.

# PART II
# CONSTITUENT MATERIALS

## II-A TRANSVERSE PROPERTIES OF FIBER CONSTITUENTS IN COMPOSITES

# II-A TRANSVERSE PROPERTIES OF FIBER CONSTITUENTS IN COMPOSITES

Senior Investigator: R. J. Diefendorf

## 1. Introduction

The transverse properties of reinforced composites are of great interest. One reason is that they may impose limitations in applications. A second reason is that they may hold the key to the realization of the full potential of the synergistic behavior of composites. In order for the full benefits of composites to be attained, a better understanding of the constituent materials is required. In the case of the transverse direction, composite properties are a function of fiber structure and fiber packing. This implies that only average transverse properties can be determined. However, only very little engineering data on transverse characteristics of the fiber constituent has been obtained. Current research efforts are aimed at collecting this data.

Direct transverse property measurement of the fiber is difficult due to the small fiber diameter (typically 8 microns). Hence, unidirectional laminates were used to supply transverse property test specimens. By carefully controlling the cure process parameters, the volume fractions of the laminates were varied while differences in thickness were kept at a minimum. The production of these laminates enabled a plot of property versus volume fraction to be constructed, from which a fiber value in the transverse direction was extrapolated.

## 2. Status

The dispersion in volume fraction versus number of fields for laminates and theoretical arrays has been investigated as a first cut at determining homogeneity. As expected, a poorly fabricated part (in this case molded) has a greater dispersion than even a laminate made by conventional press curing (see Figure II-A-1). Transverse specimen coefficients of thermal expansion (reported previously) were analyzed and corrected for the quartz push rod used in the dilatometer measuring expansion. Transverse specimen modulus measurements have been performed recently. The concept of homogeneity has helped explain some of the scatter in the transverse data results.

## 3. Progress During Report Period

The data for transverse modulus is presented in Table II-A-1 and is plotted in Figures II-A-2 through 6. The data for the AS-4 and T-300 fibers appears to have similar characteristics, and this raises the possibility that they can be treated as one data group within the experimental scatter. The combined data is plotted in Figure II-A-7, and it is apparent that the data sets can be treated as one. The reason for this is revealed by close scrutiny of the constituent fiber. Figure II-A-8 illustrates three of the transversely isotropic fiber types currently available. Figure II-A-8a is that of a "wheel-spoke" structure while Figure II-A-8b depicts an onion-like structure. A random fiber

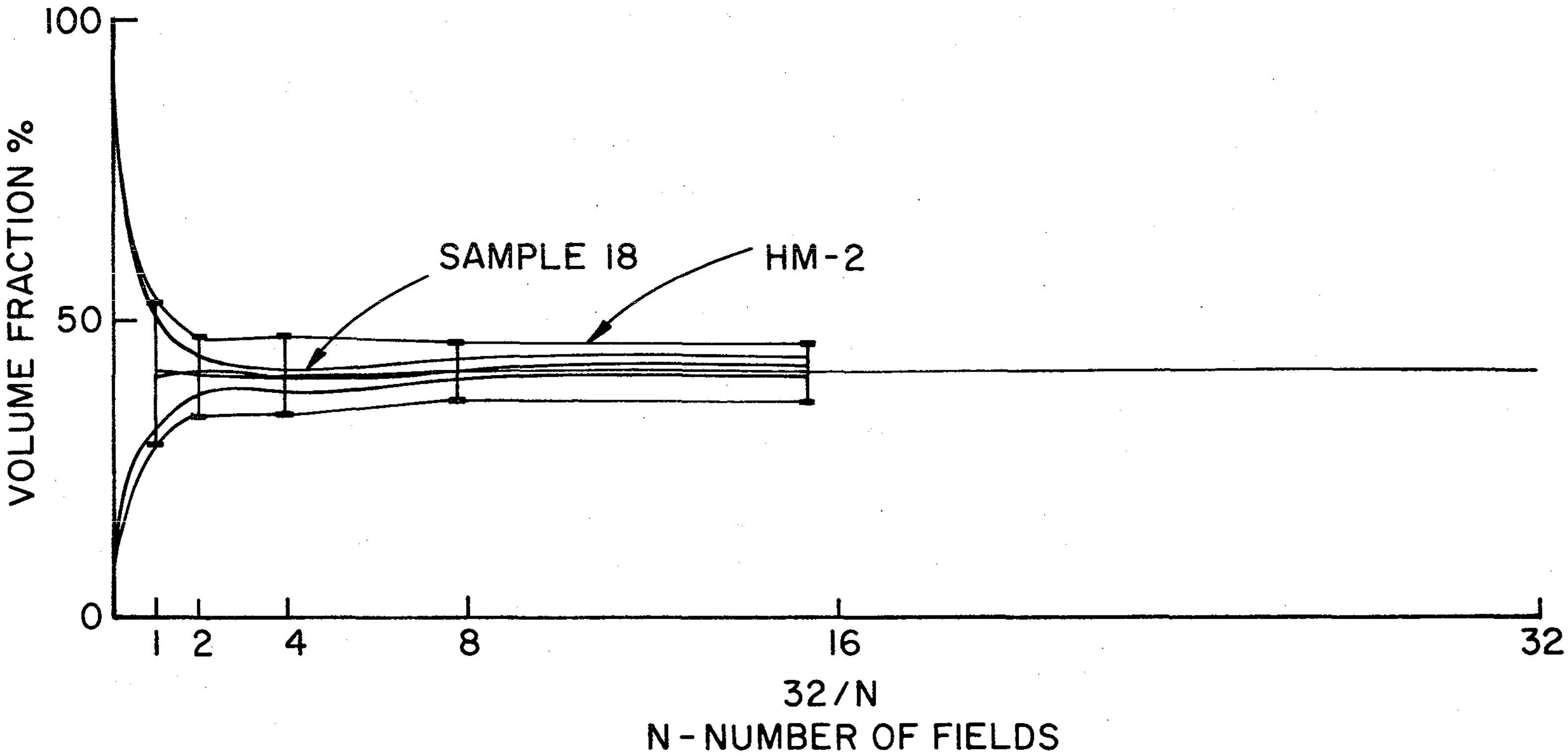


Figure II-A-1. Volume Fraction of Fibers Versus Area for Homemade Sample HM-2

## TABLE II-A-1. UNIDIRECTIONAL COMPOSITE MODULUS RESULTS

**T-300**

| Plate | $(1 - V_f)/V_f$ | $1/V_fE_2$ |
|---|---|---|
| 8-T | .8349 | 1.7277 |
| 9-T | .7668 | 1.6284 |
| 16-T | .6181 | 1.3039 |
| 20-T | .5432 | 1.0746 |
| 24-T | .7241 | 1.3428 |
| 30-T | 1.1186 | 2.2929 |
| 31-T | .6129 | 1.1208 |
| 34-T | 1.1834 | 1.8953 |

**AS-4**

| Plate | $(1 - V_f)/V_f$ | $1/V_fE_2$ |
|---|---|---|
| 11-T | .9231 | 1.797 |
| 12-T | .6529 | 1.1296 |
| 21-T | .6234 | 1.0769 |
| 25-T | .5083 | 1.0595 |
| 36-T | .6474 | 1.3702 |
| 39-T | .5290 | 1.0954 |

**Kevlar**

| Plate | $(1 - V_f)/V_f$ | $1/V_fE_2$ |
|---|---|---|
| 1-T | .5174 | 3.0602 |
| 2-T | .3141 | 2.3723 |
| 3-T | .3228 | 2.4950 |
| 5-T | .3298 | 2.1176 |
| 6-T | .2658 | 2.2898 |

**Type P Pitch**

| Plate | $(1 - V_f)/V_f$ | $1/V_fE_2$ |
|---|---|---|
| 10-T | .5244 | 1.8112 |
| 19-T | .6556 | 1.5353 |
| 23-T | .4837 | 1.6358 |
| 33-T | .7212 | 1.699 |
| 37-T | 2.7037 | 6.1316 |

**HMS**

| Plate | $(1 - V_f)/V_f$ | $1/V_fE_2$ |
|---|---|---|
| 13-T | 1.1413 | 2.5152 |
| 14-T | .6778 | 1.3263 |
| 18-T | .6556 | 1.5107 |
| 22-T | .5974 | 1.4438 |
| 26-T | .5456 | 1.4642 |
| 28-T | 1.7933 | 3.3019 |
| 29-T | .7794 | 2.0068 |
| 35-T | 1.3810 | 2.6388 |

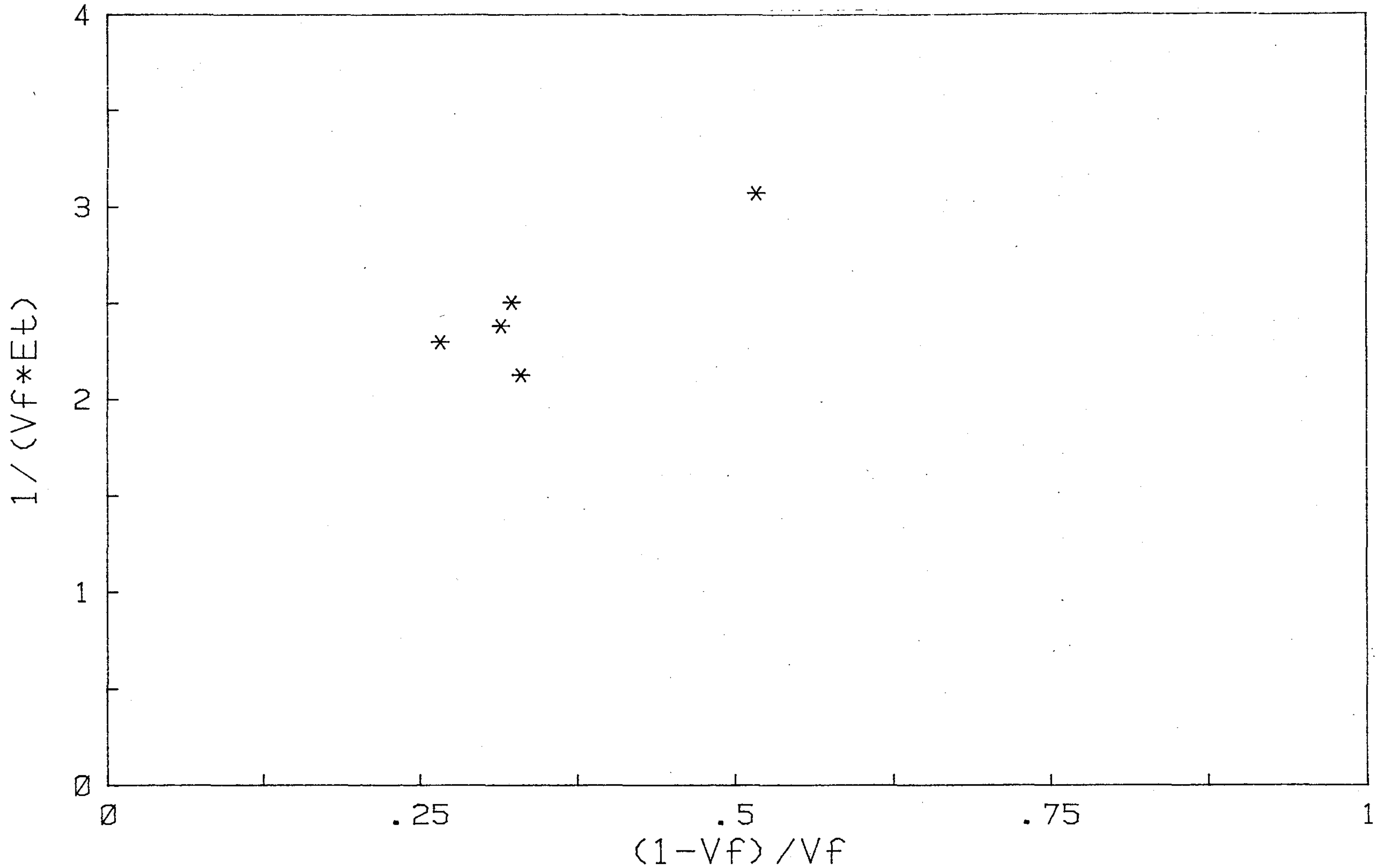


Figure II-A-2. Plot of Derived Modulus Versus Volume Fraction Parameter for Kevlar Composites

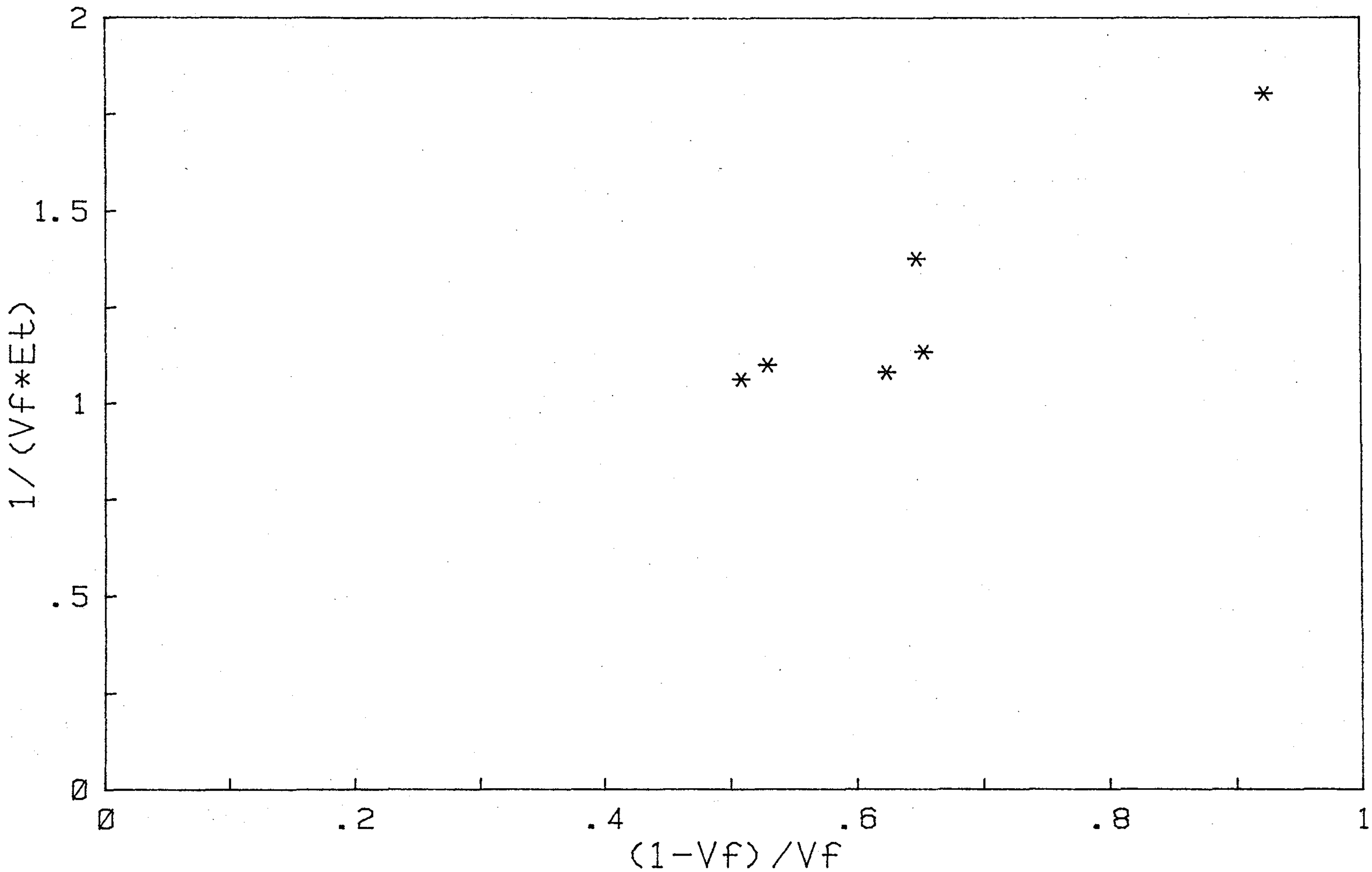


Figure II-A-3. Plot of Derived Modulus Versus Volume Fraction Parameter for AS-4 Fiber Composites

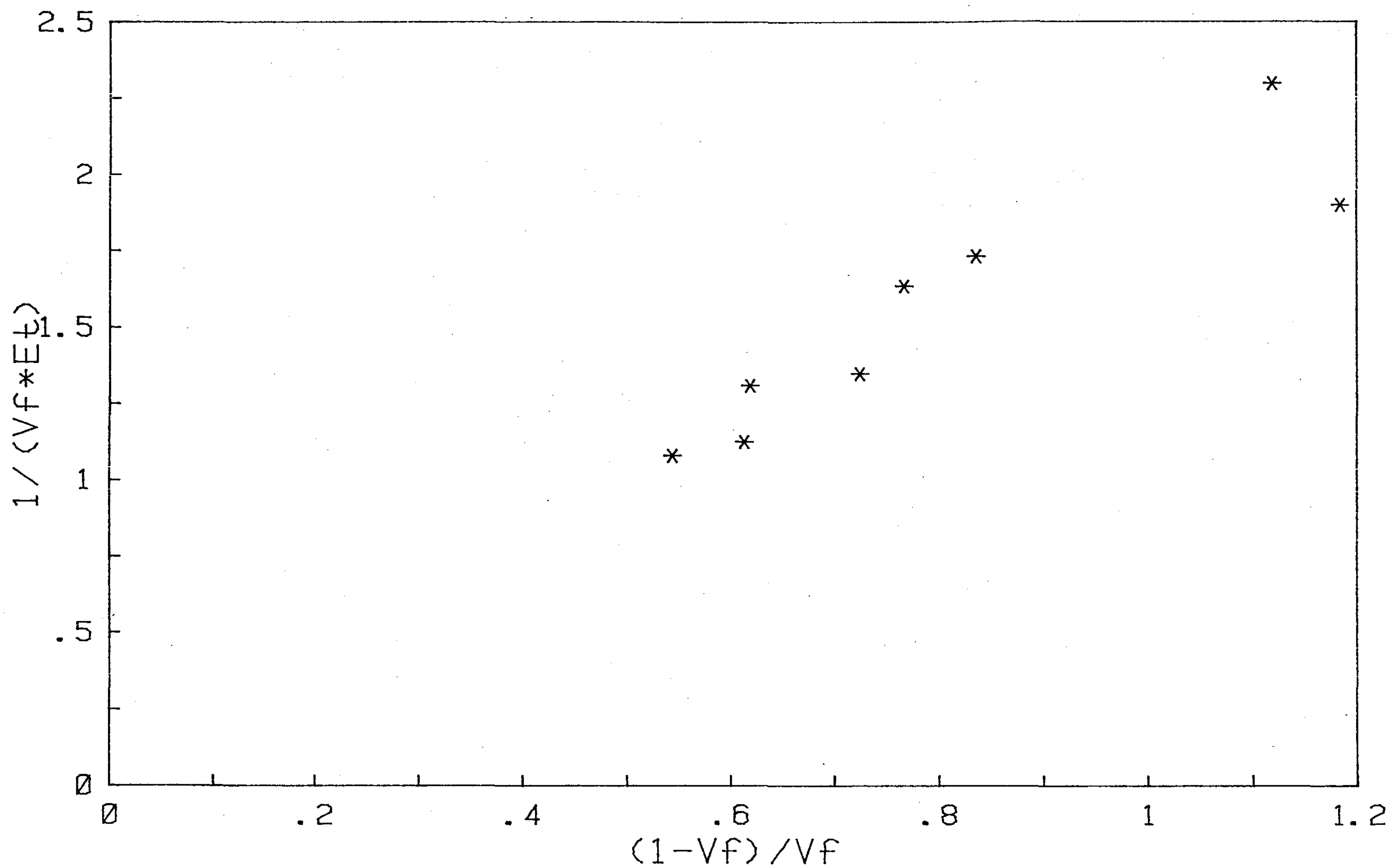


Figure II-A-4. Plot of Derived Modulus Versus Volume Fraction Parameter for T-300 Fiber Composites

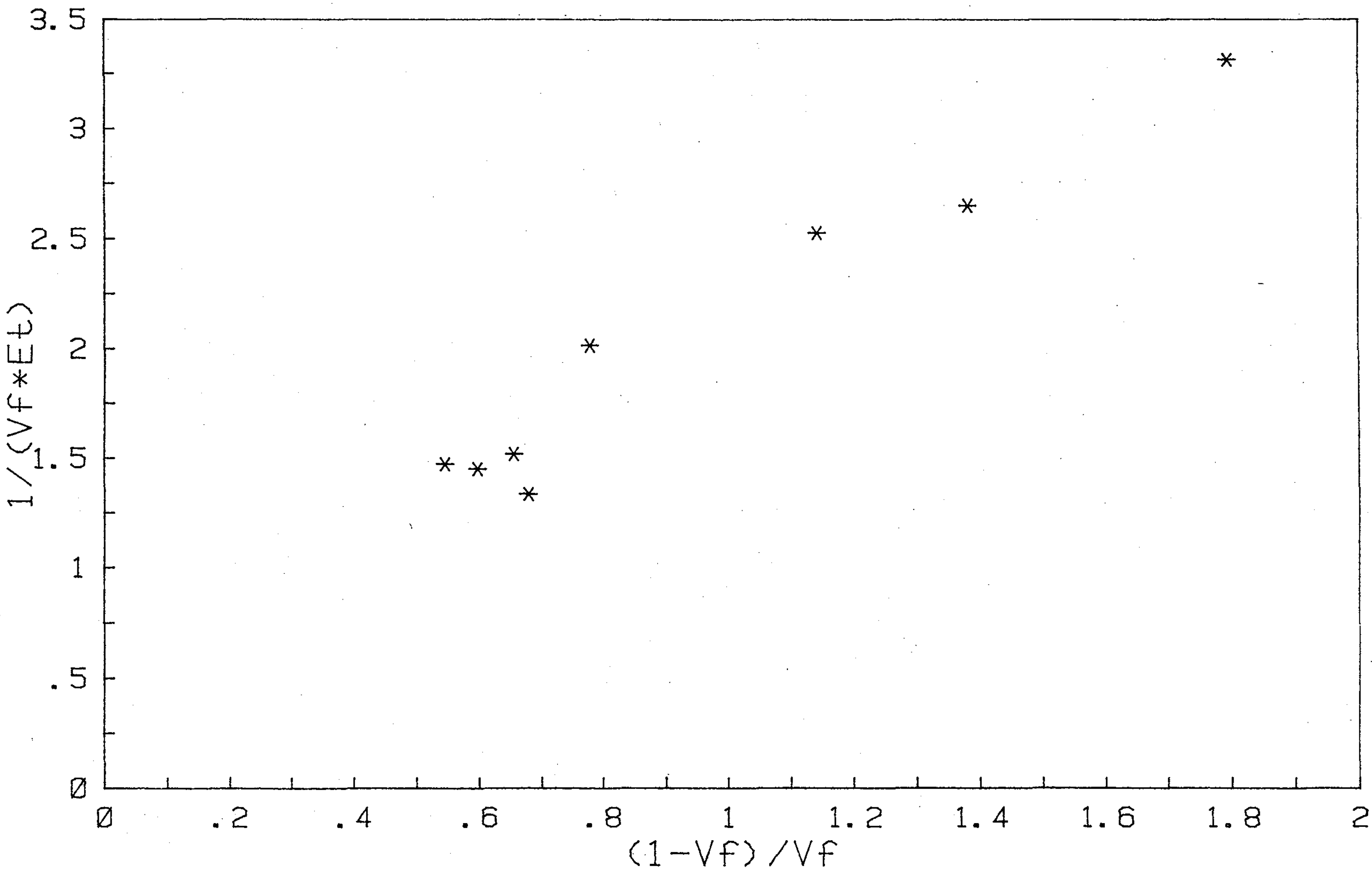


Figure II-A-5. Plot of Derived Modulus Versus Volume Fraction Parameter for HMS Fiber Composites

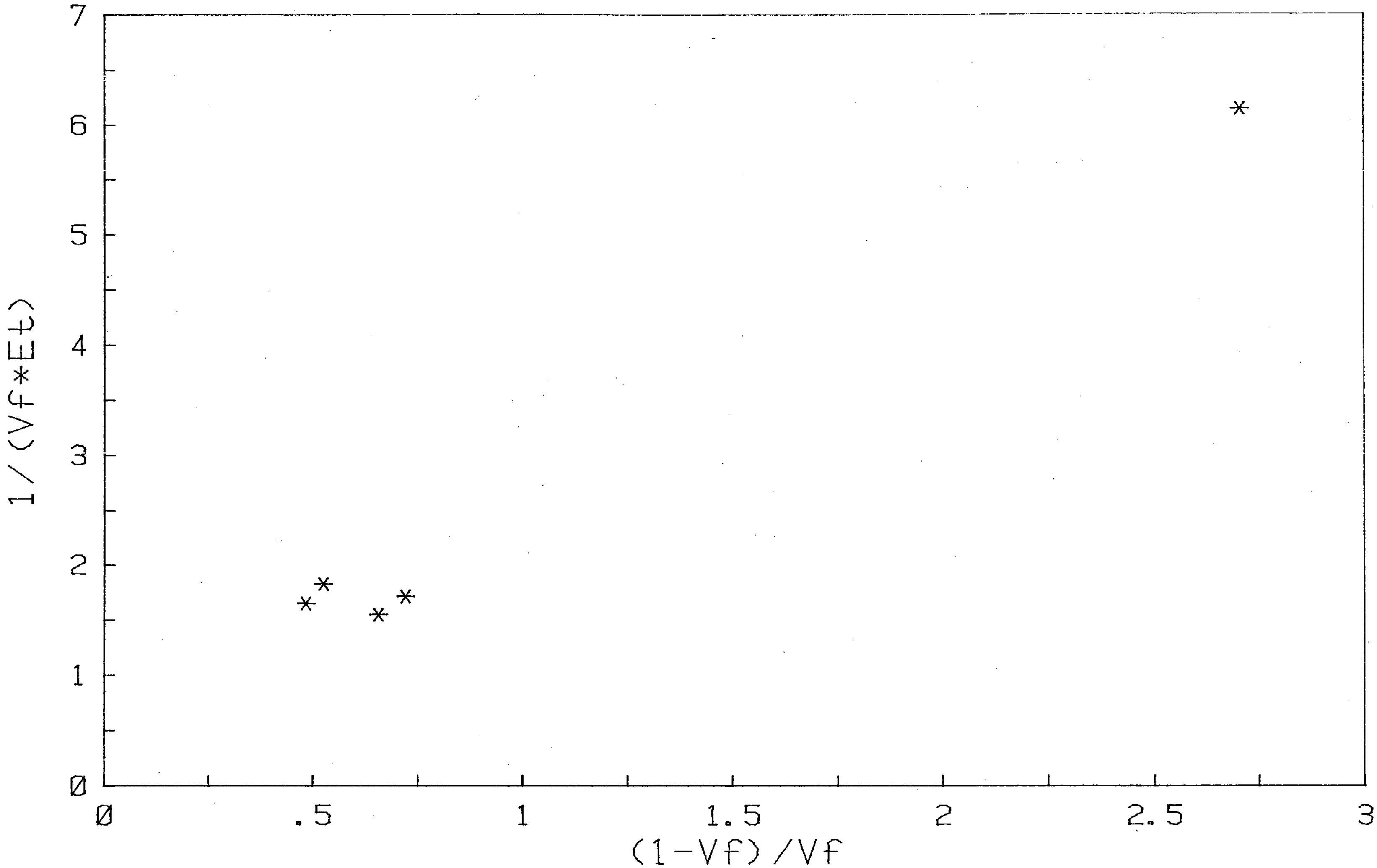


Figure II-A-6. Plot of Derived Modulus Versus Volume Fraction Parameter for Type P Pitch Fiber Composites

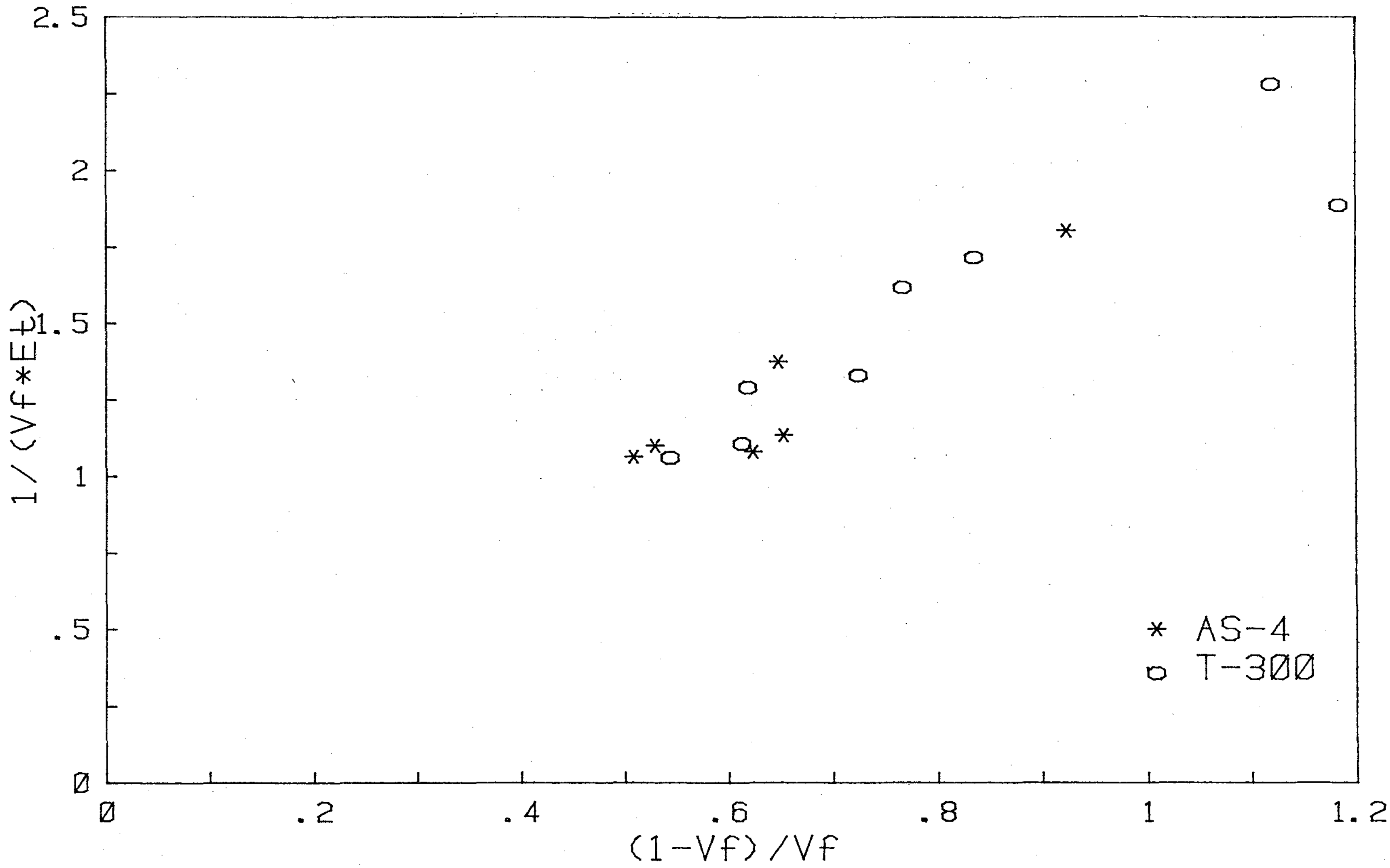


Figure II-A-7. Superimposed Modulus Data for AS-4 and T-300 Fibers

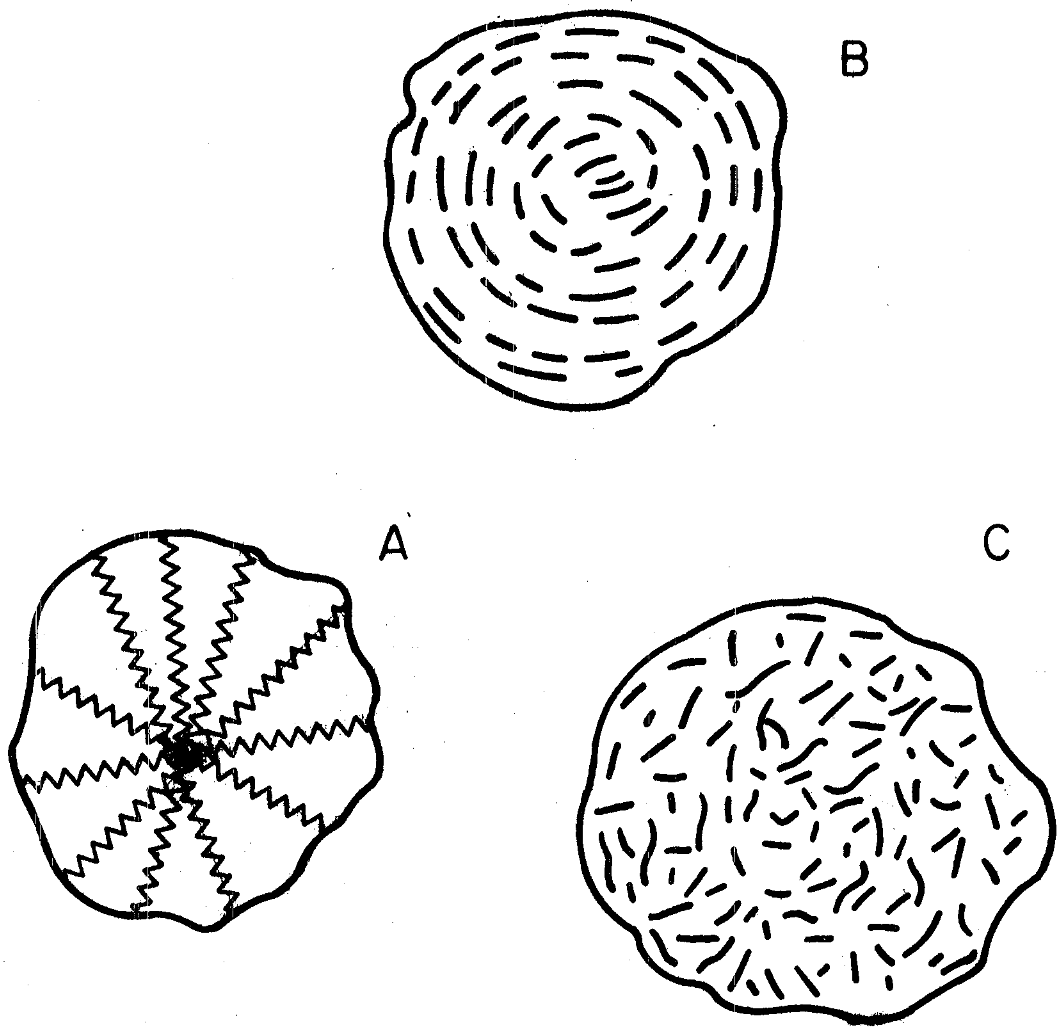


Figure II-A-8. Schematic Diagram of Structures of Transversely Isotropic Fibers structure is represented by Figure II-A-8c. From first principles, it is intuitive that structures A and B could yield similar results for transverse fiber properties. When the fibers are placed in a composite and such factors as packing and volume percent resin make significant contributions to composite behavior, it becomes easy to understand why it may well require a radically different fiber structure to produce different transverse property results for a given axial modulus. The modulus values for HMS and Type P Pitch also appear to be similar in nature. A plot (Figure II-A-9) of the combined modulus data indicates that, within the results, these two data sets can also be treated as one.

The results of individual sample CTE runs were correlated to the samples' respective volume fractions (as determined in most cases by a Bausch & Lomb FAS/II image analysis system), and the results are plotted in Figures II-A-10 through 14. As in the case of transverse modulus, the data can be separated into pairs consisting of the AS-4 and T-300 (see Figure II-A-15) and the HMS and Type P Pitch (see Figure II-A-16). The cause for concern in the CTE extrapolations is the inherent scatter in both the CTE and volume fraction measurements. In order to achieve a better estimate of the fiber property by anchoring the extrapolation at one end, the properties of the neat resin were measured. However, due to a Poisson's effect that results from the construction of the matrix in the longitudinal direction at

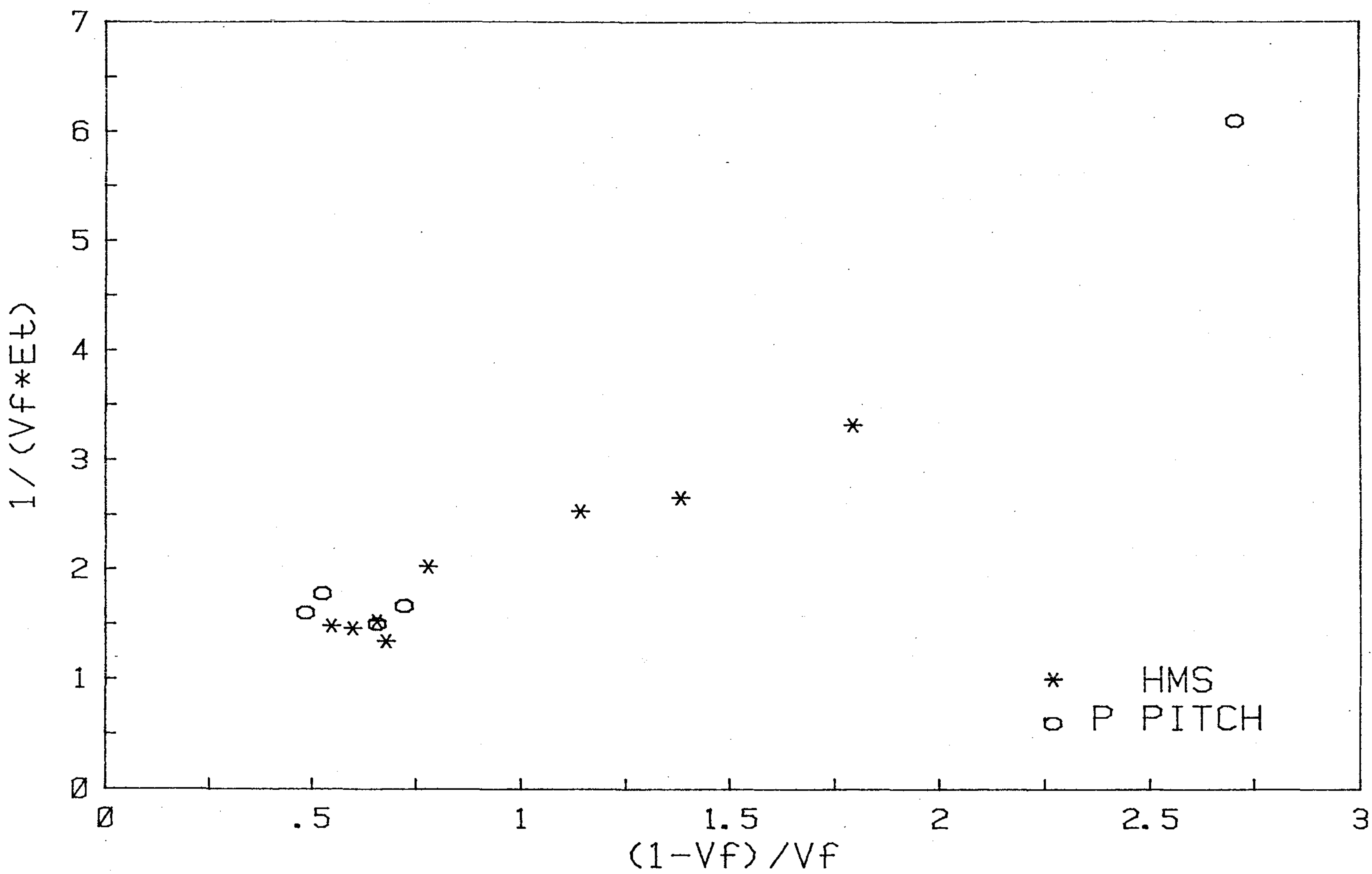


Figure II-A-9. Superimposed Modulus Data for HMS and Type P Pitch Fibers

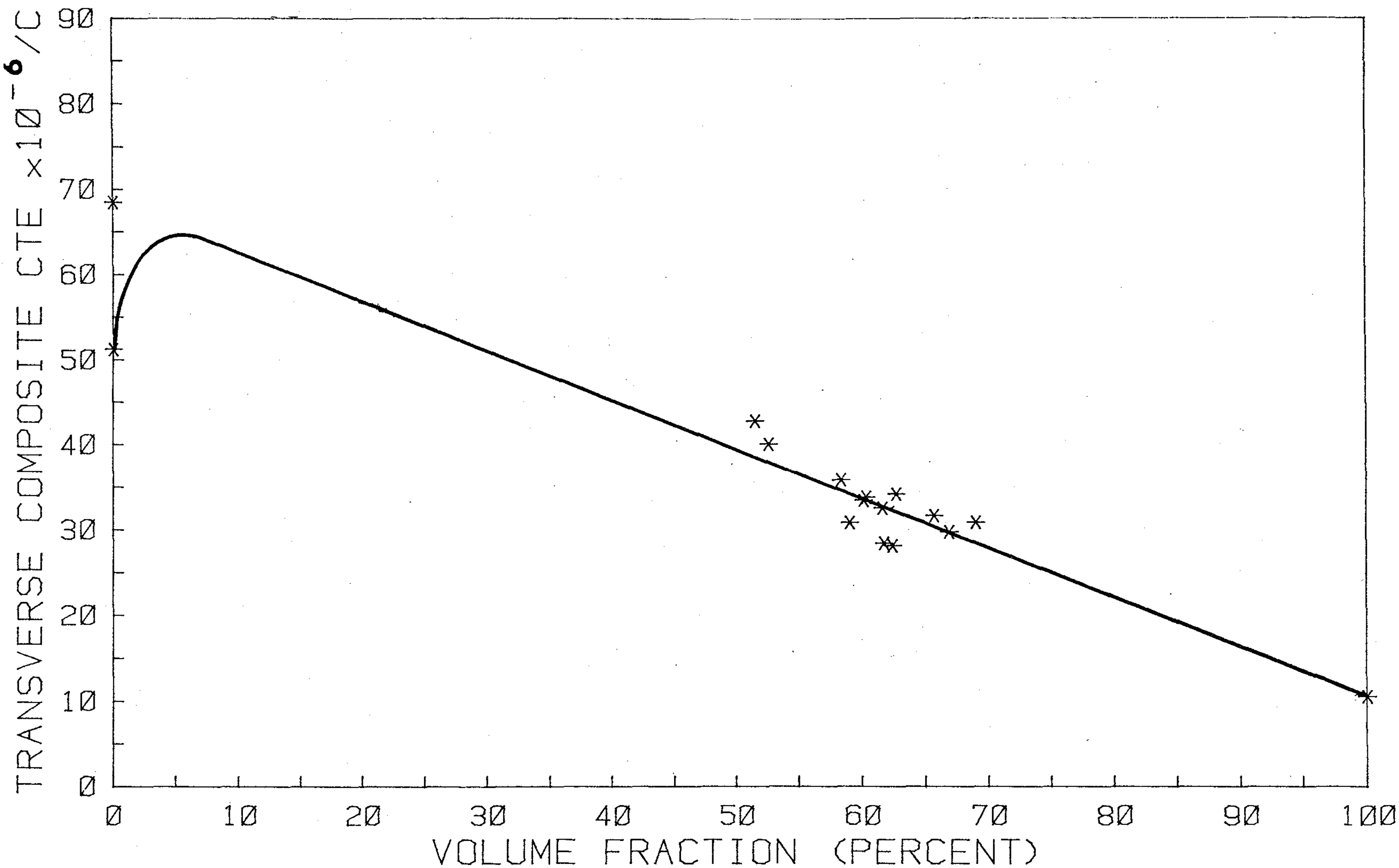


Figure II-A-10. Plot of CTE Versus Volume Fraction for AS-4 Fiber Composites

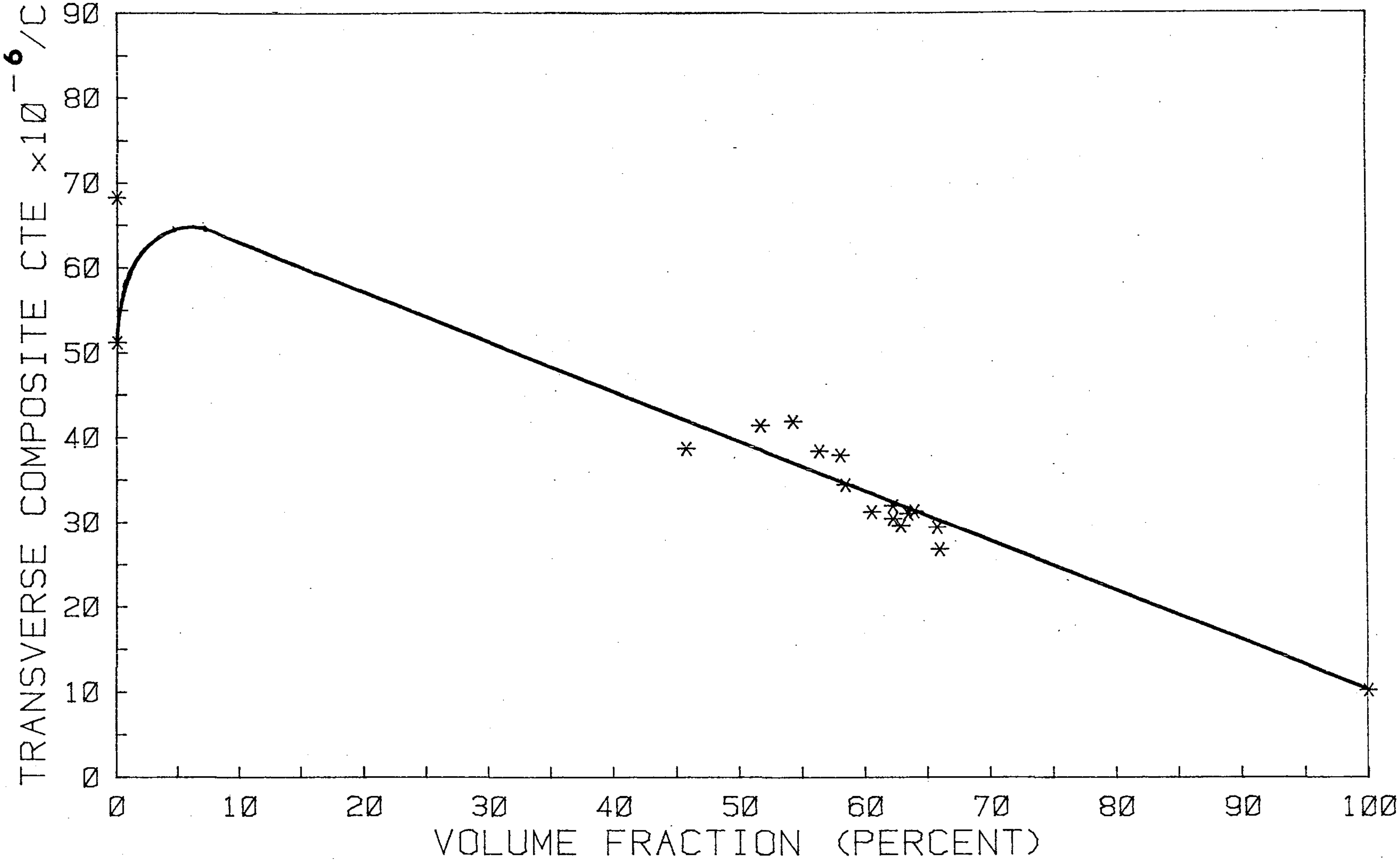


Figure II-A-11. Plot of CTE Versus Volume Fraction for T-300 Fiber Composites

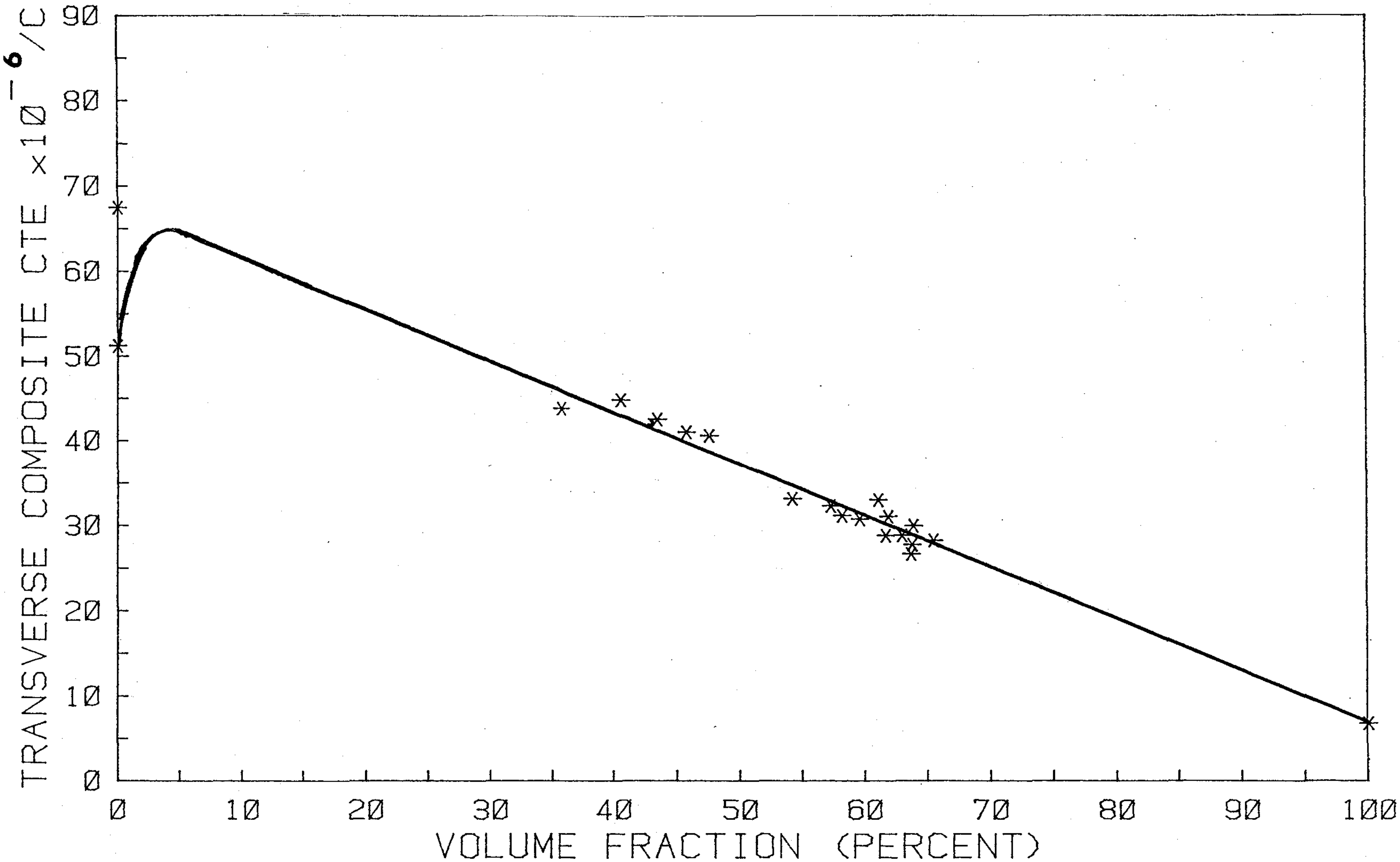


Figure II-A-12. Plot of CTE Versus Volume Fraction for HMS Fiber Composites

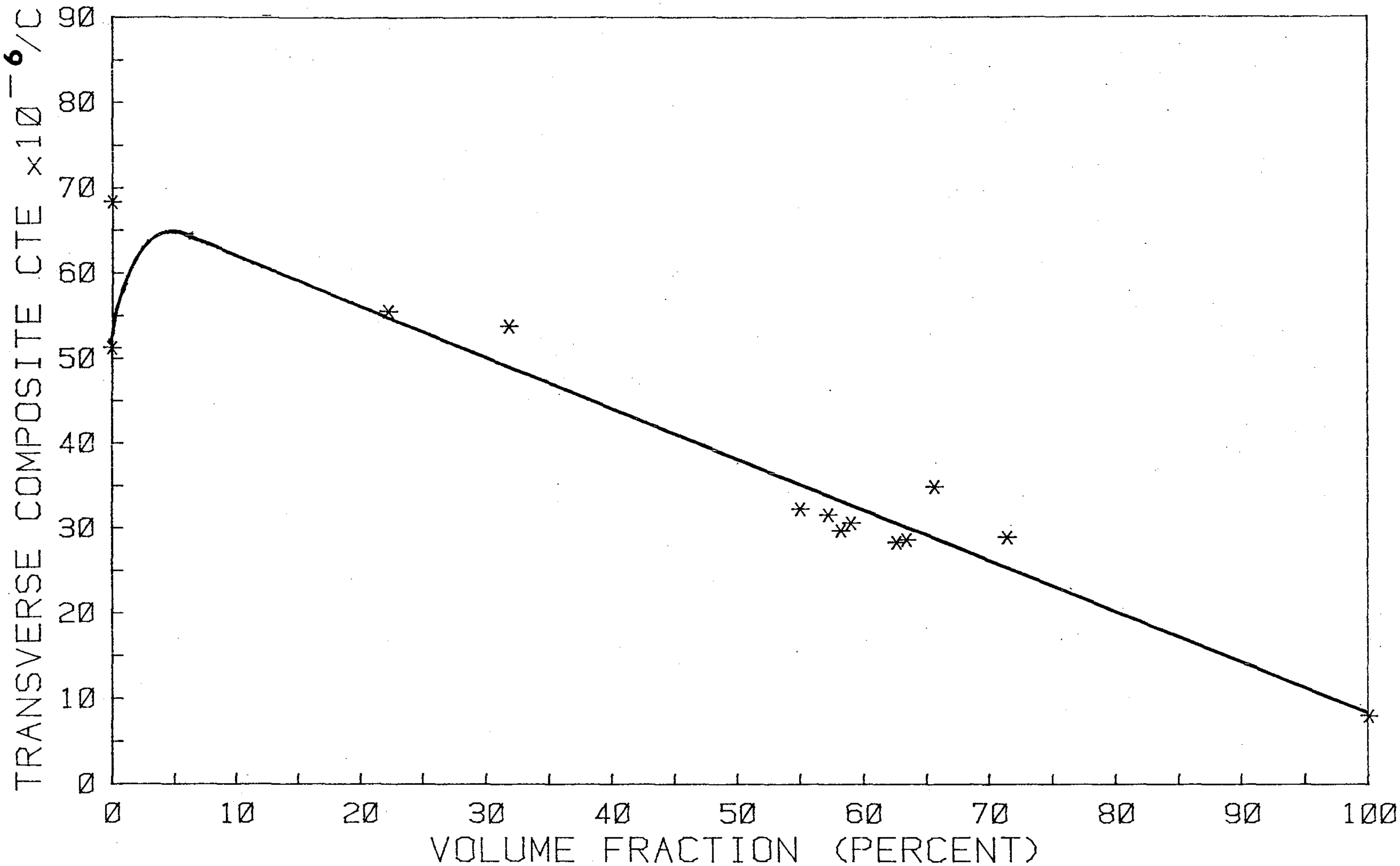


Figure II-A-13. Plot of CTE Versus Volume Fraction for P Pitch Fiber Composites

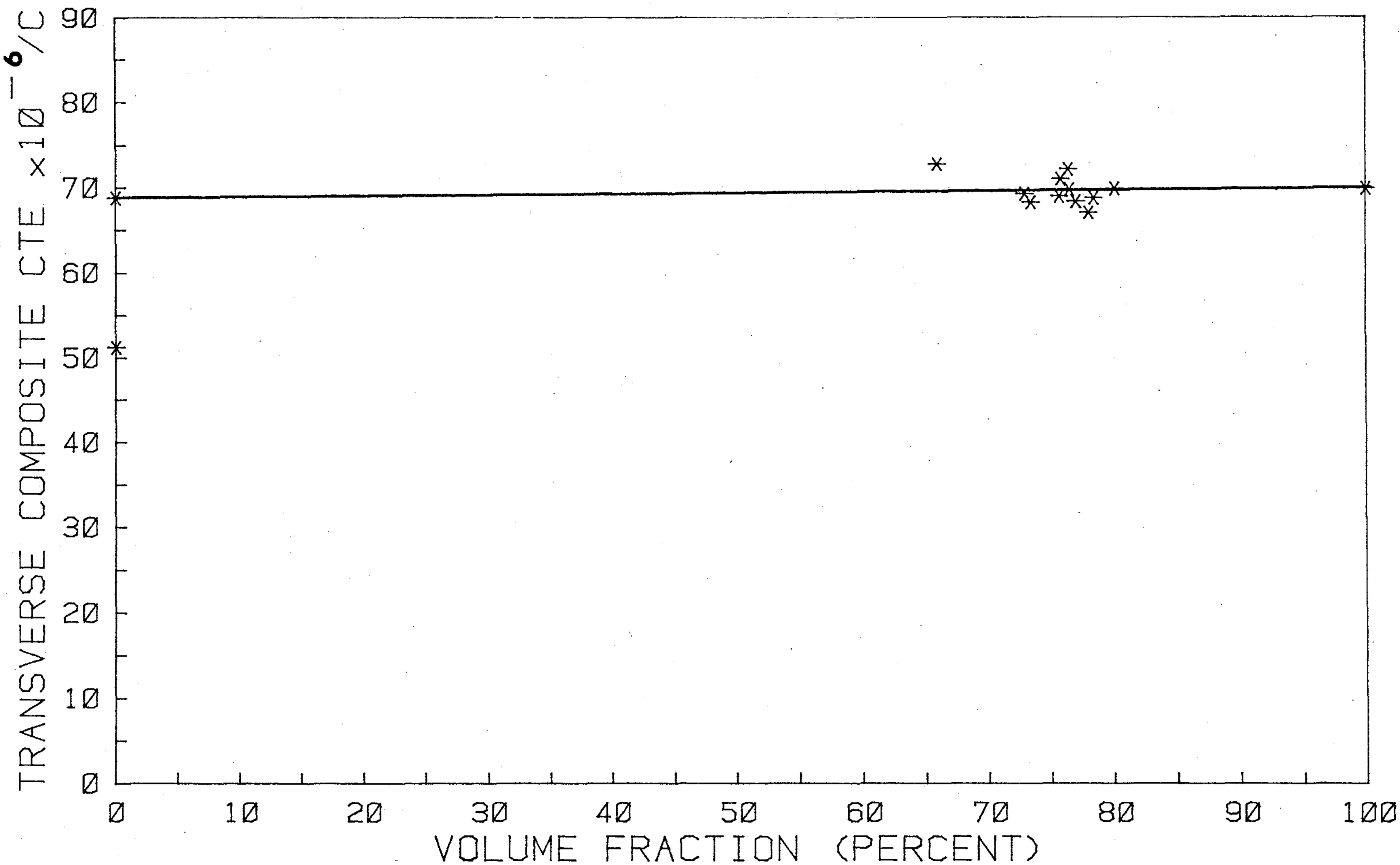


Figure II-A-14. Plot of CTE Versus Volume Fraction for Kevlar Fiber Composites

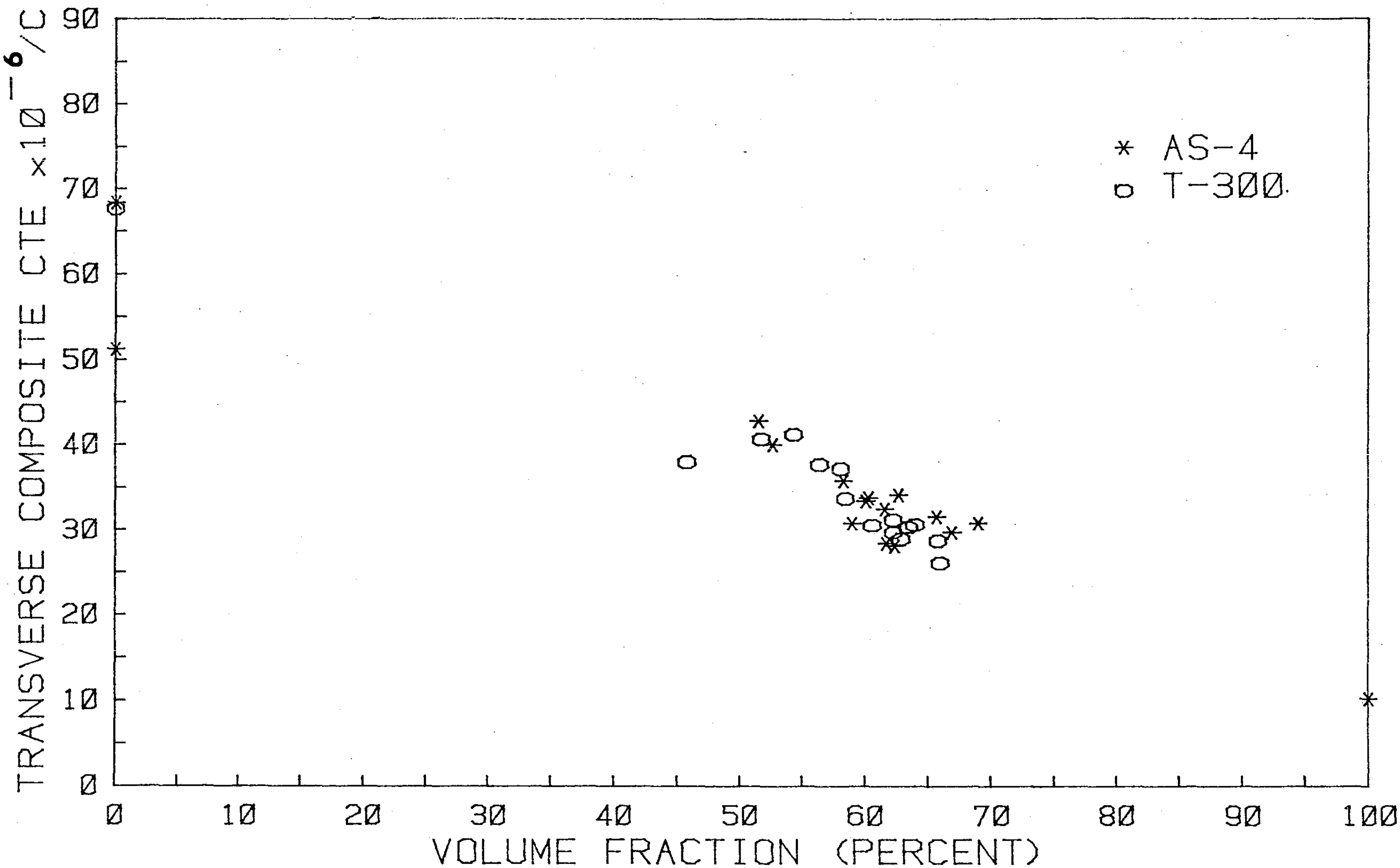


Figure II-A-15. Superimposed CTE Data for AS-4 and T-300 Fibers

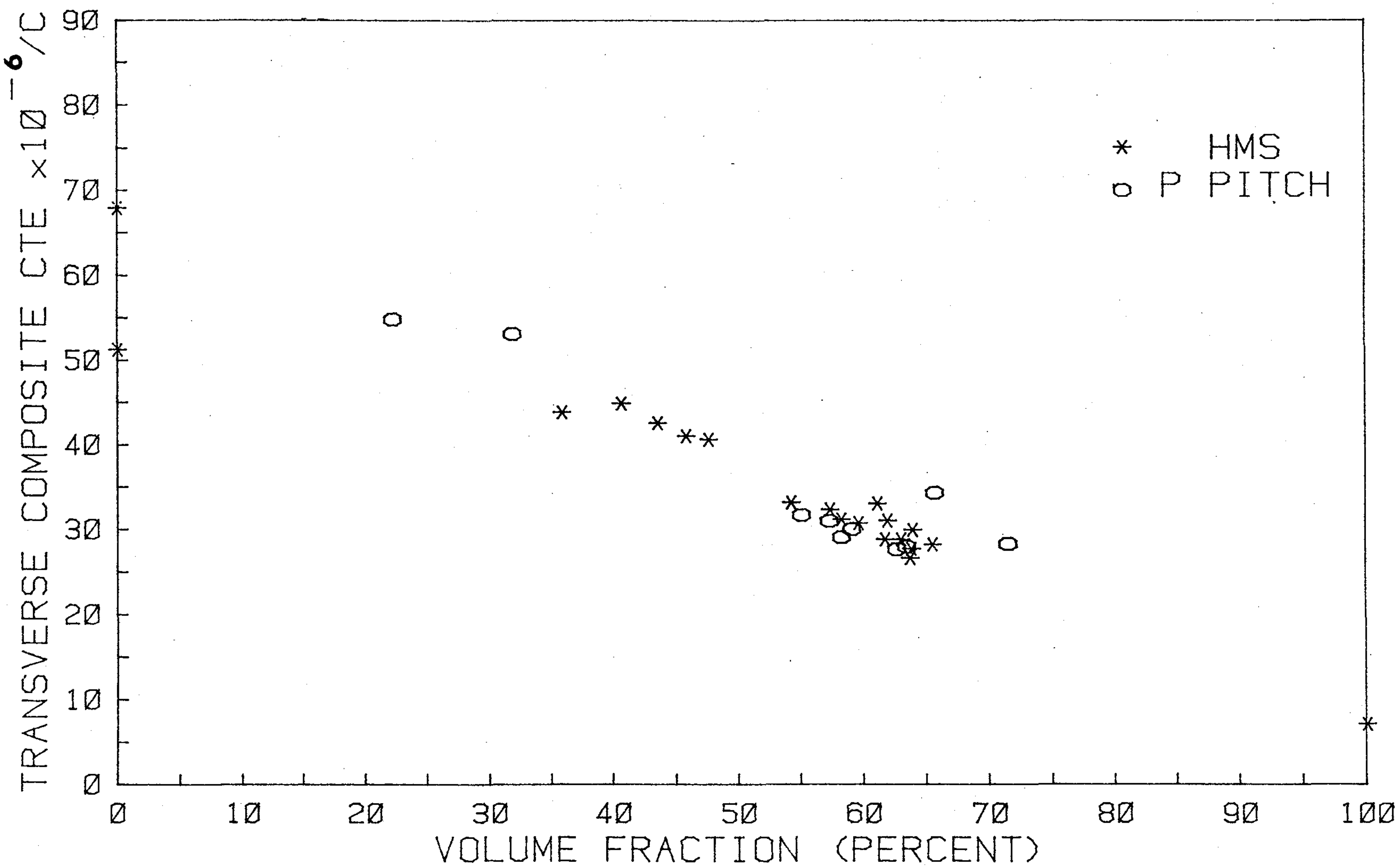


Figure II-A-16. Superimposed CTE Data for HMS and Type P Pitch Fibers low volume fractions, the direct resin expansion is not directly useful in anchoring the extrapolation. Using Schapery's [1]* equation for longitudinal composite expansion, it was possible to determine the restrained expansion case and to use this value in the extrapolation. The results for the five anisotropic fiber types for both individual and combined data sets are summarized in Table II-A-2. The values for CTE of T-300 fibers are in good agreement with those of Ishikawa and Van Schooneveld (see Table II-A-3). Little data is available for other fibers but they are judged to be reasonable based on the T-300 results.

As previously discussed, it was possible to anchor the extrapolation for the CTE values and thereby provide reliable estimates. However, it is not possible to perform a similar calculation for the modulus of the resin. Instead, to check on the reliability of the modulus estimates, statistical analysis and a t-value corresponding to plus or minus one standard deviation (about 75% confidence level), the spread in the intercept can be calculated. The results are presented in Table II-A-4. The reason for the high values determined for 1/INT(-) is that as INT(-) approaches zero, its inverse (modulus) blows up disproportionately with respect to INT(+). However, inspection of the 1/INT and 1/INT(+) terms indicates the spread is not so great as to make the

---

*Numbers in brackets in this section refer to the references which are listed on page 34.

## TABLE II-A-2

## PAIRED CTE RESULTS

| Fiber | CTE (E-6) |
|---|---|
| Kevlar | 69.6 |
| HMS | 6.6 |
| T-300 | 10.0 |
| AS-4 | 10.3 |
| P Pitch | 7.8 |

| Fiber Pairs | CTE (E-6) |
|---|---|
| HMS & P Pitch | 6.8 |
| AS-4 & T-300 | 10.0 |

---

## SUMMARY OF TRANSVERSE FIBER PROPERTIES

| Fiber | Modulus psi (E+6) | CTE in/in/C (E-6) |
|---|---|---|
| Kevlar | .75 | 69.6 |
| HMS / P Pitch | 3.10 | 6.8 |
| AS-4 / T-300 | 5.82 | 10.0 |

## TABLE II-A-3

## COMPARISON OF TRANSVERSE T-300 FIBER CTE RESULTS

| | CTE | Temperature Range (°C) | $\alpha_m$ |
|---|---|---|---|
| Ishikawa | $8.6 \times 10^{-6}$ | 20-60 | $63.9 \times 10^{-6}$ |
| Van Schooneveld | $8.8 \times 10^{-6}$ | 30-98 | $53.2 \times 10^{-6}$ |
| This work | $10.0 \times 10^{-6}$ | 35-110 | $51.0 \times 10^{-6}$ |

## TABLE II-A-4

## SCATTER AND INTERCEPT OF EXTRAPOLATED MODULUS RESULTS

| Sample | Standard Error of Estimate | $t \rightarrow 70\%$ $\pm 1\sigma$ Standard Deviation | Intercept | $\pm\Delta$ | Int. (+) | 1/Int. (-) | Int. (-) | 1/Int. (-) | 1/Int. |
|---|---|---|---|---|---|---|---|---|---|
| Kevlar | .1582 | .95 | 1.33528 | .1503 | 1.4856 | .6731 | 1.1850 | .8440 | .7489 |
| HMS/Pitch | .3304 | .75 | .32224 | .2478 | .5700 | 1.7543 | .0744 | 13.4336 | 3.1033 |
| T-300/AS-4 | .1453 | .75 | .17192 | .1090 | .2809 | 3.5600 | .0629 | 15.9032 | 5.8166 |

data invalid, and the modulus values obtained are also reasonable.

## 4. Plans for Upcoming Period

During the course of this work it became apparent that there were a few research areas that might be worth investigating. First, the concept of an index of homogeneity requires more development. Second, Poisson's ratio data, which is practically non-existent for the fiber constituent, might be a useful piece of information. The effect of nonuniformities in producing and processing fiber batches on property variances might be addressed. Third, the role of the "3rd phase" in fiber reinforced composites (i.e., the interface between the fiber and matrix) must be more fully developed.

## 5. References

1. Schapery, R. A., "Thermal Expansion Coefficients of Composite Materials Based on Energy Principles", Journal of Composite Materials, Vol. 2, No. 3, July 1968, p. 380.

# PART III

# COMPOSITE MATERIALS

# III-A FATIGUE IN COMPOSITE MATERIALS

Senior Investigator: E. Krempl

## 1. Introduction

The deformation and failure behavior of graphite-epoxy tubes under biaxial (axial and torsion) loading is being investigated. The aim of this research is to provide basic understanding and design information on the biaxial response of graphite-epoxy composites.

## 2. Status

Static, axial and torsional strength, elastic moduli and fatigue strength under completely reversed load-controlled axial loading were measured for graphite-epoxy $[\pm 45]_s$ thin-walled tubes and reported[1]*. A new specimen lay-up $[0, \pm 45]_s$ consisting of four layers oriented in the 45° directions sandwiched between an outer and an inner zero-degree layer was established. Static tests of this configuration were completed.

## 3. Progress During Report Period

Preparation of two technical papers has begun. One will cover the static elastic and strength properties of the $[0, \pm 45]_s$ tubes; the other will be devoted to their fatigue performance.

---

*Numbers in brackets in this section refer to the references which are listed on page 41.

Two batches of six-layer $[0, \pm 45]_s$ tubes were prepared using the same prepreg and the same curing cycle. The only difference in their manufacture was the use of a seal between the shrink tube and the aluminum mandrel in the second batch. (See Reference [1] for a description of the specimen manufacture procedure.) This seal prevented both the bleeding of epoxy during the curing process and pressure equalization.

The results are given in Table III-A-1 and are reproduced as Figure III-A-1. It is seen that each batch has different strength properties. The specimens of the first batch have generally inferior strength properties when compared with those of the specimens of the second batch. This is surprising, since the only obvious difference in the fabrication procedure is the use of seals for the second batch.

With the exception of the second quadrant, where low strengths are observed for specimens of the second batch (no specimens of the first batch were tested in this direction), the failure points seem to form an ellipse.

Compared to the properties of the $[\pm 45]_s$ 4-layer tubes reported in Figure III-B-1 of Reference [2], the addition of the layers of 0° fibers has roughly doubled the axial tensile failure stress and has caused a difference between the tensile and compressive strengths. The marked asymmetry in the torsional strengths shown in Figure III-B-1 of Reference [2] for the $[\pm 45]_s$ tubes has disappeared. However, the torsional

TABLE III-A-1

BIAXIAL STATIC FAILURE STRENGTH OF $[0, \pm 45]_s$ GR/E TUBES

| Tube No. | Stacking Sequence | | σ MPA | τ MPA | Failure Location Upper | Central | Lower | Batch No. |
|---|---|---|---|---|---|---|---|---|
| 141 | $[0/\pm 45]_s$ | | -262 | 0 | | | x | 1 |
| 142 | " | " | 0 | -132 | | x | | " |
| 143 | " | " | 0 | +159 | | x | | " |
| 144 | " | " | +290 | 0 | | | x | " |
| 145 | " | " | -161 | -93 | x | | | " |
| 146 | " | " | +218 | +127 | | | x | " |
| 1 | " | " | -116 | +65 | | | x | 2 |
| 2 | " | " | +147 | -159 | | | x | " |
| 3 | " | " | 0 | -181 | x | | | " |
| 4 | " | " | 0 | +130* | | x | x | " |
| 5 | " | " | +341 | 0 | | | x | " |
| 6 | " | " | 0 | +191 | | | x | " |
| 7 | " | " | -271 | 0 | | x | | " |
| 8 | " | " | +252 | +144 | | | x | " |
| 9 | " | " | -145 | +84 | x | x | x | " |
| 10 | " | " | -221 | -126 | x | | | " |

*Preloaded Specimen

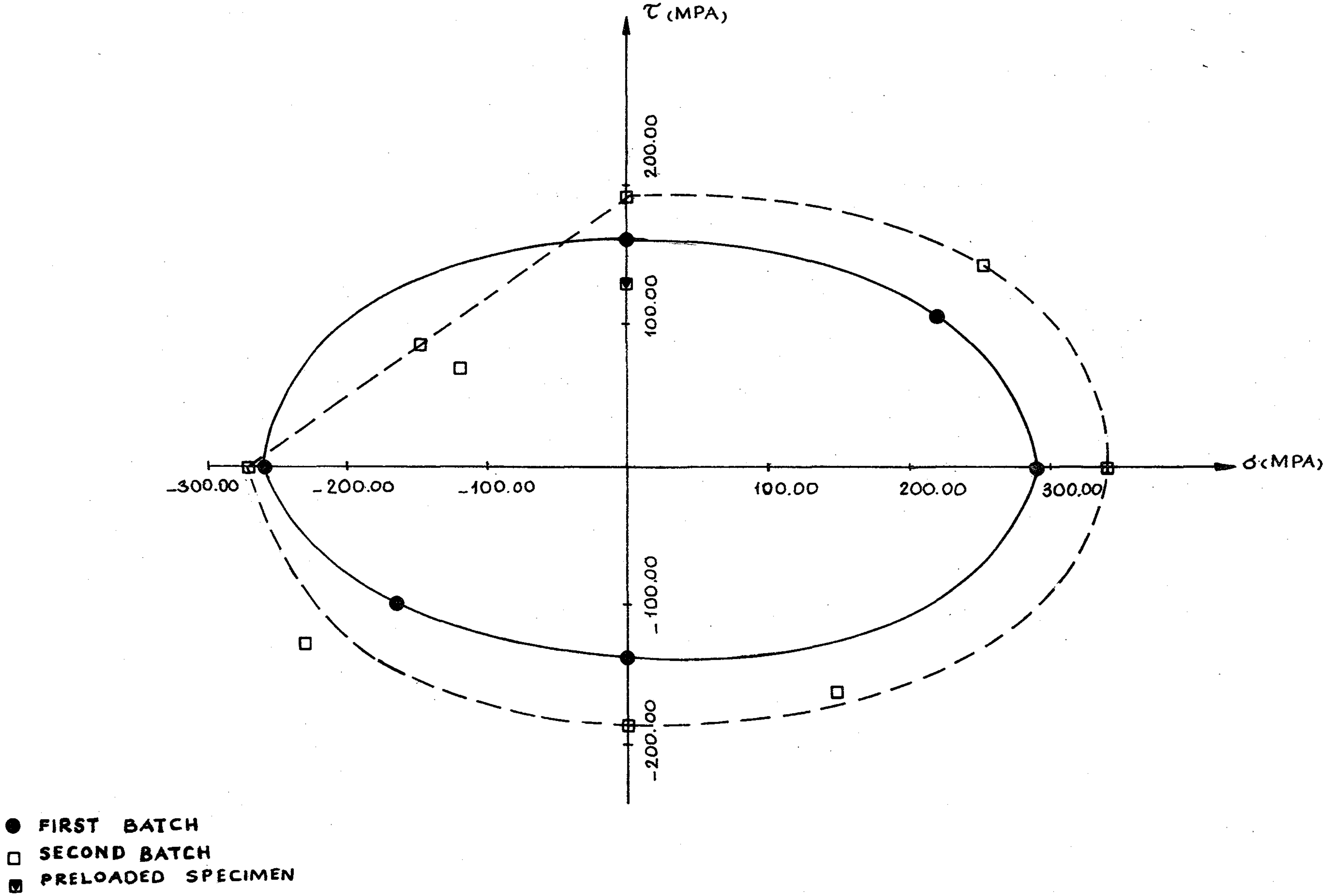


Figure III-A-1. Biaxial Static Failure Strengths of $[0,\pm 45]_s$ (5-layer) Graphite/Epoxy Tubes. During positive twist the outermost 45-degree fibers are compressed.

failure stress of the $[0, \pm 45]_s$ tubes is smaller than the failure torsional stress of the $[\pm 45]_s$ tubes. (Failure stress properties are based on the total, i.e., fibers plus resin, original cross-sectional area of the tubes.)

## 4. Plans for Upcoming Period

The static and fatigue properties of $[0, \pm 45]_s$ tubes will be explored further. The two papers mentioned earlier, stemming from the Doctor of Engineering thesis of T.-M. Niu, will be prepared for submission to an appropriate journal.

## 5. References

1. Krempl, E. and T.-M. Niu, "Graphite-Epoxy $[\pm 45]_S$ Tubes. Their Static Axial and Shear Properties and Their Fatigue Behavior Under Completely Reversed Load Controlled Loading", Journal of Composite Materials, Vol. 16, 1982, pp. 172-187.

2. 42nd Semiannual Progress Report, Composite Structural Materials, RPI, Sept. 30, 1981 - April 30, 1982, July 1982.

## 6. Current Publications or Presentations by Professor Krempl on this Subject

"Biaxial In-Phase and Out-of-Phase Behavior of Graphite-Epoxy Tubes"

Presented at the ASTM Conference on Biaxial/Multiaxial Fatigue, San Francisco, California, December 15-17, 1982.

## III-B MATRIX DOMINATED PROPERTIES OF HIGH PERFORMANCE COMPOSITES

Senior Investigator: S. S. Sternstein

### 1. Introduction

This project is concerned with those properties of high performance composites which are strongly dependent on the polymeric matrix.

Moisture is known to adversely affect the properties of both neat epoxy resin and epoxy matrix composites. A major contribution to the moisture degradation of mechanical properties in neat epoxy is due to the internal stresses and strains caused by inhomogeneous swelling. The swelling is inhomogeneous since neat resin contains structural fluctuations, or nodular regions of nonuniform crosslink density, which are produced during curing. Several factors which contribute to the nodular structure include improper mixing of the reagents, thermodynamically based partial segregation, excessive intramolecular reaction and incipient formation of nodules before macrogelation.

In addition, swelling is inhomogeneous in composite laminates because of the additional nonuniformity of the system due to the fibers or any other filler having swelling properties different from those of the matrix.

### 2. Status

To date, specific investigations have included viscoelastic characterization of the glass transition region in both laminates and neat resins, delamination studies, moisture interactions and inhomogeneous swelling phenomena.

### 3. Progress During Report Period

During the present report period, our objective has been to further quantify both experimentally and theoretically the interactions of water with epoxy based systems and other amorphous, glassy polymers.

#### a. Experimental Studies

A set of composite samples, exposed for various periods of time to a 100°C, 100% relative humidity environment (as opposed to the boiling water environment described in the previous semiannual report), were tested, and the in-phase (storage) stiffness (M') results are shown in Figure III-B-1 versus weight gain (moisture). The values of M' are normalized by the value of M' for the dry sample and also normalized by the cube of the thickness for the wet sample (as tested). It is clear that, at about 2.5% moisture pickup, the close of the curve markedly increases, suggesting a change in the structure-moisture interaction mechanism. The loss factor, M"/M', for composite samples is given in Figure III-B-2. The ordinate represents the increase (or increment) in loss factor which is obtained in a wet sample relative to a dry sample. If moisture content is increased only (no drying), all samples indicate a linear increase of loss factor with moisture content. If the sample is dried, then

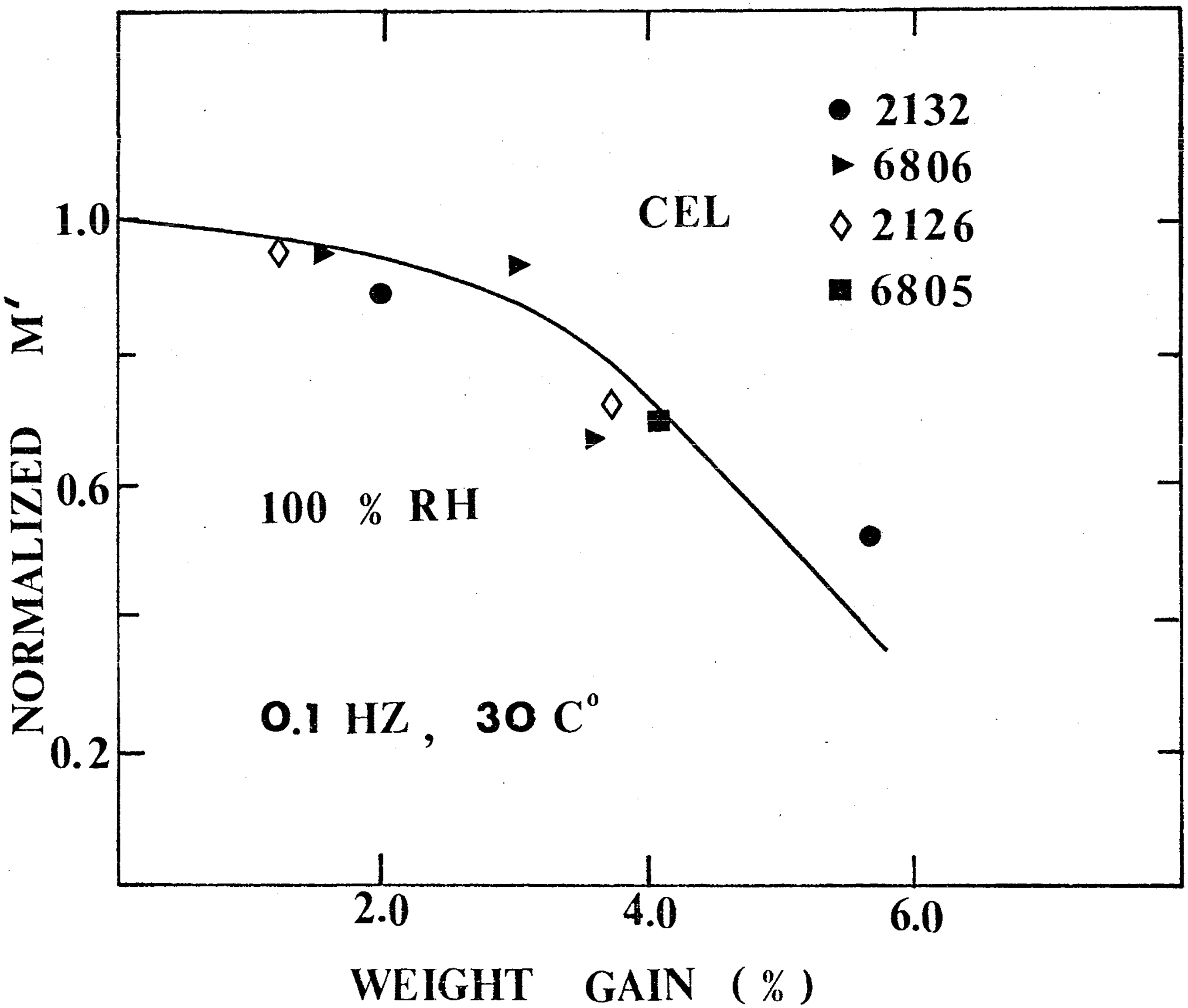


Figure III-B-1

Normalized In-Phase Stiffness as a Function of Moisture Weight Gain for Samples Exposed to Water Vapor

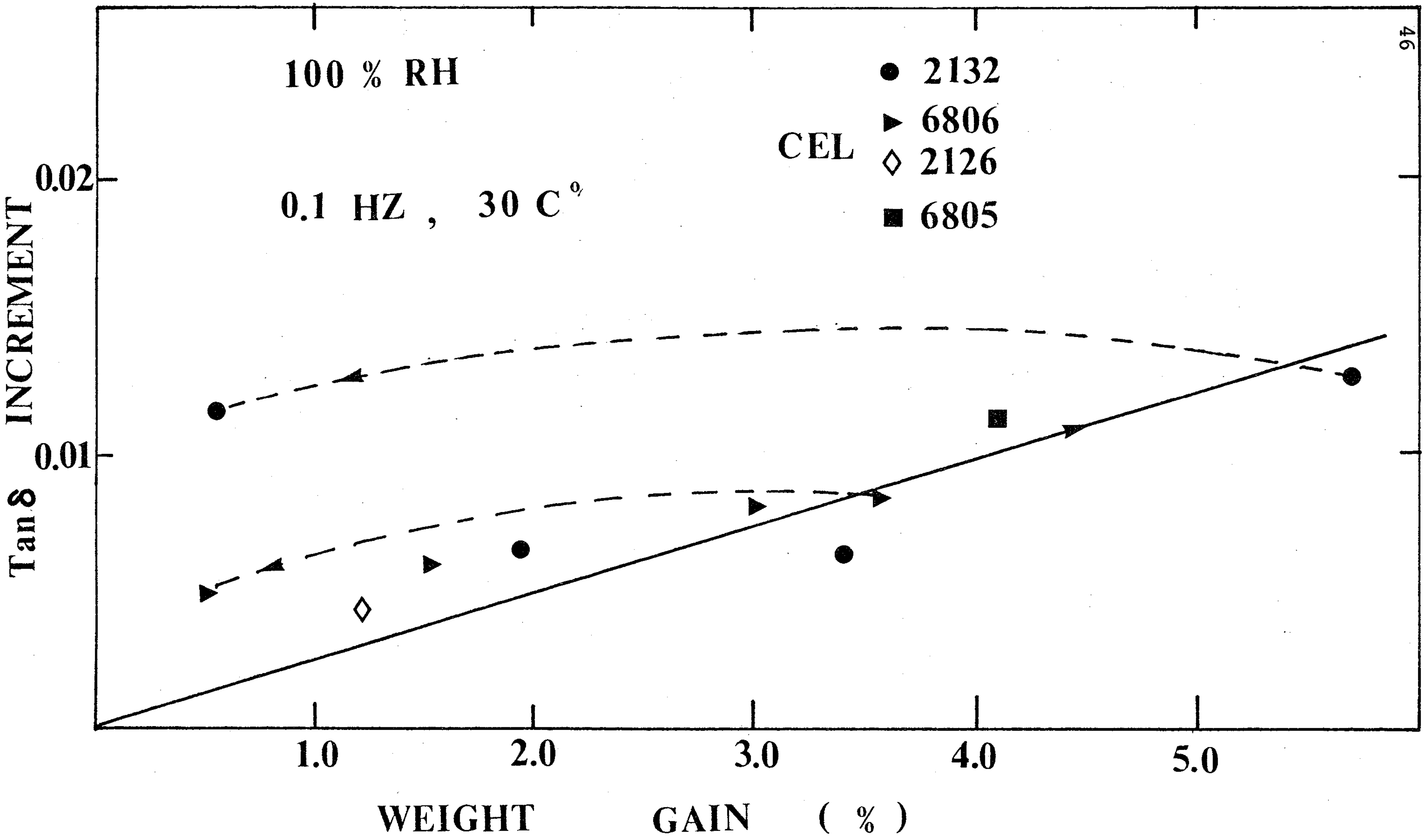


Figure III-B-2. Loss Factor Versus Moisture Uptake a permanent residual increase in loss factor (tan $\delta$) is observed. The same behavior was reported previously, when composite samples were exposed to a boiling water environment. This indicates that the moisture effects on dynamic mechanical properties of composite materials are the same regardless of different states of moisture environment.

The hysteresis effect in loss factor (shown in Figure III-B-2 and the previous report) indicates that composite samples are permanently damaged. The micrograph of a composite sample with 5.1% weight gain is shown in Figure III-B-3. The damage is easily visible at 50 magnafication. Note that cracks occur mostly at interfaces between laminae, with a small amount of interply crackings. The micrograph suggests that the large weight gain and thickness increase are due to moisture trapped in the separated laminae. It is clear that the reduction in stiffness is due to the delamination induced by moisture uptake.

During the previous period, we reported that the change in M' of neat resin occurs at about 7% moisture uptake. Since the composite samples are about 35% resin, this suggested that the slope change in the composite is strongly related to the failure of the matrix and is therefore matrix controlled.

In order to further investigate the damage mechanism induced by moisture uptake, the polarized light microscope was used to provide microscopic evidence of the failure

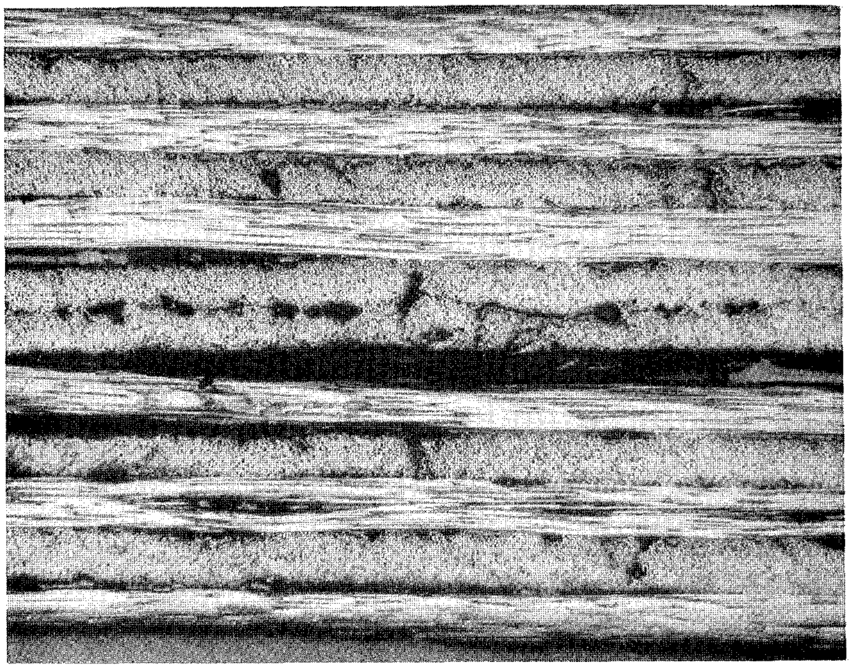

200 u     50 X

Figure III-B-3. Micrograph of Composite with Moisture Uptake of 5.1%

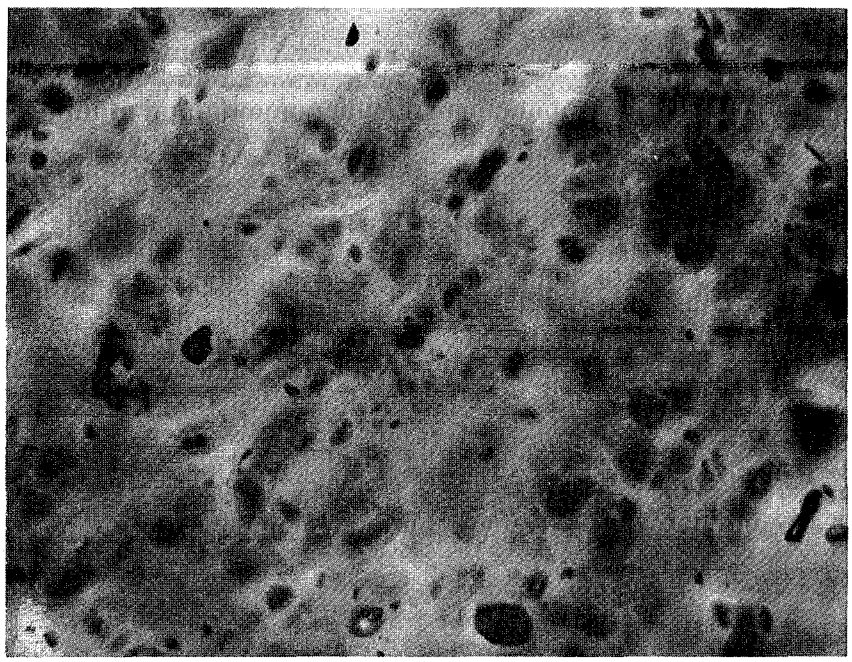

100 u     100 X

Figure III-B-4. Birefringence Pattern of Dry Epoxy patterns. The micrograph at 100 magnification of a dry, thick epoxy resin (~ 2 mm) sample when viewed with polarized light, is shown in Figure III-B-4. The light intensity pattern suggests that the epoxy resin is not a homogeneous material. As a matter of fact, the pattern is an overlapping image of multiple layers of epoxy resin. The pattern is diminished when moisture uptake is about 6% as shown in Figure III-B-5. Further moisture uptake (about 8%) actually causes the sample to produce microcracks as shown in Figure III-B-6.

A corresponding study in thin films (~ 0.1 mm) reveals that inhomogeneous swelling occurred in the epoxy resin upon exposure to moisture. The 100 magnafication of a dry, thin film shows a distinct light intensity pattern as shown in Figure III-B-7. It is believed that the bright areas are the precipitates of curing agent (dycyanodiamide) of the cured epoxy. The birefrigence patterns are observed (gray areas) due to the thermal mismatch between the precipitate and the surrounding matrix (network of epoxy resin). The light intensity pattern produced by swelling in the vicinity of precipitate, when the sample is exposed to 20-hour boiling water environment, is shown in Figure III-B-8. The complete extinction along the polarizer axis (vertical) and analyzer axis (horizontal), approximate symmetry of the four quadrants, maximum interfacial retardation and decay of retardation with distance from the interface, is typical of birefringence patterns which retained their interfacial integrity upon swelling.

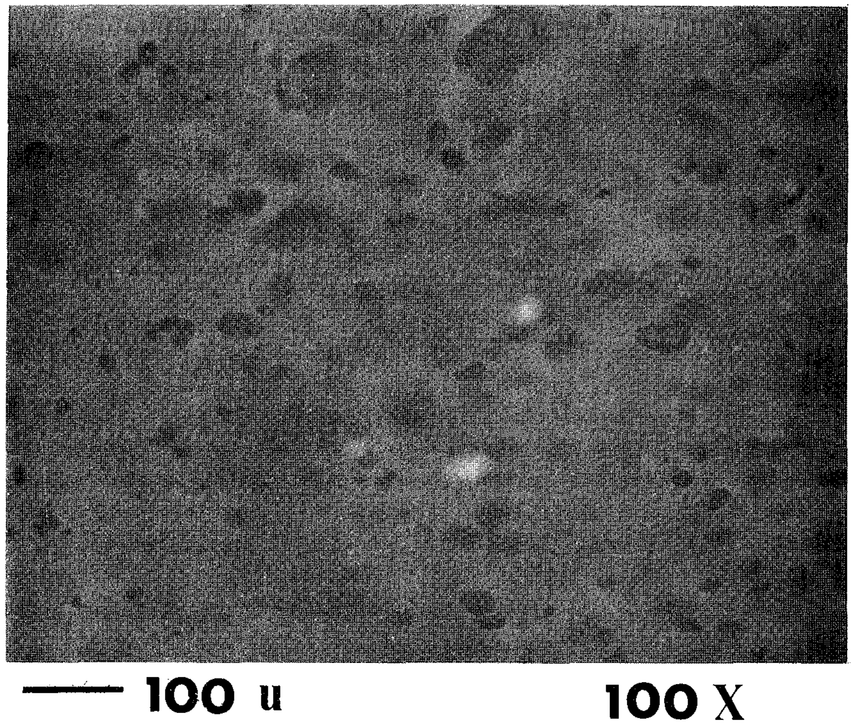


Figure III-B-5. Birefringence Pattern of Epoxy with Moisture Uptake of 6.2%

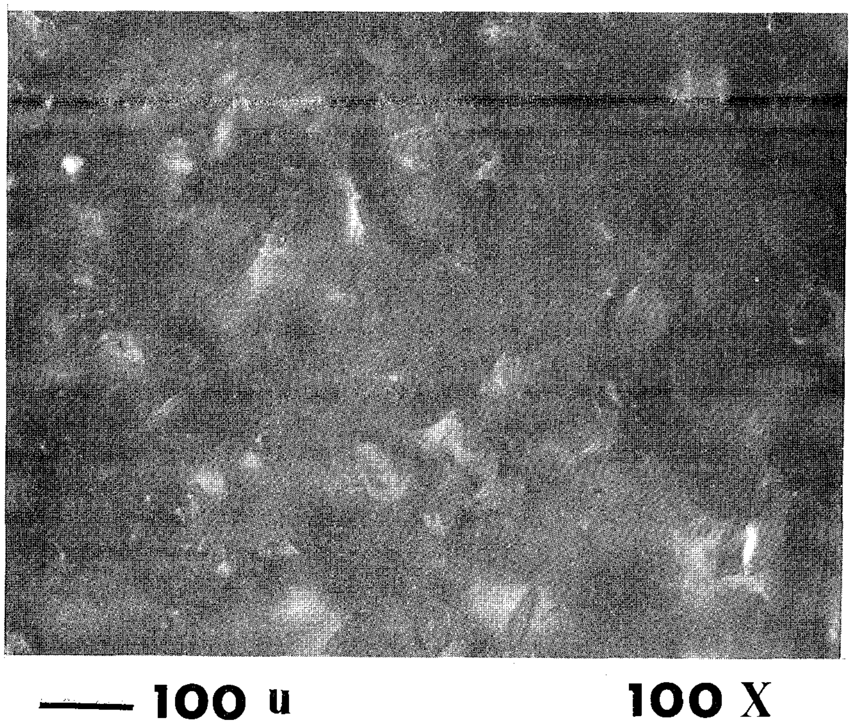


Figure III-B-6. Birefringence Pattern of Epoxy with Moisture Uptake of 7.9%

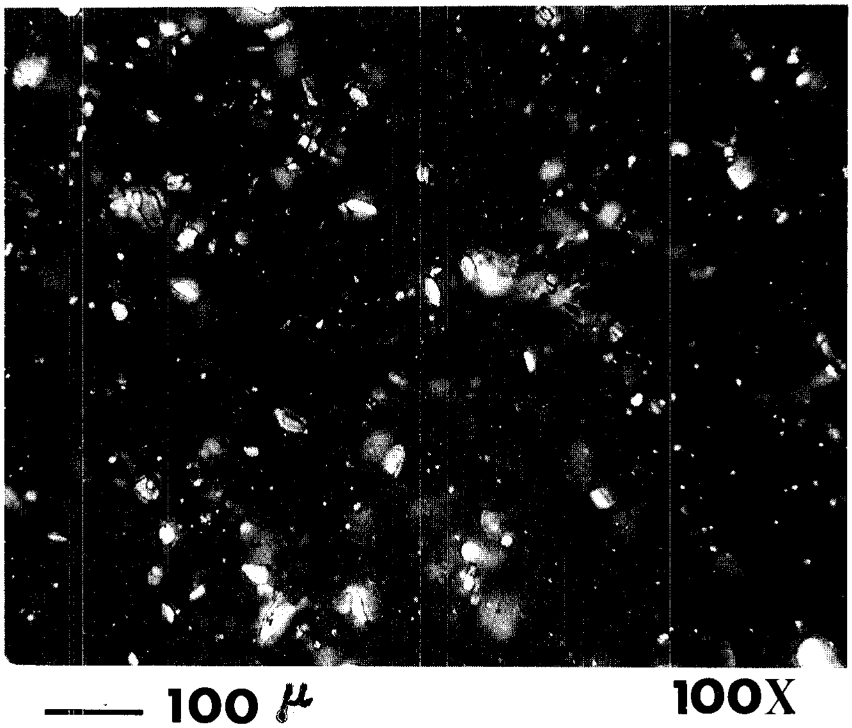


Figure III-B-7.  Birefringence Pattern of Dry Epoxy Film

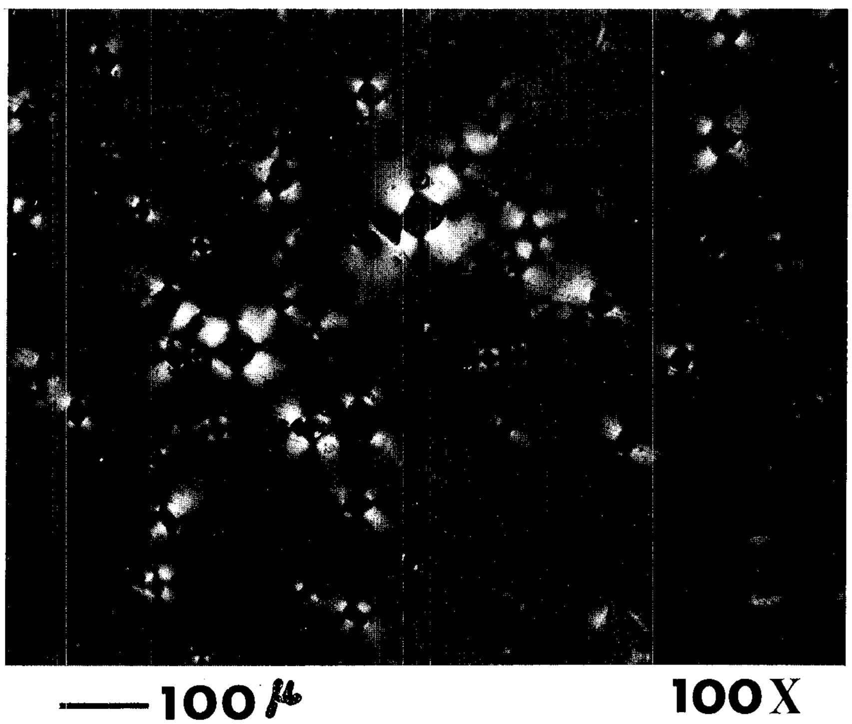


Figure III-B-8.  Birefringence Pattern of Epoxy Film
Exposed to Boiling Water for 20 Hours

The changes in birefringence pattern, when the epoxy samples are exposed to a boiling water environment for various periods of time (i.e., 120 hours, 370 hours and 440 hours), are shown in Figures III-B-9, 10 and 11, respectively. In Figures III-B-9 and 10, more birefringence patterns are observed, and they suggest that the epoxy resin is so inhomogeneous that the diffusion and swelling process are strongly dependent on the local structure of the material. Previously, other investigators have suggested that inhomogeneity of crosslink density in cured epoxy exists, based on electron microscopy of fracture surfaces. It has been known that, if the crosslink density was insufficient to produce a network structure capable of withstanding the high radial extension ratio at the interface, a cohesive failure in the interfacial region developed. This is shown, in Figure III-B-11, by the disappearance and/or relaxation of light intensity pattern, when epoxy is exposed to boiling water for 440 hours. The difference in birefringence patterns between Figures III-B-8 and 11 indicates that the cohesive failure occurred in the interfacial region.

The dynamic mechanical data and microscopic evidence suggests that the effect of moisture and temperature on the mechanical performance of composites and neat resin is detrimental, that the matrix stiffness is a significant factor in the out-of-plane stiffness of composites and that inhomogeneous swelling in the epoxy matrix is the major mechanism responsible

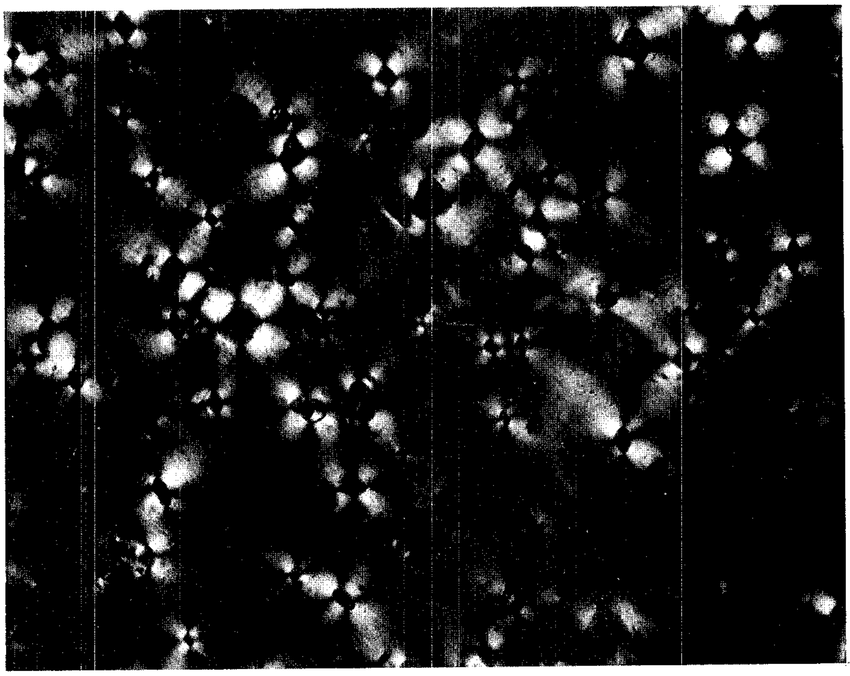

— 100 μ 100X

Figure III-B-9. Birefringence Pattern of Epoxy Film Exposed to Boiling Water for 120 Hours

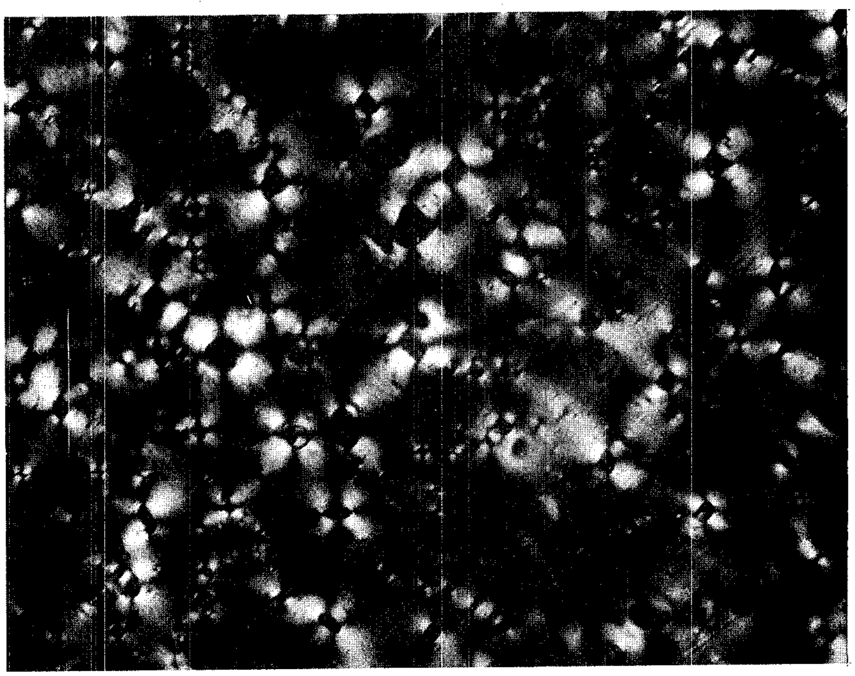

— 100 μ 100X

Figure III-B-10. Birefringence Pattern of Epoxy Film Exposed to Boiling Water for 370 Hours

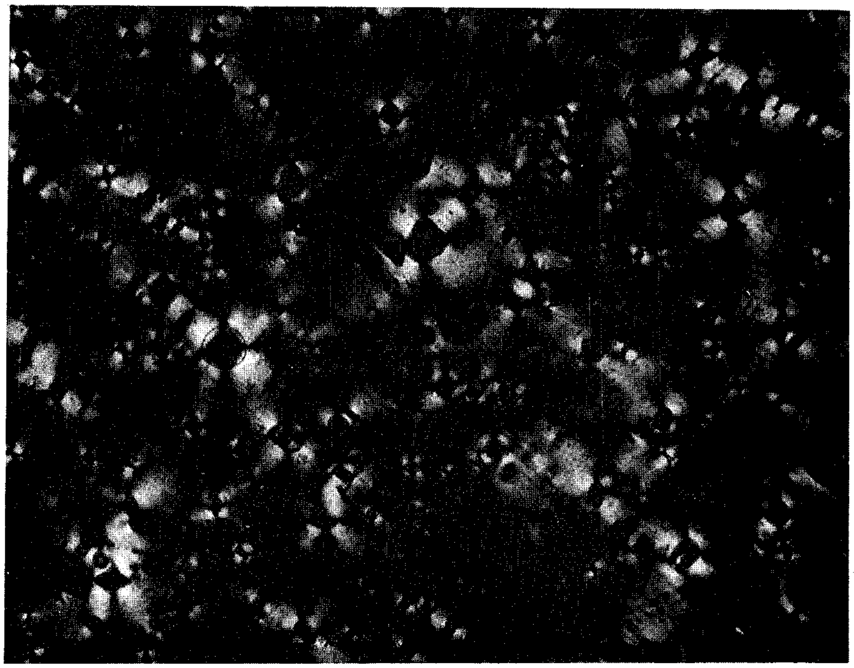

— 100 μ 100X

Figure III-B-11. Birefringence Pattern of Epoxy Film Exposed to Boiling Water for 440 Hours for the degradation of mechanical properties of composites and neat resins upon exposure to moisture.

b. Theoretical Studies

Using the thermodynamic concepts of swelling and mixing, a constitutive equation relating stress, strain and volume fraction of liquid in the swollen polymer has been developed. This nonlinear constitutive equation is applicable in the reversible regions of swelling to amorphous network polymers in swelling equilibrium with a solvent at constant temperature and constant external pressure. Equations for inhomogeneous swelling in polymeric materials with a spherical inclusion have then been developed for the case of zero external load by minimizing the total Gibbs' free energy. The spherical inclusion, here, may represent a filler particle dispersed in a structural fluctuation field. It is assumed that the inclusions are isotropic and stress-free in the unswollen state and are located far from each other so that they do not interact with the inhomogeneous swelling field of others. The numerical solution of the equations for Narmco 5208 epoxy resin and 100% relative humidity at 25°C surrounding environment is given in Figures III-B-1 through 6 for a few cases of inhomogeneities.

Figures III-B-12 and 13 show the stresses and volume fraction of water, respectively, as functions of reduced radius (starting from the inclusion interface) for the case of a rigid (nonswelling) spherical inclusion imbedded in and

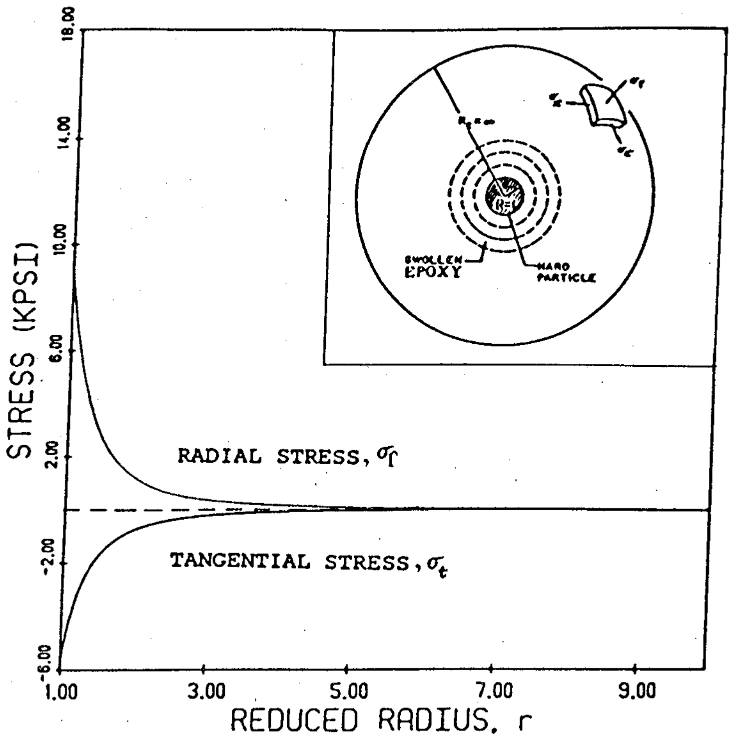


Figure III-B-12. The Radial and Tangential Stresses in a Swollen Epoxy Matrix of Infinite Extent as Functions of Reduced Distance From a Rigid Spherical Inclusion. Inset shows the schematic of stress field.

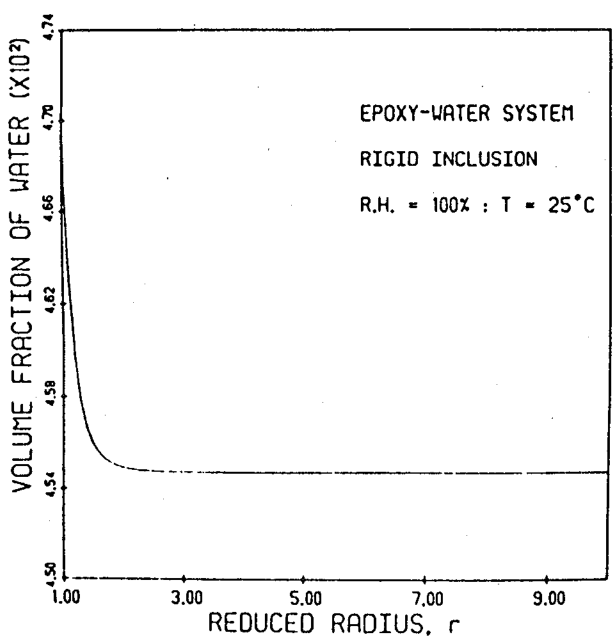


Figure III-B-13. The Volume Fraction of Water as Functions of Reduced Distance for the Same Case as Figure III-B-12.

bonded to a homogeneous, infinite epoxy matrix. The reduced radius is the radius normalized with respect to the inclusion radius, R. Stress and volume fraction of water are maximum at the inclusion interface, thus indicating that any damage would most likely start there.

Because of limited knowledge about the mechanism of formation of inhomogeneities in neat or in situ resin and a lack of experimental work, a precise characterization of the structural fluctuation field is difficult. At present a single parameter, $\rho$, defined as a material property of which the bulk and shear moduli of the neat resin are a linear function, is assumed to characterize the structural fluctuation field. Also, it is assumed that the fluctuation field is spherically symmetrical and thus can be expressed as a continuous or discontinuous function (i.e., Gaussian, exponential, step, etc.) of the reduced radius. The reduced radius in this case is radius normalized with respect to some characteristic radius like the radius where fluctuation ($|\rho - 1|$) first reaches a fixed fraction [here exp $(-\frac{1}{2})$] of maximum fluctuation. Figure III-B-14 shows the stresses as functions of reduced radius (starting from the center of the fluctuation field) for a positive Gaussian fluctuation field (shown in the inset). The corresponding distribution for volume fraction of water is shown in Figure III-B-15. As expected, it is seen that the stress fields produced in neat resin by a large structural fluctuation field (large $\rho$) of

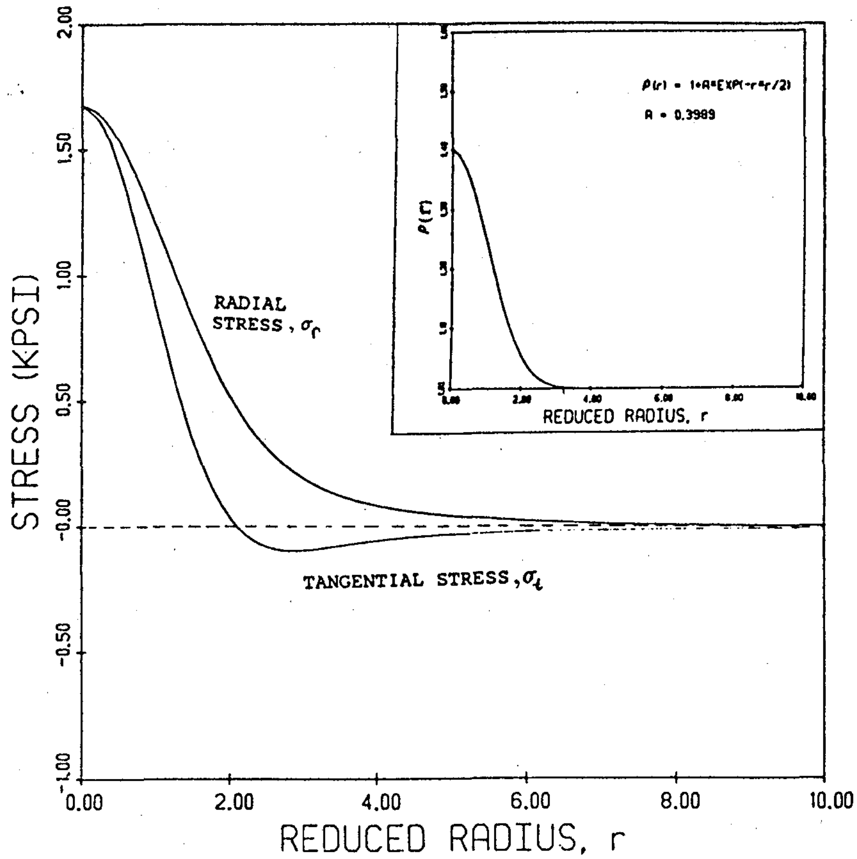


Figure III-B-14. The Radial and Tangential Stresses Associated with a Positive Gaussian Fluctuation Field in Neat Resin, as Functions of Reduced Radius. Inset shows the nature of fluctuation field.

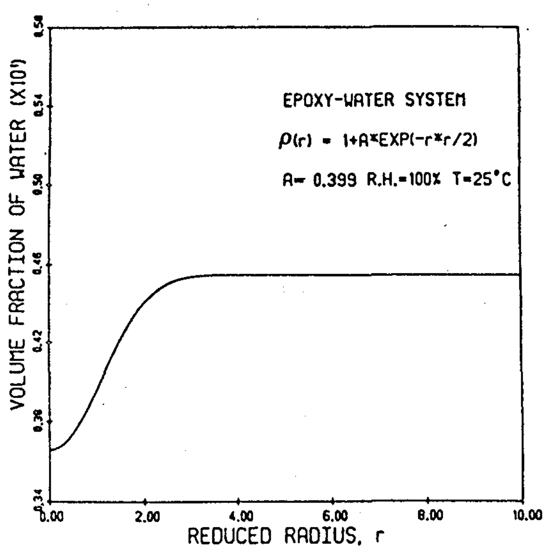


Figure III-B-15. The Volume Fraction of Water as Functions of Reduced Distance for the Same Case as III-B-14.

step function profile is the same as the stress field produced by a rigid filler particle (Figure III-B-12). Figure III-B-16 shows the stress field for a negative Gaussian fluctuation field, and Figure III-B-17 shows the stress field for a positive fluctuation field dispersed in a negative fluctuation field. As is obvious from all these figures, a small structural fluctuation field can produce a large stress concentration due to swelling, and these stresses alone or in conjunction with a stress field due to an external load (The two are not simply additive.) can initiate damage at the interface.

## 4. Plans for Upcoming Period

The experimental moisture interaction studies will be continued using postcured samples. Improvements in the theoretical constitutive equation and a more realistic characterization of structural fluctuations will be sought.

## 5. Current Publications or Presentations by Professor Sternstein on this Subject

"Characterization of the Matrix Glass Transition in Carbon-Epoxy Laminates using the CSD Test Geometry", with P. Yang.

Published in The Role of the Polymeric Matrix in the Processing and Structural Properties of Composite Materials, J. C. Saferis and L. Nicolais, eds., 1983.

"Dynamic-Mechanical Response of Graphite/Epoxy Composite Laminates and Neat Resin", with P. Yang and L. Carlsson.

Published in Polymer Composites, Vol. 4, No. 2, April 1983.

"Characterization of High Performance Composites"

Presented Invited Plenary Lecture to the High Polymer Physics Division of the American Chemical Society, Los Angeles, CA, March 22, 1983.

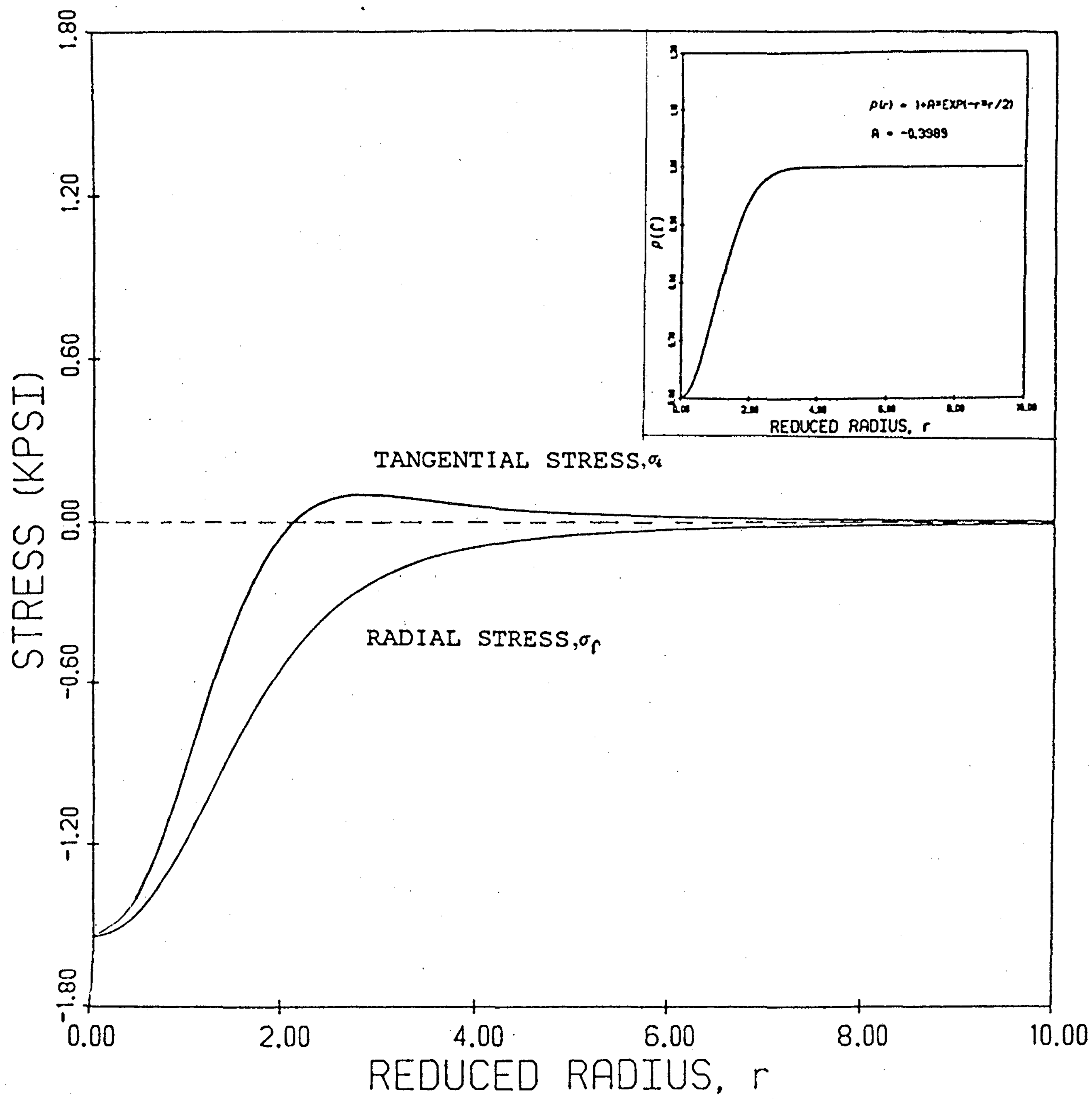


Figure III-B-16. The Radial and Tangential Stresses Associated with a Negative Gaussian Fluctuation Field in Neat Resin, as Functions of Reduced Radius. Inset shows the nature of fluctuation.

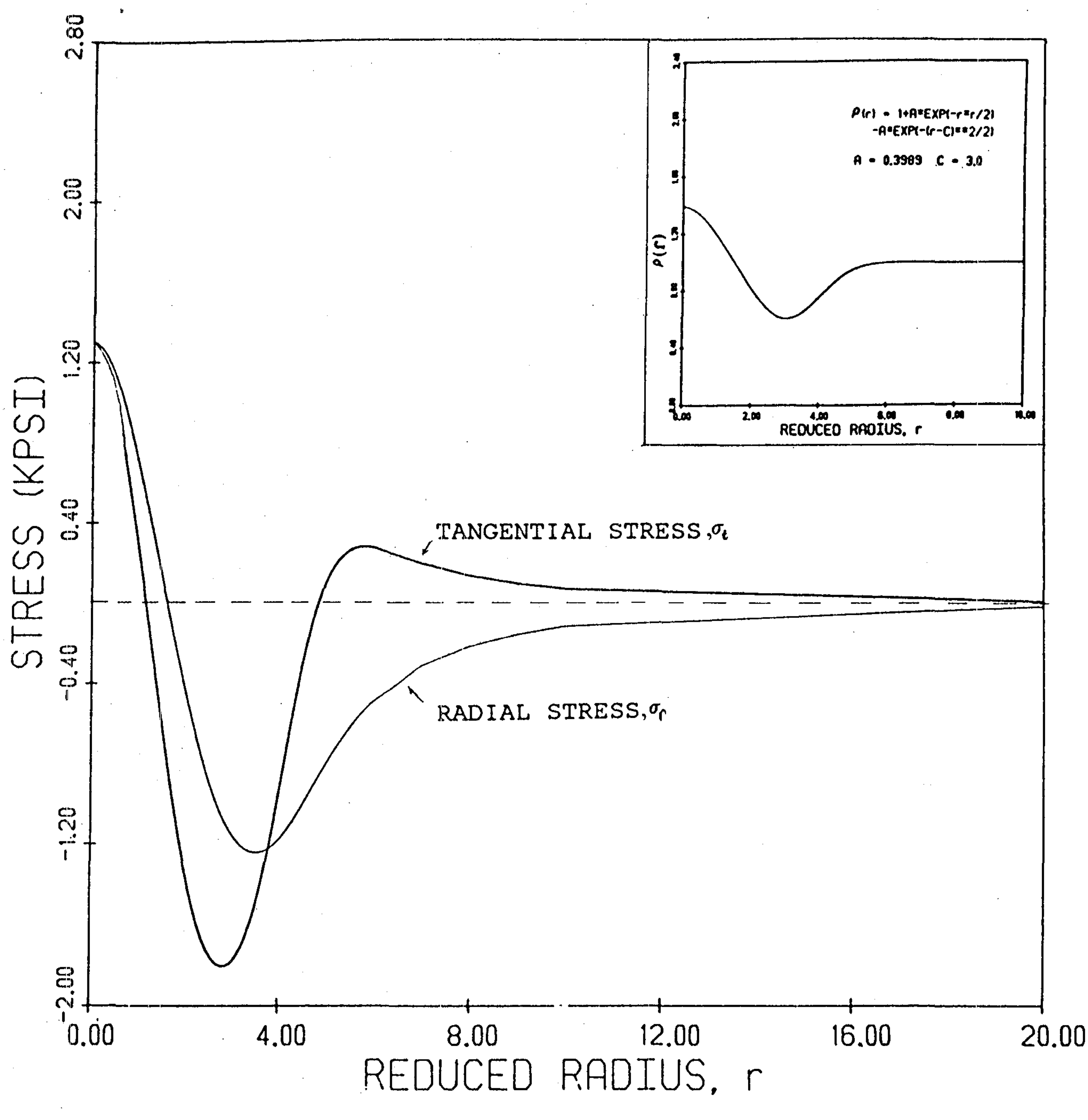


Figure III-B-17. The Radial and Tangential Stresses Associated with a Fluctuation Field of Nature Shown in the Inset

## III-C NUMERICAL INVESTIGATION OF MOISTURE EFFECTS

Senior Investigator: M. S. Shephard

### 1. Introduction

This analysis builds on the theoretical developments of Professor S. Sternstein (as reported in the semiannual progress reports on this program, dated December 1979 and June 1980), in which the fully-coupled, non-linear thermomechanical equations of inhomogeneous swelling of composites in the presence of moisture and temperature are analyzed. In the research reported here, the one-dimensional case of a single fiber in an infinite matrix has been extended to two-dimensional, multiple fiber cases with far field stresses.

### 2. Status

As discussed in earlier progress reports, moisture effects were introduced into the problem through a nonlinear constitutive relation, the principle of virtual displacements was employed to develop a nonlinear matrix equation using displacement-based finite elements, and these nonlinear equations were solved using quasi-Newton finite element analysis. Subsequently, the constitutive equation was built into the finite element analysis. Test cases with multiple fiber packings have been analyzed, in the presence of various humidity levels and applied far field stresses.

## 3. Progress During Report Period

During the current report period, additional cases were run using the subject analyses, which is the work of graduate student Frida Lumban-Tobing. The problems run included both one and two fiber problems considering additional loadings and humidities. The results confirm the trends previously reported and are discussed in detail in Dr. Lumban-Tobing's thesis[1]*.

## 4. Plans for Upcoming Period

These studies are now considered to be complete, and the only remaining tasks are to document the computer program for future use and modification.

## 5. References

1. Lumban-Tobing, F. E. R., "Finite Element Analysis of Moisture and External Load Effects in Composites", Ph.D. Thesis, Rensselaer Polytechnic Institute, Troy, NY, May 1983.

## 6. Current Publications or Presentations by Professor Shephard on this Subject

"Finite Element Analysis of Moisture Effects in Graphite-Epoxy Composites", with F. E. R. Lumban-Tobing and S. S. Sternstein.

Published in Computers and Structures, Vol. 16, No. 1-4, 1983, pp. 457-469.

Presented at the Symposium on Advances and Trends in Structural and Solid Mechanics, Washington, D.C., October 4, 1982 (Given by F.E.R. Lumban-Tobing).

---

*Numbers in brackets in this section refer to the references which are listed on page 64.

# III-D NUMERICAL INVESTIGATION OF THE MICROMECHANICS OF COMPOSITE FRACTURE

Senior Investigator: M. S. Shephard

## 1. Introduction

To understand the mechanisms of failure in composites it is necessary to develop insight into their micromechanical behavior, including interactions between matrix and fibers as the load is increased from zero to that corresponding to failure. Investigations of these phenomena, either experimental or numerical , are difficult. The purposes of this project, being carried out by graduate student Nabil Yehia, are to develop the nonlinear finite element analysis capability required for and to perform numerical investigations of the micromechanical failure of composites.

## 2. Status

The overall structure of a general purpose finite element code for fracture problems has been designed (under this project) and is currently being implemented and tested. The major requirements for the program are that it (a) accommodate various types of fracture problems and (b) house a variety of algorithmic approaches to fracture and debonding analysis. The linear portion of the program has been coded and tested. The fracture criteria are currently being implemented and tested. The automatic crack-tracking algorithms have been developed and are being tested in a stand-alone mode by graduate student Gary Burd.

## 3. Progress During Report Period

During the last reporting period, effort concentrated on two areas of development; implementation and testing of numerical algorithms required for the fracture problem and development of a meshing algorithm to automatically generate finite models accounting for crack growth. Efforts on the fracture problem have focused on procedures to predict crack growth increments and to insure the level of accuracy obtained in the calculation of crack-tip stress intensity values. The meshing algorithm being developed to automatically track crack growth employs the modified-quadtree mesh generator discussed in the semi-annual progress report for this program, dated July 1982, in an algorithm that automatically meshes a geometry after it has changed due to crack growth.

### a. Stress Intensity Factors Calculation

The stress intensity factors, $K_I$ and $K_{II}$, are evaluated from the local displacements of the two crack-tip/crack-surface singular elements, using the displacement correlation technique[1]*. The proper elastic, crack-tip singular element can be obtained from the standard quadratic isoparametric element by appropriate positioning of the node points[2,3]. Tests have been run on both the singular quadratic isoparametric triangle (SLST) and collapsed quadratic isoparametric quadrilateral (SQ8).

*Numbers in brackets in this section refer to the references which are listed on page 82.

To test this module, three sample problems for fracture mode 1, as suggested in Reference [4], are analyzed. The geometry and dimensions used in the analysis are shown in Figure III-D-1. The portions of the geometry analyzed and conditions applied for the double edge-notched plate are shown in Figure III-D-2. Figure III-D-3a shows a typical element mesh used to analyze a problem while Figure III-D-3b shows a typical mesh at a crack tip. Although it has been repeatedly reported in numerous meetings and papers [1,2] that the element side-length of the crack tip affects the accuracy with which the crack-tip stress intensity factors can be calculated, we have found in this research that this effect is almost within the level of engineering accuracy for the range of element side lengths under half of the mesh length. Figure III-D-4 shows the percent error in evaluating $K_I$ for different element side lengths, for the three sample problems. It has been also found that the strain energy density field is not a strong function of the element side length for a reasonable range of edge lengths, as shown in Figures III-D-5 and 6.

b. Crack Propagation Module

The purpose of this module is to determine the direction and magnitude of incremental crack growth, after it has been determined that the crack will propagate. Two criteria have been chosen as candidates for this module; namely, the minimum strain energy density criterion and the maximum dilatational strain energy criterion.

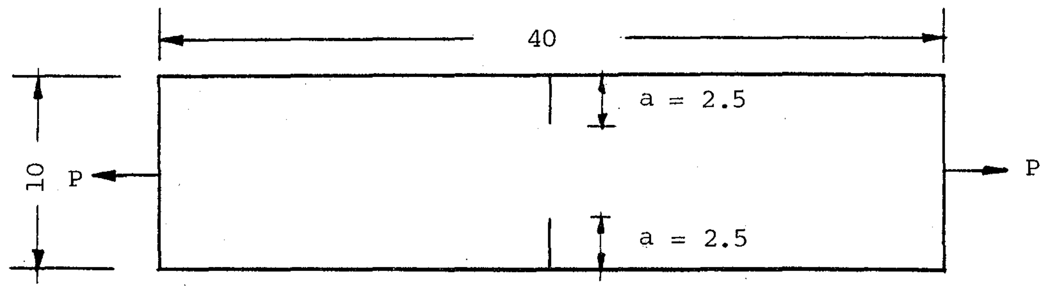


a. Double Edge Notched Plate (DEN)

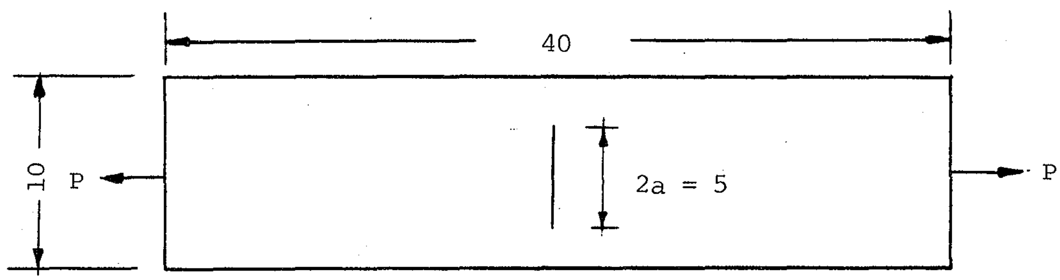


b. Central Notched Plate (CN)

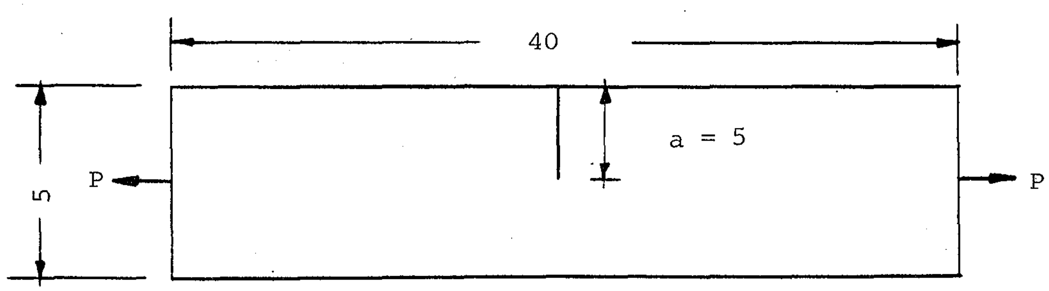


c. Single Edge Notched Plate (SEN)

Figure III-D-1. Mode I Notched Plate Test Geometries

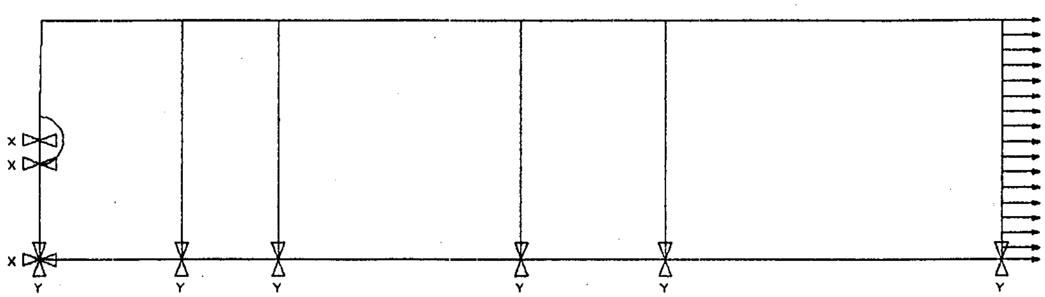


Figure III-D-2. Quarter of Double Edge Notched Plate Analyzed

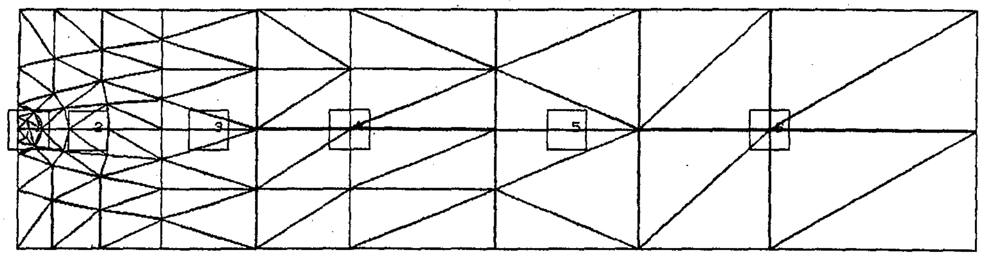


Figure III-D-3. Typical Finite Element Mesh
a. Entire Mesh

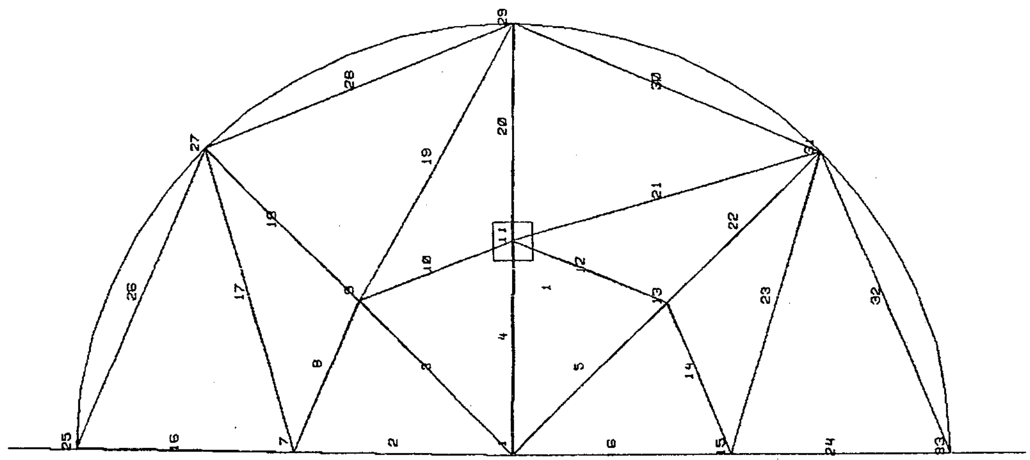


Figure III-D-3. Typical Finite Element Mesh
b. Closeup of Mesh at Crack Tip

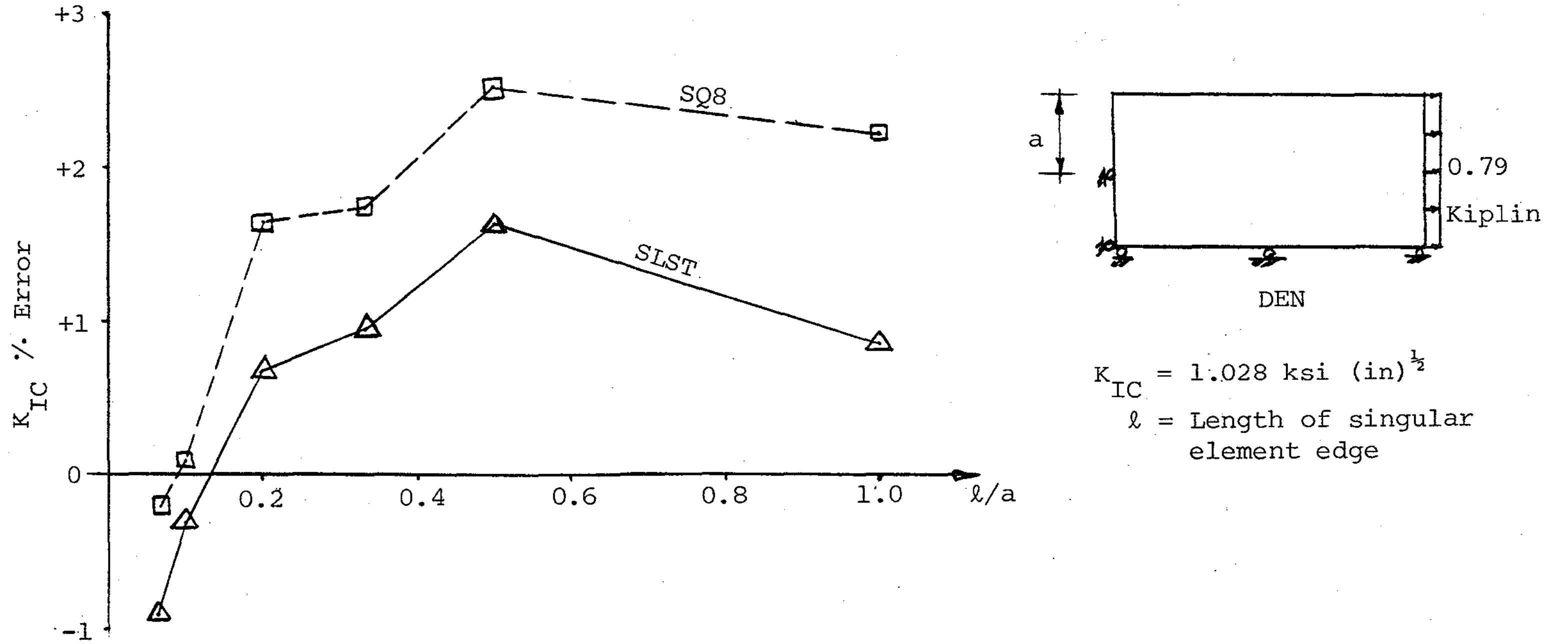


Figure III-D-4. Error in Computing $K_{IC}$ as a Function of Element Side Length

a. Double edge notched plate (DEN)

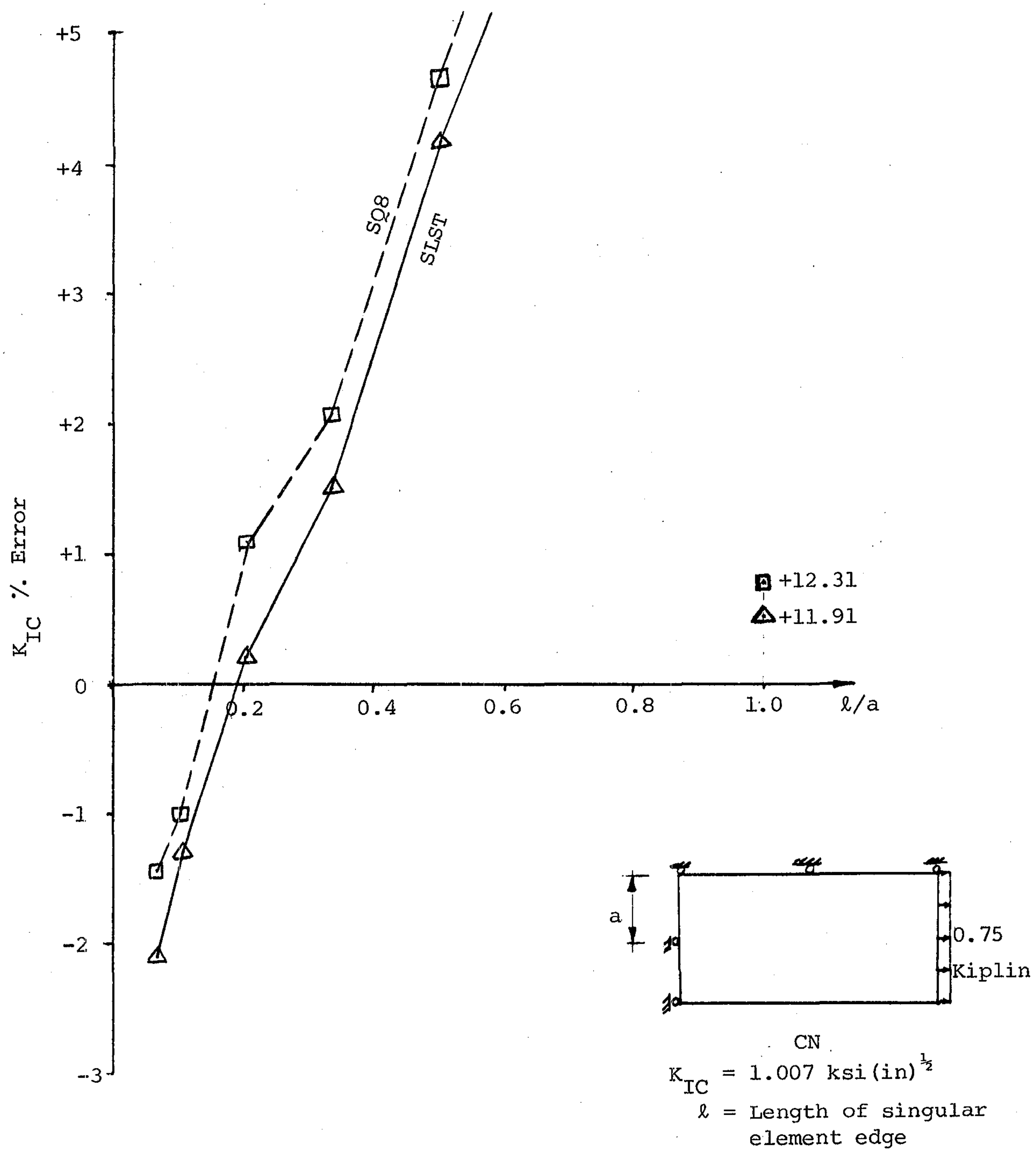


Figure III-D-4. Error in Computing $K_{IC}$ as a Function of Element Side Length
b. Central notched plate

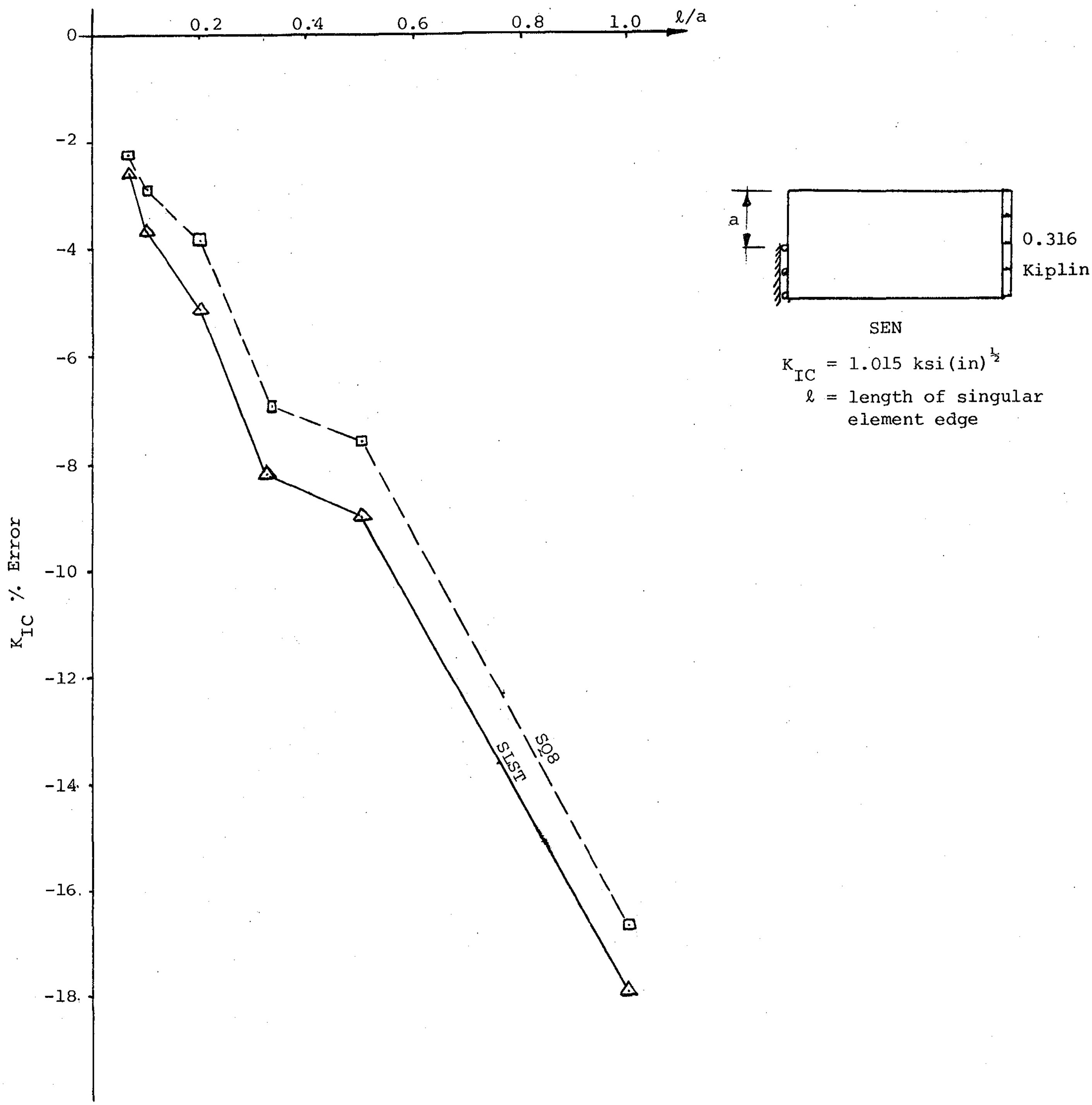


Figure III-D-4. Error in Computing $K_{IC}$ as a Function of Element Side Length
c. Single edge notched plate (SEN)

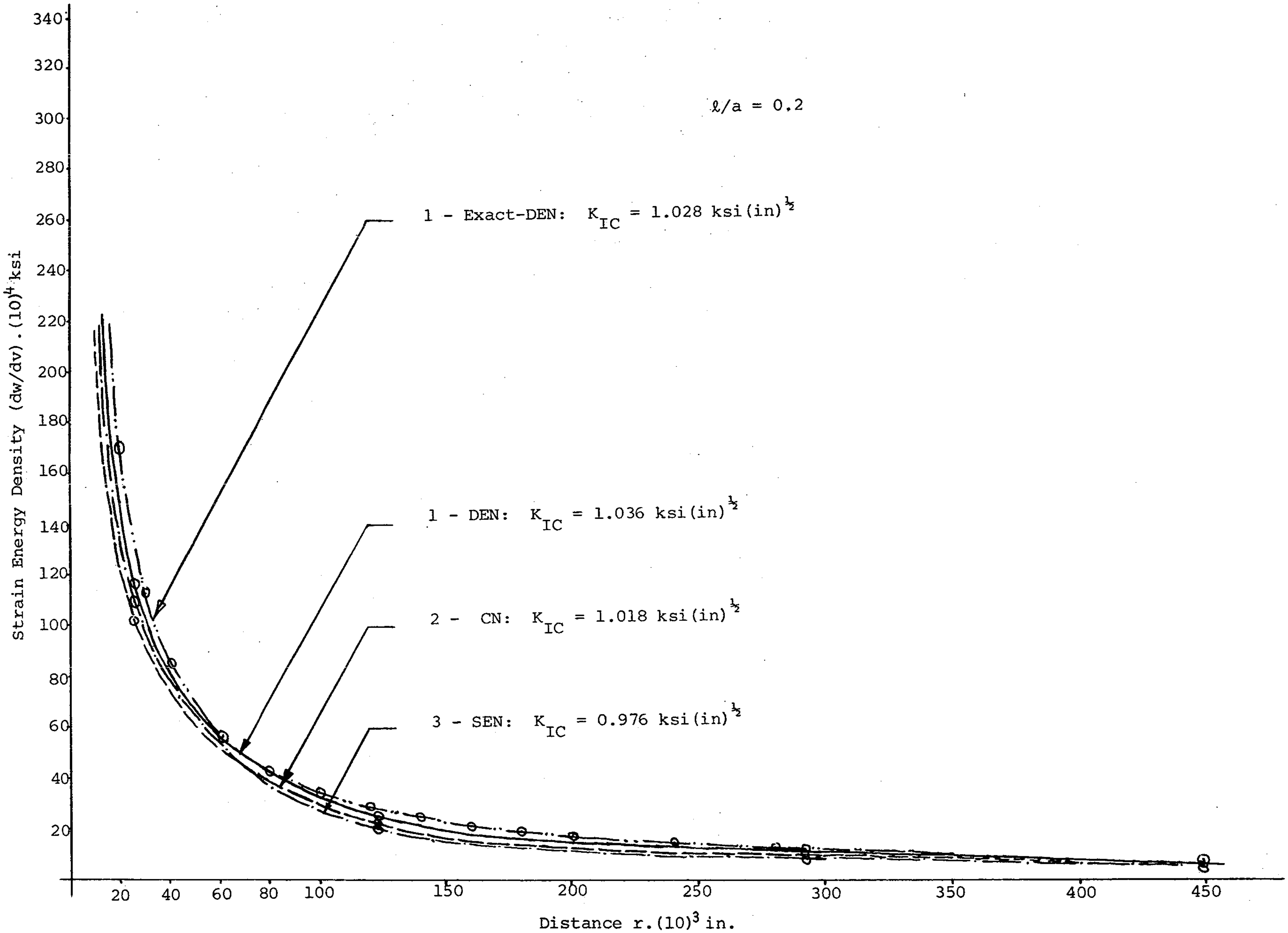


Figure III-D-5. Strain Energy Density Field for Element Side Length Equal To 20% of Cracked Length

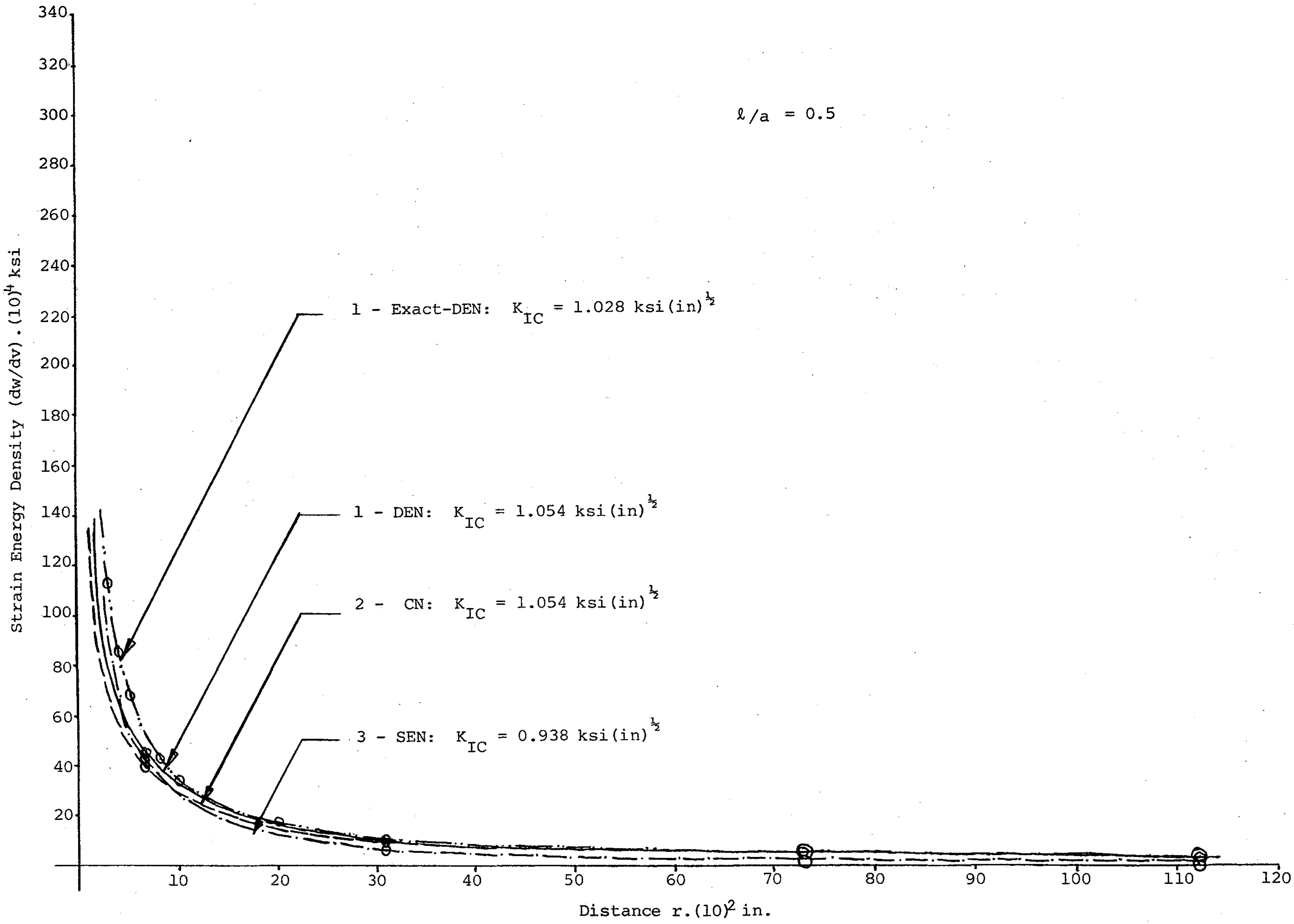


Figure III-D-6. Strain Energy Density Field for Element Side Length Equal To 50% of Cracked Length

The minimum strain energy density[5] has been used[6] to predict the crack propagation increment. This approach assumes that the critical strain energy of the material is a material property and is known for the material under study. The latter assumption is not easy to live with in most cases, since it requires experimental determination of the strain energy density at fracture for each material. A procedure has been suggested[7] for determining this value. Once the material critical strain energy is known, the crack propagation angle and the crack-tip stress intensity factors are determined; the propagation increment can be determined as shown schematically in Figure III-D-7.

The maximum dilatational strain energy criterion has been suggested[8,9] to determine the angle of crack propagation. This criterion defines a material critical parameter, $T_{vcr}$, as the particular value of the proper point as the value of this quantity which indicates that the crack will propagate. The Von Mises elastic-plastic boundary is used as the curve on which the maximum value of $T_v$ is evaluated. To determine the crack propagation angle, one can decompose the total strain energy at a point a distance, r, from the crack tip as follows:

$$T = T_v + T_d$$

where

$T_v$ = the dilational strain energy component

$T_d$ = distorsional strain energy component

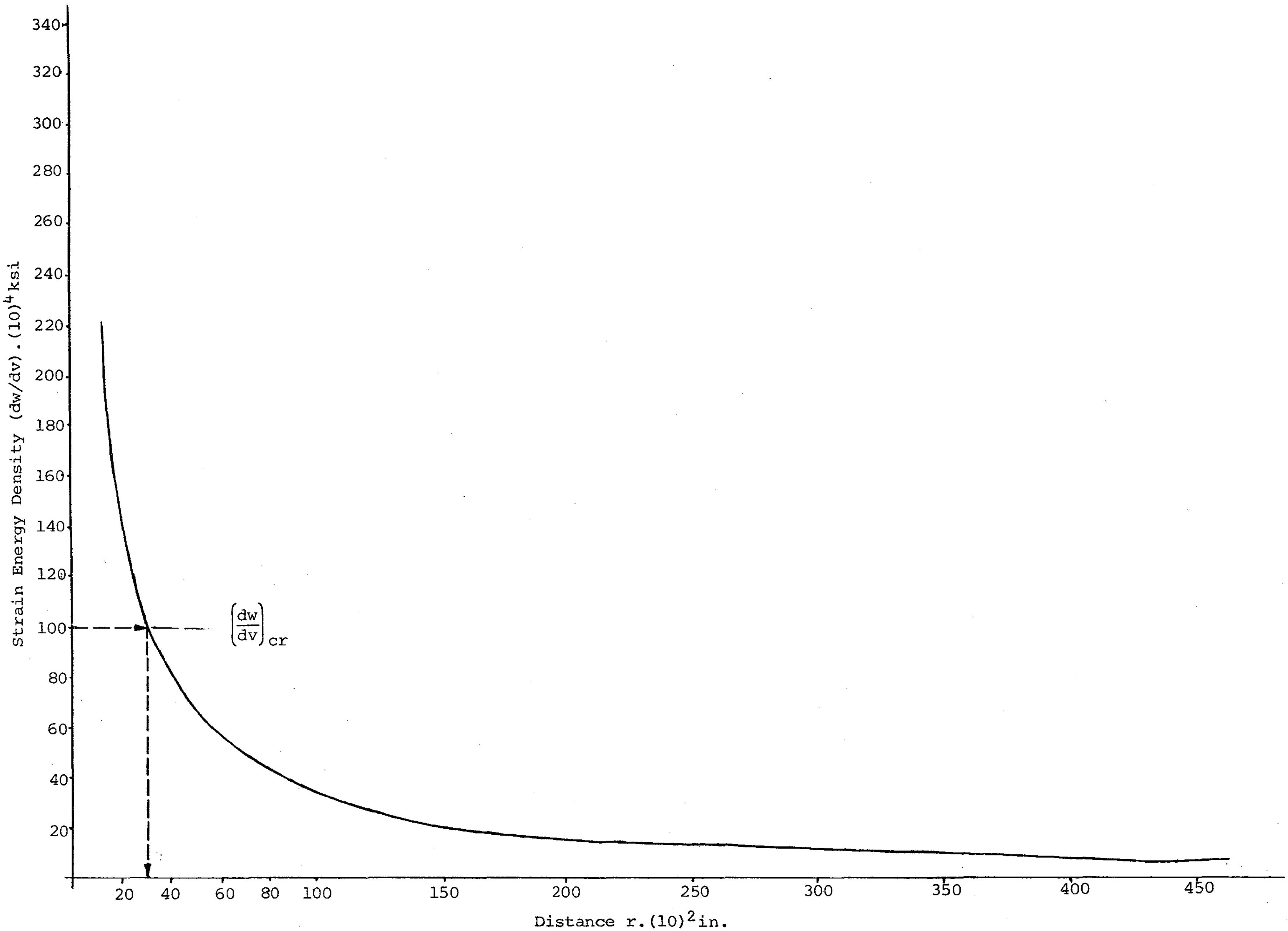


Figure III-D-7. Determination of Crack Propagation Increment and each can be defined as follows:

$$T_v = \frac{S_v}{r} = \frac{1}{r}\left(b_{11}K_I^2 + 2b_{12}K_IK_{II}^2 + b_{22}K_{II} + b_{33}K_{III}^2\right)$$

$$T_d = \frac{S_d}{r} = \frac{1}{r}\left(c_{11}K_I^2 + 2c_{12}K_IK_{II}^2 + c_{22}K_{II} + c_{33}K_{III}^2\right)$$

where:

$K_I$, $K_{II}$ and $K_{III}$ are the crack-tip stress intensity factors and

$b_{ij}$ and $c_{ij}$ are functions of the local angle $\theta$ and the material properties.

Although this criterion has been used just to determine the crack propagation angle[8,9], it can be extended to determine the magnitude of the crack propagation increment as well. To determine the crack propagation increment, one can use either the critical dilatational strain energy approach or the critical distance to the elastic plastic boundary and check against the appropriate value of the predicted direction of propagation on the elastic-plastic boundary around the crack tip. Unlike the minimum strain energy density criterion[5,6], both critical values mentioned above can be easily determined for a given material provided that the material fracture toughness is given.

The T criterion has been implemented and preliminarily tested on the sample problems mentioned earlier in this report. Reasonable results were obtained. Further testing is required, however.

### c. Error in Predicting the Crack Increment

In Figures III-D-5 and 6, the error in $K_I$ is defined as:

$$(K_I)_{ER} = \frac{K_I - K_{IC}}{K_{IC}}$$

where:

$K_I$ is the calculated value and

$K_{IC}$ is the critical value.

The error in predicting the crack propagation increment, using either of the criteria discussed above, can be obtained as follows:

$$(r)_{ER} = \frac{r_I - r_{IC}}{r_{IC}} = \frac{K_I^2 - K_{IC}^2}{K_{IC}^2} = (K_I)_{ER}\left(\frac{K_I}{K_{IC}} + 1.0\right)$$

This implies that the error in predicting the magnitude of the crack propagation increment is about twice as much as evaluating the crack-tip stress intensity factor. In other words, the shorter the singular element side length, the better will be the prediction of the crack increment, based on the results obtained, with a range of L/a between 0.0 and 0.3 required to yield results within ten percent (reasonable engineering accuracy).

### d. Automatic Mesh Generation for Crack Tracking

The ability to automatically track the crack growth requires an automatic mesh operator [10,11] and an adaptive geometry data base. Alterations are being made to the modified-quadtree automatic mesh generator so that it can be used for this purpose. Thus far, work has been done in three major areas. These areas are (a) converting the input of the mesh generator so as to work from an adaptive geometry data base, (b) allowing a quadrant to have several boundaries within it and (c) adding pointers to the quadtree.

Because several changes of geometry will have to be made during the analysis of a given problem, an adaptive data structure is required. Linked lists lend themselves quite nicely to this job. A region can be represented as an area enclosed by a linked list of curves; and a curve can be represented by a linked list of x-y coordinate pairs. As the geometry changes, only a few pointers need to be changed rather than reorganizing the storage of data in memory. The curve discretization algorithm, used by the present version of the modified-quadtree program, has been recoded to work from this linked-list data structure.

The original version of the modified-quadtree program allows only one boundary to be represented within a quadrant. At least two boundaries will always have to be represented in the analysis of crack growth. In order to make this task more manageable, the possible number of cutting points in a quadrant has been limited to four. If the diagonals used to convert quadrilaterals into triangles are chosen properly, the limitation on the number of cutting points does not adversely affect the quality of triangular meshes. An algorithm for choosing diagonals has been successfully implemented.

Because several meshes will be generated during a crack growth problem, it is important that the mesh generation process be as inexpensive as possible. A significant improvement in the cost of generating a mesh can be made by keeping pointers from a parent to its sons, rather than by deriving this information by a tree traversal every time it is needed. Accordingly, portions of the mesh generator are being rewritten so that it will use pointers.

## 4. Plans for Upcoming Period

During the next reporting period, effort will concentrate on the following:

a) interfacing the automatic mesh generator for remeshing as cracks propagate with the analysis routines,

b) continuing the testing of crack propagation modules and

c) carrying out specific micromechanical analysis on composites that can be properly represented with those features available in the program.

## 5. References


1. Ingraffia, R. A. and C. Manu, "Stress-Intensity Factor Computation in Three Dimensions with Quarter-Point Element", Int. J. Num. Meth. Engng., Vol. 15, 1980, pp. 1426-1445.

2. Barsoum, R. S., "On the Use of Isoparametric Finite Elements in Linear Fracture Mechanics", Int. J. Num. Meth. Engng., Vol. 10, 1976, pp. 25-37.

3. Barsoum, R. S., "Triangular Quarter-Point Elements as Elastic and Perfectly-Plastic Crack Tip Elements", Int. J. Num. Meth. Engng., Vol. 11, 1977, pp. 87-98.

4. Brown, William, T., Jr. and S. E. Srawley, "Plane Strain Crack Toughness Testing of High Strength Metallic Materials", ASTM, STP410, 1966.

5. Sih, G. C., "Strain-Energy Density Factor Applied to Mixed Mode Crack Problems", Int. J. Fracture, Vol. 20, No. 3, September 1974, pp. 305-321.

6. Sih, G. C., "Mechanics of Ductile Fracture", Fracture Mechanics and Technology, G. C. Sih and C. L. Ches, eds., Vol. 11, 1977, pp. 767-784.

7. Leslie, F. Gillenet, "Criterion of Crack Initiation and Spreading", Eng. Fract. Mechanics, 1976, Vol. 8, pp. 239-253.

8. Theocaris, P. S. and N. P. Andrianopoulos, "The Mises Elastic-Plastic Boundary as the Core Region in Fracture Criteria", Eng. Fract. Mechanics, 1982, Vol. 16, No. 3, pp. 425-432.

9. Theocaris, P. S. and N. P. Andrianopoulos, "The T-Criterion Applied to Ductile Fracture", Int. J. of Fracture, 20, 1982, pp. R125-R130.

10. Yerry, M. A. and M. S. Shephard, "Finite Element Mesh Generation Based on a Modified-Quadtree Approach", IEEE Computer Graphics and Applications, Vol. 3, No. 1, 1983, pp. 36-46.

11. Yerry, M. A. and M. S. Shephard, "Approaching the Automatic Generation of Finite Element Meshes", Computers in Mech. Engng., Vol. 1, No. 4, 1983, pp. 49-56.

## 6. Current Publications or Presentations by Professor Shephard on this Subject

"The Effective Use of Finite Element Methods in Engineering Design"

Published in Proc. 2nd Chautauqua on Productivity in Eng. and Design, The CAD Revolution, Nov. 1982, pp. 299-312.

Presented at 2nd Chautauqua, Kiawal Island, SC, November 17, 1982.

"Finite Element Mesh Generation Based on a Modified-Quadtree Approach", with M. A. Yerry.

Published in IEEE Computer Graphics and Applications, Vol. 3, No. 1, 1983, pp. 36-46.

"Approaching the Automatic Generation of Finite Element Meshes"

Published in Computers in Mechanical Engineering, Vol. 1, No. 4, 1983, pp. 49-56.

"A Comment on the Effectiveness of Uniform Finite Element Refinements", with S. M. Yunus.

Accepted for publication, Int. J. Num. Meth. Engng.

"Automatic Three-Dimensional Finite Element Generation Using a Modified-Octree Technique"

Presented to the Engineering Mechanics and Solid Modeling Group at General Motors Research Laboratories, Warren, MI, January 28, 1983.

"Finite Element Mesh Generating Techniques and the Interfacing of Finite Element Modeling and Geometric Modeling"

Presented at the Finite Element Modeling Workshop, NASA Langley Research Center, Hampton, VA, February 3, 1983.

"Developments in Mesh Generation and Adaptive Analysis Techniques"

Presented at the Applied Mechanics Colloquia, University College, Swansea, U. K., March 18, 1983.

## III-E ADVANCED ANALYSIS METHODS

Senior Investigator: E. J. Brunelle

### 1. Introduction

The effort to find solutions for individual lamina in terms of a minimum number of generalized variables has gradually widened to finding solutions for composite plates with commonly used stacking sequences. In particular, anti-symmetric cross-ply and anti-symmetric angle-ply plates (for particular boundary conditions) have been analyzed in some detail. This report continues in the same spirit.

### 2. Status

The principal results of the last period are summarized as follows:

a) The complete Kármán-Rostovstev plate problem was stretched into the correct affine space and appropriate solutions for uniform static load and for ultimate uniaxial load were presented to show the sweeping generality of the results.

b) New material parameters R and X were introduced, which are combinations of the four orthotropic constants; $E_1$, $E_2$, $\nu_{12}$ and $G_{12}$. These new parameters embody the characteristics of the fundamental plate parameters $D^*$, $\varepsilon$ and $H^*$. It was found that many common orthotropic materials cluster within the rather narrow bands $1 \leq R \leq 3$ and $5 \leq X \leq 15$.

## 3. Progress During Report Period

Progress in the last reporting period has been made principally in the following three areas.

(a) The following P. D. E. describes the behavior of regular symmetric cross-ply plates.

$$\frac{\partial^4 w}{\partial x_o^4} + 2\omega\frac{\partial^4 w}{\partial x_o^2 \partial y_o^2} + \frac{\partial^4 w}{\partial y_o^4} + kx_o\left(\frac{\pi}{b_o}\right)^2\frac{\partial^2 w}{\partial x_o^2} + ky_o\left(\frac{\pi}{a_o}\right)^2\frac{\partial^2 w}{\partial y_o^2} + M\ddot{w} = q(x_o, y_o, t)$$

Examination reveals that this equation differs from the specially orthotropic plate equations only in that the constant, $\omega$, is interchanged with D*. Hence, all solution techniques, similarity rules and similarity variables used in the orthotropic case are available to facilitate the solution of the above cross-ply composite plate equation.

Few specific solutions exist (all of them in untransformed real space) for the cross-ply symmetric plate, and they are not helpful in understanding how solutions change in response to material constant changes.

The central strong-point of the present formulation, the dependence of specific solutions (i.e., static loading, vibration, stability) on only one parameter, $\omega$, remedies that situation.

A particularly revealing solution of the vibrating, axially-loaded simply supported plate is available in terms of the author's similarity variable, $T$. The results are shown in Figure III-E-1 (for all possible axial loadings less than the buckling load) for $\Omega mn/n^2$ versus $T$ with a

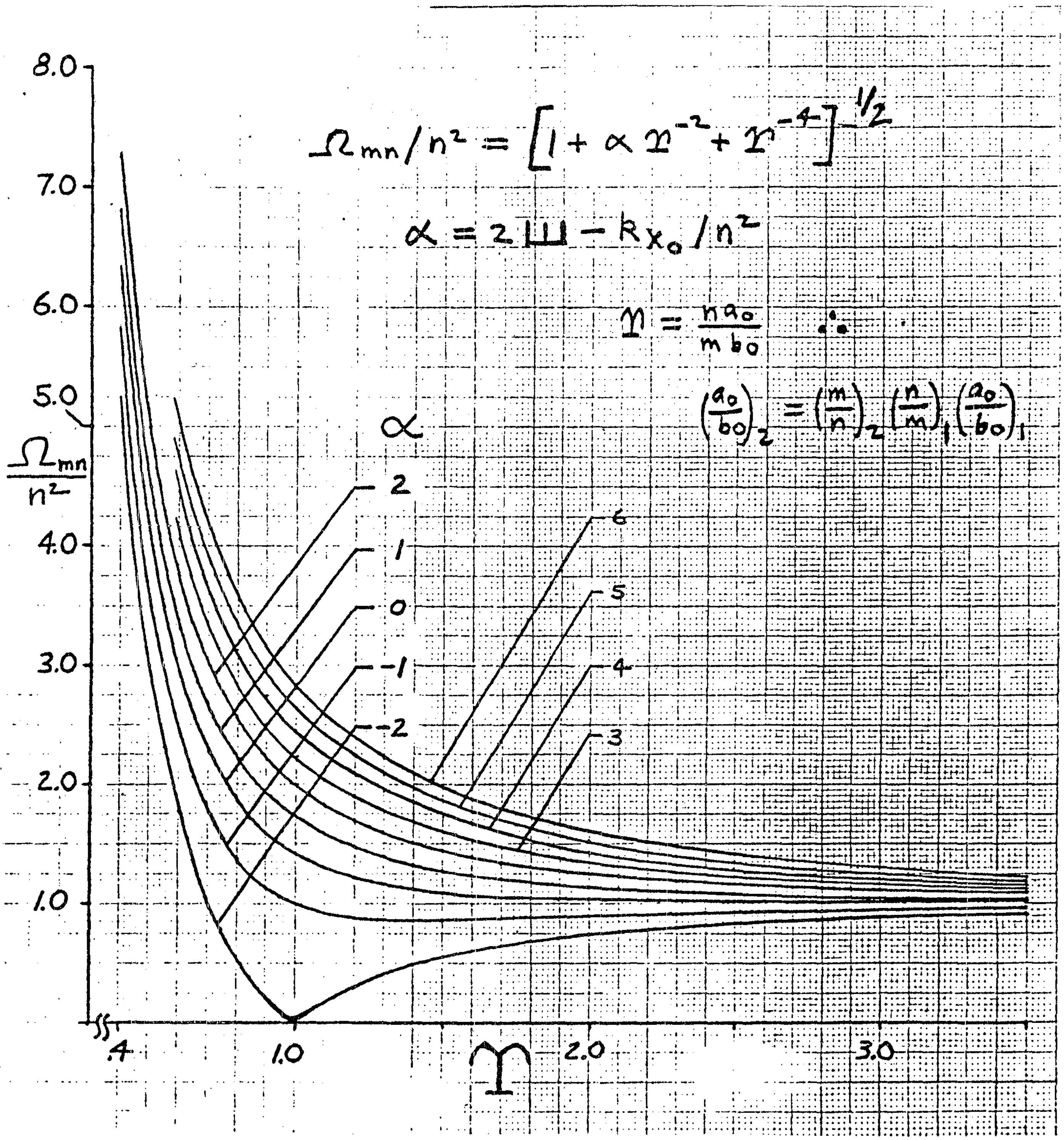


Figure III-E-1. Similarity Solution for All Sides Simply Supported parametric dependence on the parameter $\alpha$. Notice that the entire frequency spectrum is displayed.

(b) A chance reading of a 1982 Winter ASME paper (authored by S. Batdorf) prompted the author to write an extended note using affine transformation theory to make Batdorf's equations independent of any constants present in his original equations. This procedure removes the only known barrier to the effective use of Batdorf's results in assessing local stress distributions in damaged composites.

(c) The rotational derivatives (about some unit vector $\underset{\sim}{n}$) of arbitrary order tensors have been derived and detailed results have been worked out for fourth order systems, $T_{ijkl}$. In particular, the extremum paths of the elasticity tensor, $E_{ijkl}$, can be calculated, and in fact, these derivative results are linearly related to the tensor components themselves. This work was motivated by the "derivative-results" due to Tsai (and independently derived by the author a few months later); it seemed natural to expect a generalization of these very useful results.

## 4. Plans for Upcoming Period

The author, having taken an extended leave of absence from RPI, regretfully must end his association with the NASA/AFOSR research effort. This association afforded the author ideal conditions for creative work, and the ever-steady support of the NASA and AFOSR project monitors is gratefully acknowledged.

## 5. Current Publications or Presentations by Professor Brunelle on this Subject

"An Overview of Composite Plate Solution Techniques"

Presented Invited Lecture at the United States Air Force Institute of Technology, Dayton OH, December 28, 1982.

"The Affine Equivalence of Local Stress Distributions in Damaged Composites and Batdorf's Electric Analogue"

To be published in the AIAA Journal, July 1983.

"Generic Buckling Curves for Specially Orthotropic Rectanular Plates", with G. Oyibo.

To be published in the AIAA Journal, August, 1983.

# PART IV
# GENERIC STRUCTURAL ELEMENTS

## IV-A COMPACT LUG DESIGN

# IV-A COMPACT LUG DESIGN

Senior Investigator: D. B. Goetschel

## 1. Introduction

A critical aspect of many aerospace structural elements is the load transfer that takes place between the connecting lugs at the ends of the structure and the portions of the structure wherein the loads are well-distributed if not uniform. Such lugs are often highly loaded and have very complex stress states. Further, since they must mate with connecting parts, these lugs are usually designed within rather stringent dimensional envelope constraints. As compared to lugs which are made from high-strength steel, for example, meeting the geometric constraints, even with a composite structural design making maximum use of unidirectional graphite-epoxy, has proven to be a difficult task. This research is intended to solve the load-volume problem in favor of composites rather than either reverting to designs using 200 ksi steel lugs attached to a composite strut or forcing the dimensional constraints to be relaxed with a redesign of the mating parts.

The drag strut of the Lockheed L-1011 is a specific primary structure which has been taken as an example to investigate heavily loaded pinned connections. While it is readily assumed that the column aspect of the structure (see Figure IV-A-1a) could be redesigned of graphite/epoxy, it is

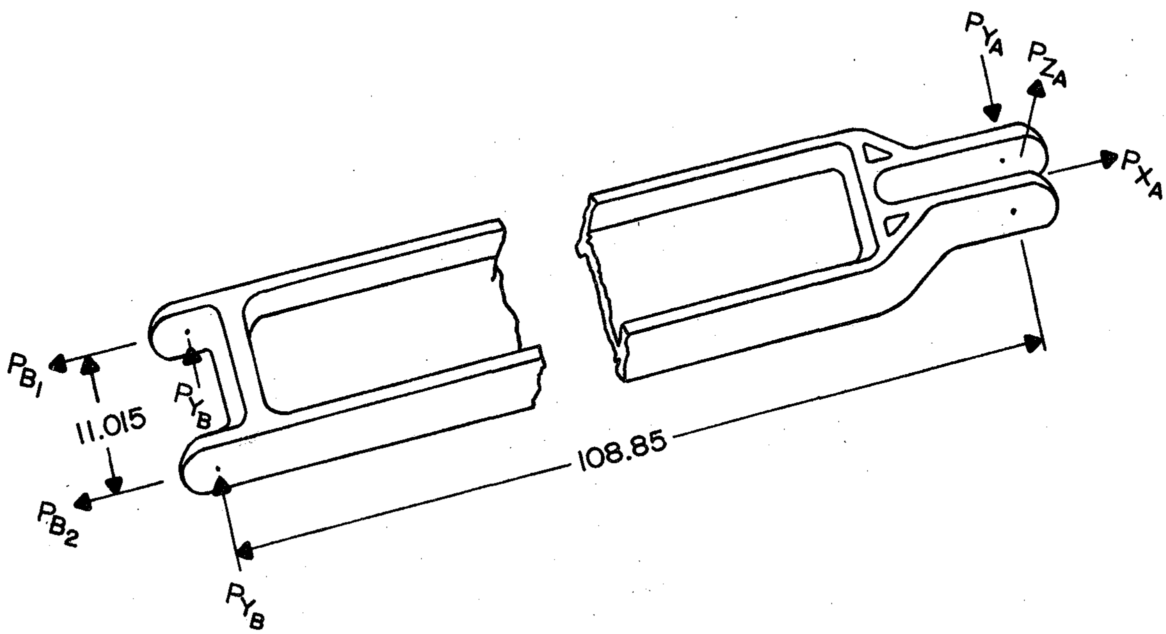


Figure IV-A-1a. Lockheed L-1011 Engine Drag Strut (Schematic)

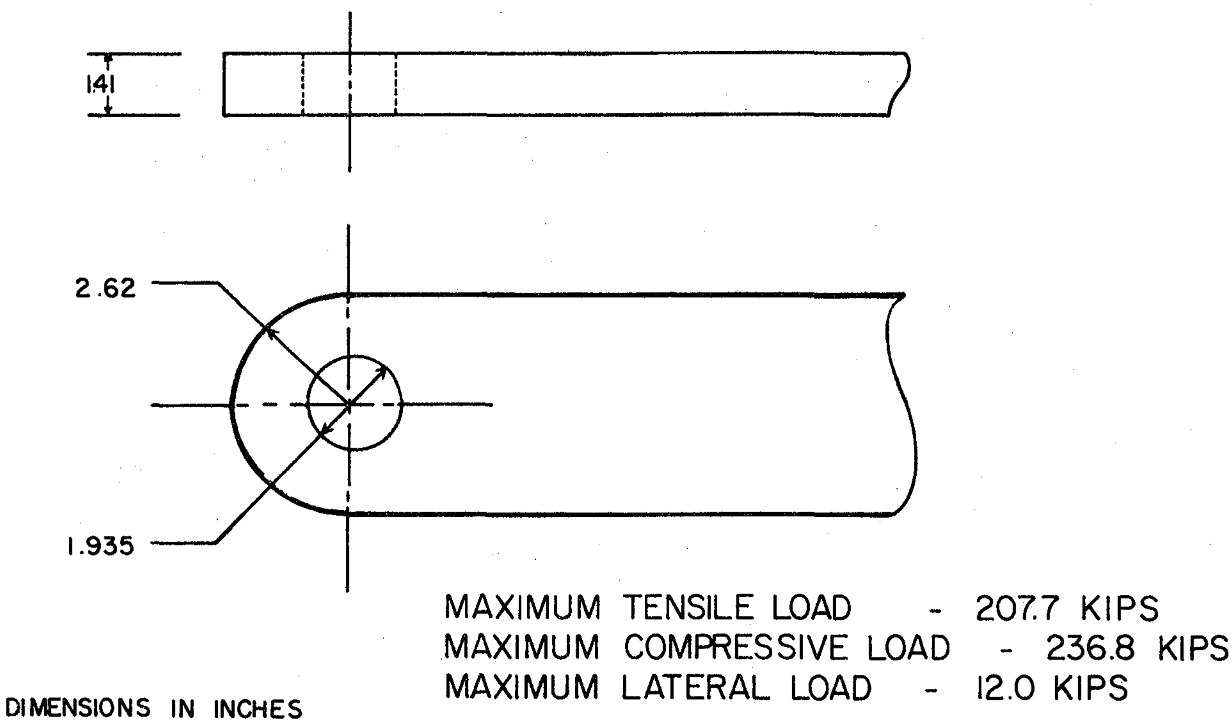


Figure IV-A-1b. Lug Experiment: Full-Scale L-1011 Drag Strut not so clear as to whether a graphite/epoxy pinned lug connection can be designed to withstand the design loads, given the original geometric constraints.

## 2. Status

A number of lug configurations using ply layups (see Figure IV-A-1b, for example) and several means intended to force failure modes into net tension were fabricated and tested. Specimens included quasi-isotropic strips $[0/\pm45/90]_s$ not scaled to any particular design, $[0/\pm45]_s$ quarter-scaled to the L-1011 engine drag strut lug; with round and rectangular ends; with and without stress relieving, longitudinal slots at the ends of the holes; with and without steel bushings in the bolt-loaded holes; with and without cap strips. Twelve tests specifically comparing slotted and unslotted lugs all resulted in failure in combined shear-out and net-tension. Although the failure loads all fell within roughly the same scatter, all specimens without slots showed a more nearly pure tension failure. This showed that the slots improve stress distributions in the direction intended.

## 3. Progress During Report Period

### a. Stress Relief Cut

The stress relief cut concept which was applied to the quarter-scale lug (72-ply) models and reported in the previous progress report[1]* was further investigated. Since, in the

*Numbers in brackets in this section refer to the references which are listed on page 109.

earlier work both the slotted and unslotted (see Figure IV-A-2a and 2b) lugs exhibited failure modes involving shear-out at similar load levels, the stress redistribution effect expected from the slotted geometry was not verified. The occurrence of a failure more closely approaching a net tensile mode would show the benefit of the slots, if such benefits exist.

To isolate the effect of the slots, twelve 16-ply (quasi-isotropic layup $[0/45/-45/90]_{2s}$) specimens with rectangular extended heads were tested during the current period (see Figure IV-A-2c). The squared ends were intended to force tensile failure. Bearing failure unexpectedly occurred at 955 pounds, however, with the first four specimens tested, a 35% decrease in bearing strength is shown to be expected for these 16-ply specimens as compared to 72-ply specimens, according to $F^{br}$ vs. D/t plots given in the advanced composites design guide[2]. Thus, the premature bearing failures can probably be attributed to increasing diameter to thickness ratio.

Similar testing done at the University of Delaware[3] has shown that bearing stresses, in similar specimens, are much higher than those predicted by finite element modeling. Three-dimensional effects are suspected as playing a large role in this phenomenon. This appears even more likely in the case of thin laminates, where free edge stress may cause break-away of the outer plies, reducing the effective bearing surface by a greater percentage than for thick specimens.

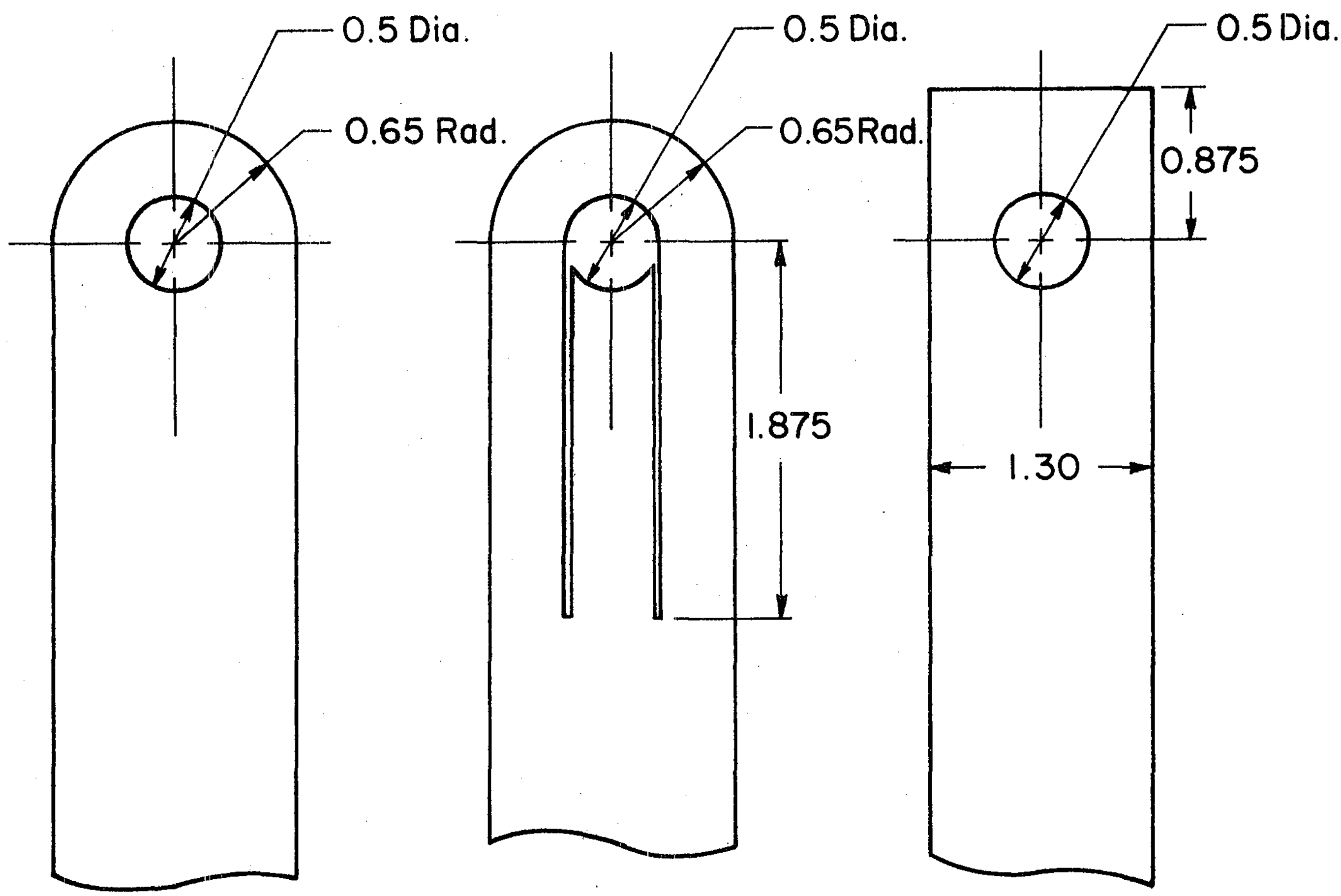


(2a)

Unslotted Lug

(2b)

Slotted Lug

(2c)

Squared Lug
(modified to prevent
shear-out failure)

Figure IV-A-2. Trial Lug Configurations

To overcome the D/t effect, the area of the net tension plane was reduced by reducing the width from 1.3 inches to 0.7 inches on the remaining eight specimens. Net tension failure then was clearly evident in each of the subsequent tests. The slotted lug specimens showed, on the average, 21% higher ultimate load capability than unslotted specimens. Further, there is no overlap in the data scatter (see Table IV-A-1). This result strongly suggests that the stress relief cuts are effective in reducing tensile stress concentrations at the edge of the loaded hole. It should be noted that the final width to diameter ratio (W/D = 1.4) is shown to result in relatively lower tensile stress concentrations[4,5] than the original width [Note: Here tensile stress concentration is defined as peak tensile stress divided by av. net tensile stress, $K_{TN} = (\sigma\theta)_{max}/\bar{\sigma}_{NT}$.] The effect of slots may be even more pronounced in geometries with larger W/D ratios. Despite the success of these tests, the stress relief cut modification appears to be of rather limited application. In terms of increased ultimate strength, it appears most effective for pinned connections with large W/D that would otherwise still fail in tension. It has been shown[1] to have negligible effect on shear failures and is vulnerable to transverse loading through the pin.

Attempts to verify these results with finite element analyses were frustrated by the assumption of a cosine normal load distribution in the available program, and such is not

TABLE IV-A-1

SUMMARY OF FAILURE INFORMATION: SLOTTED AND UNSLOTTED TENSION LUGS

| Specimen | Description | Failure Load Lbs. (psi) | Mode of Failure |
|---|---|---|---|
| 1 | Unslotted* | 359.6 (40,864) | Net tension |
| 2 | " " | 311.3 (35,375) | " " |
| 3 | " " | 338 (38,410) | " " |
| 4 | " " | 364.1 (41,375) | " " |
| 5 | Slotted | 410.2 (46,610) | " " |
| 6 | " " | 429.3 (48,780) | " " |
| 7 | " " | 383.2 (43,550) | " " |
| 8 | " " | 433.8 (49,295) | " " |
| Av. | Unslotted | 343 (38,980) | |
| Av. | Slotted | 414 (47,060) | |

*All specimens $[0/45/-45/90]_{2s}$

valid for W/D < 2.0[6]. The measured failure stresses were roughly 30% lower than the peak stresses predicted by the finite element model, probably because of the inaccuracy of the model for this particular geometry.

b. Capstrips

Another approach pursued in this research was the use of a partial capstrip made from unidirectional strips of graphite/epoxy to strengthen lug designs. The concept is that the stiff capstrip will cause a stress redistribution, reducing the peak stress at the hole edge and raising the average stress, at which the inner laminate will fail.

Our first attempts were reported in the previous progress report. In that case, a .1-inch capstrip (see Figure IV-A-3a) was bonded to an inner laminate of $[0/\pm 45]_{12s}$. The resulting mode of failure involved the capstrip shearing off along one side of the lug. Whether or not this precipitated a subsequent failure, or whether it occurred after failure of the inner laminate, was not clear. This specimen failed at a load of 12,750 pounds (40,220 psi).

It was decided to attempt to wrap the capstrip entirely around the inner laminate, forming a tension loop (see Figure IV-A-3b) to reduce the tendency of the capstrip to shear off. There are, of course, manufacturing difficulties. Whenever a laminate is laid up on a surface with curvature and then cured, the laminate thickness changes by a significant percentage, as the resin bleeds out, resulting in slack material.

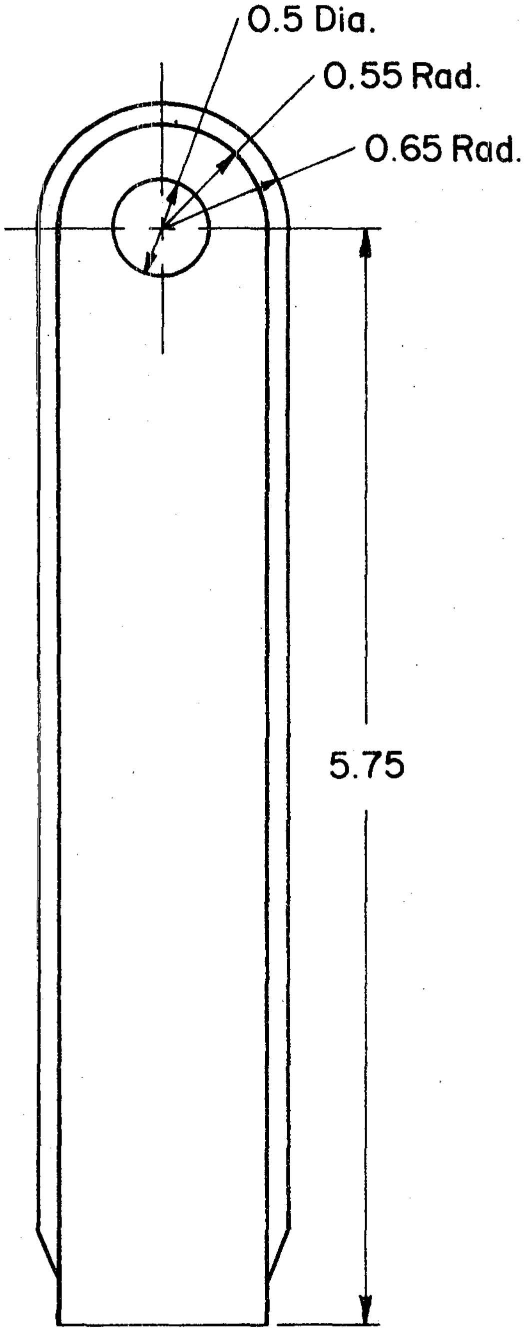


(3a)

Straight Capstrip

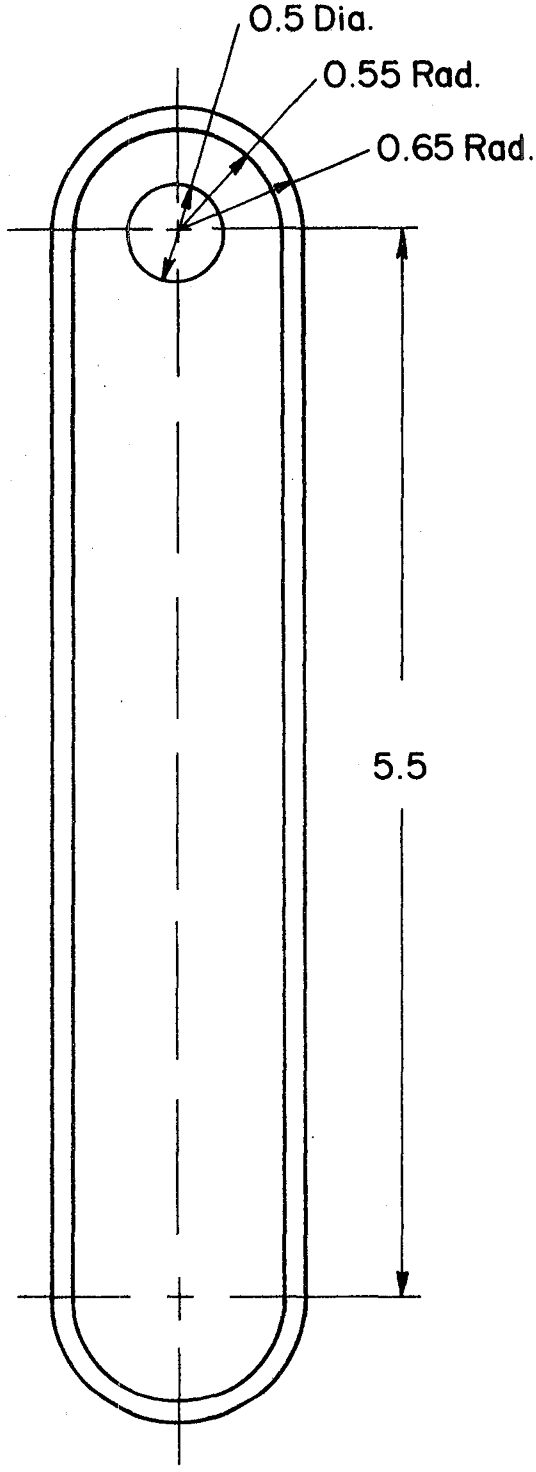


(3b)

Tension Loop Capstrip

Figure IV-A-3. Capstrip Lug Configurations

Some means must be applied to prevent resin pockets from occurring on the curved inner surface, since such imperfections can be highly detrimental.

A fixture was developed (see Figure IV-A-4) which effectively pulls out any slack to the bottom of the lug (see Figure IV-A-5a). This fixture was found to work very well in eliminating the slack. It was difficult to tightly bag the entire apparatus for cure, however, and as a result, uneven pressure on the capstrip caused uneven capstrip thickness through the depth of the lug (see Figure IV-A-5b).

Despite such fabrication imperfections, tests were conducted to determine the effect of capstrip width on strength and failure mode. These tests involved specimens with .1", .2" and .3" depth capstrips. The results (see Table IV-A-2) are encouraging, although more work will be required to establish trends. All three failures were of the shear-out type, with the failure occurring on a shear plane extending radially about 25 degrees above the net tension plane. The failures appeared to initiate in the inner laminate at the hole edge.

Two concepts were considered in an effort to address the apparent initiation of failure at the hole edge. The first was the use of a steel bushing that could plastically deform to redistribute and reduce the peak stresses. The second was the use of some material near the hole which has a greater fracture toughness and lower stiffness than graphite-epoxy to reduce the peak stress.

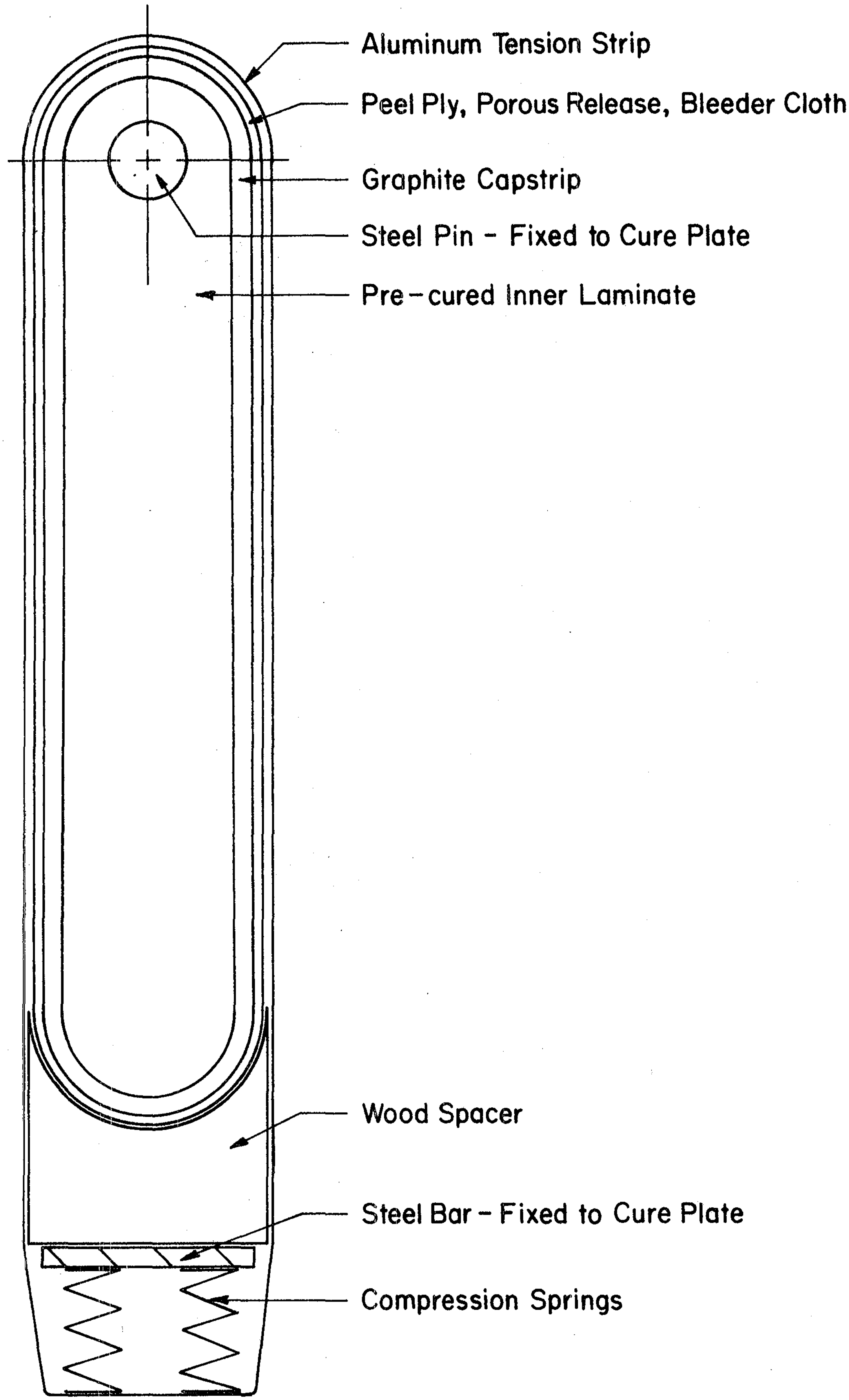


Figure IV-A-4. Capstrip Cure Apparatus

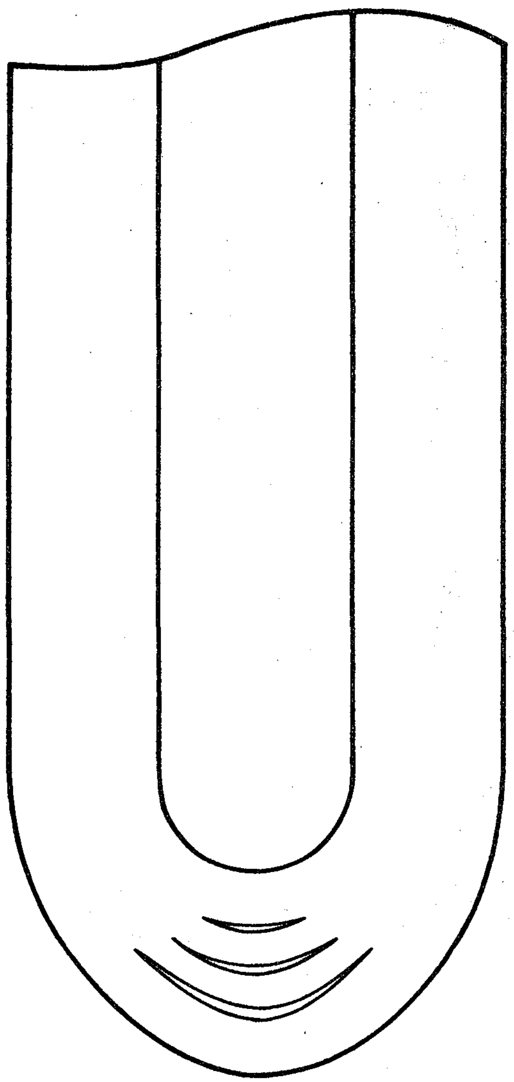

(5a)

Typical Epoxy Gaps and
Fiber Slack Resulting From
Curing Around a Corner

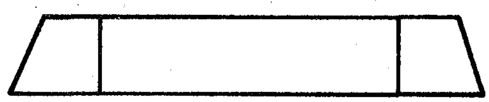

(5b)

Cross-Section of Lug
(uneven capstrip thickness)

Figure IV-A-5. Effects of Capstrip Manufacturing Fixture

TABLE IV-A-2

SUMMARY OF FAILURE INFORMATION: LUGS WITH VARIOUS CAPSTRIPS

| Description | Failure Load Lbs. (psi) | Mode of Failure |
|---|---|---|
| .1" Straight* graphite capstrip | 12,750 (40,220) | Capstrip shear off/ Shear out at hole |
| .1" Continuous graphite capstrip | 10,783 (38,238) | Shear out at hole |
| .2" Continuous graphite capstrip | 11,512 (40,823) | Shear out at hole |
| .3" Continuous graphite capstrip | 10,536 (37,361) | Shear out at hole |
| Hybrid capstrip with bushing | 11,620 (41,205) | Splitting of cap- strip |

*This specimen $[0/\pm45]_{12s}$;

All other specimens $[0_2/\pm45]_{8s}$

A combination of these concepts was tried in a hybrid capstrip specimen (see Figure IV-A-6), incorporating a 1/16" steel bushing with a .169" inner capstrip of unidirectional fiber glass/epoxy and a .169" outer capstrip of unidirectional graphite-epoxy. To minimize the capstrip slack around the curved end of the lug, the specimen was cured in two cycles, one for each successive capstrip.

An initial failure was reached at 11,620 pounds (41,200 psi), and load application halted at that point. Cracks had propagated through the capstrip in the plane of the lug. The addition of ±45° plies or metallic layers interspersed throughout the capstrip would deter this mode of failure and result in a higher strength. However, because the individual contributions of the bushing, fiber glass and graphite capstrips are undeterminable from one specimen involving all three, it can only be said that an optimum lug design would probably incorporate some degree of each.

## c. Computational Aspects

An important attribute of the design procedure is its ability to predict failure loads in preliminary stages so as to prevent the squandering of manufacturing and testing resources in the pursuit of invalid designs. The method of analysis used extensively in this study is the finite element package, "POFES" (People Oriented Finite Element System), developed at RPI by Dr. M. S. Shephard. The model being used in the process of the research has advanced in sophistication

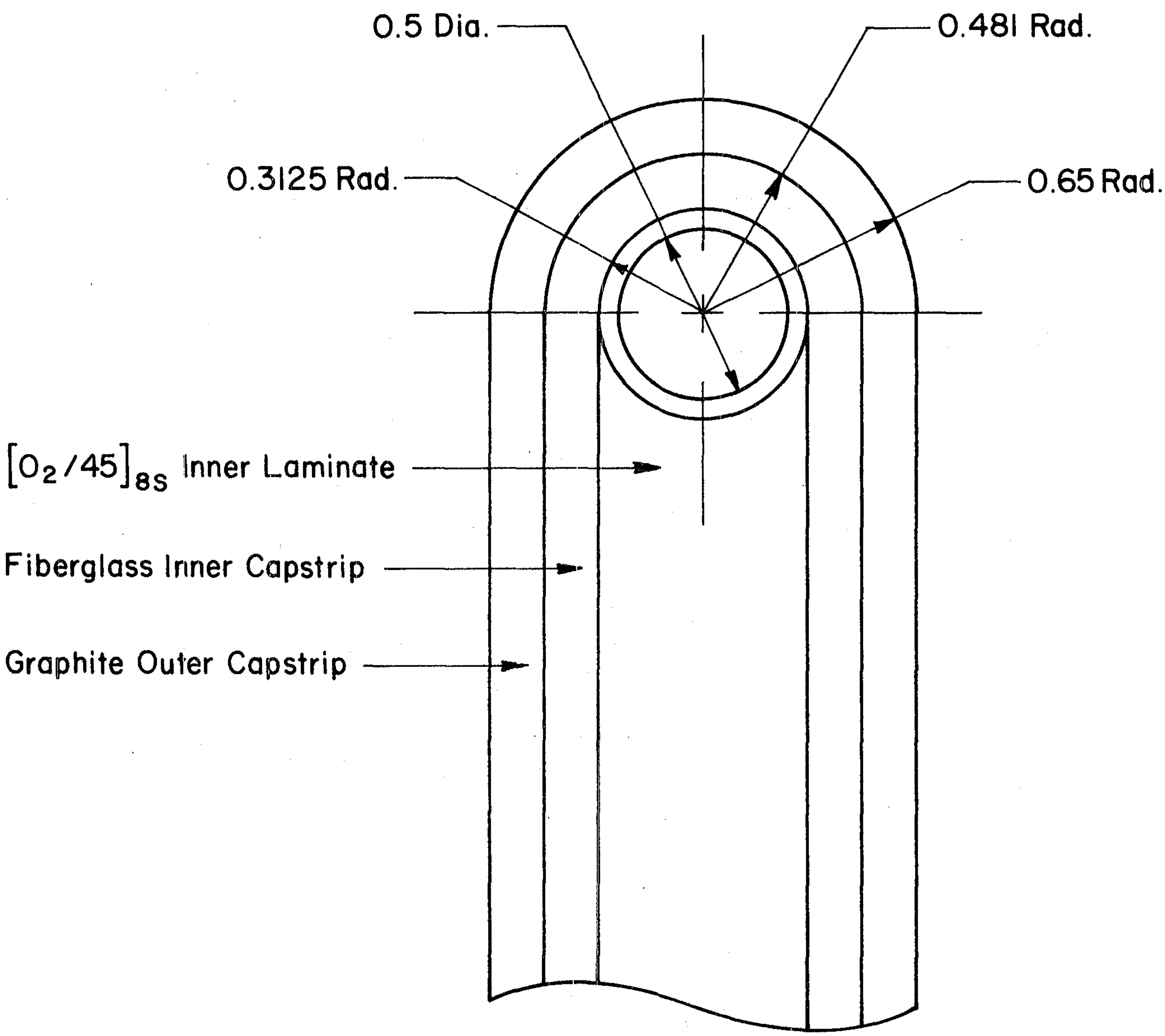


Figure IV-A-6. Hybrid Capstrip with Steel Bushing by stages. Initially, a constant strain triangle mesh with a discrete cosine-normal load distribution and isotropic material properties was used. Now, second order quadrilateral elements with a continuous, work equivalent, cosine-normal load distribution generated by a program developed in this study and anisotropic material properties are available in the model. Verification of the model with the results of De Jong[7] has been quite successful.

It is still recognized, however, that neither the results of our finite element analysis, nor De Jong's for that matter, provide exact replications of the actual stress field around the pin-loaded hole. The necessity of assuming a load distribution at the bolt-hole interface and of ignoring three-dimensional effects certainly can be expected to lead to inexactness. However, it has been shown that use of an assumed load distribution such as the cosine normal distribution can produce stress results which correlate reasonably with experimental failure data when averaged over a certain characteristic distance[8]. We are rigorously testing this stress averaging technique for application to bolted joints.

## 4. Plans for Upcoming Period

It appears from our studies to date, that no feasible composite lug design is likely to reach high density design criteria such as imposed by Lockheed for the L-1011 drag strut pinned connection. A graphite lug constrained to the same maximum dimensions as a high strength steel lug doesn't seem capable of withstanding as high a tensile load. Composite pinned connections as typified by the lug studied here, however, are potentially advantageous under more general design envelopes. Despite the lower load/volume efficiency of graphite/epoxy in this case, it is clearly more efficient in terms of load/weight. Our research indicates that the graphite lug is nominally 85% as strong as the 200 ksi steel lug, yet it only weighs 20% as much as the same steel lug. The composite thus demonstrates a load/weight efficiency 425% greater than steel. The weight savings resulting from use of graphite lugs would seem to justify their use in aircraft design.

This project will be concluded with the work reported here and further predictive analytical studies making use of averaged stress and characteristic distance techniques.

## 5. References


1. "Composite Structural Materials", RPI 43rd Semi-Annual Progress Report under NGL 33-018-003, April 30, 1982 through September 30, 1982, pp. 85-100.

2. "Advanced Composites Design Guide", Vol. II, 3rd ed., Contract No. F33615-74-C-5075, Flight Dynamics Lab., U. S. Air Force, 1976, p. 2.4.2-24.

3. Wilson, D. W., J. W. Gillespie, J. L. York and R. B. Pipes, "Failure Analysis of Composite Bolted Joints", Center for Composite Materials, University of Delaware, Newark, DE, sponsored by NASA Grant 1409, 1980, p. 15.

4. See p. 31 of Reference 3.

5. See p. 2.4.2-7 of Reference 2.

6. Oplinger, D. W., "On the Structural Behavior of Mechanically Fastened Joints in Composite Structures", Fibrous

Composites in Design (4th Conf., Nov. 14-17, 1978), E. Lenoe, D. Oplinger, J. Burke, eds., Army Materials and Mechanics Research Center, Watertown, MA, Plenum Press, pp. 578-580.

7. De Jong, T., "Stresses Around Pin-Loaded Holes in Elastically Orthotropic or Isotropic Plates", Journal of Composite Materials, Vol. II, July 1977, pp.313-331.

8, Agarwal, B. L., "Static Strength of Bolted Joints in Composite Materials", AIAA Journal, Vol. 18, No. 11, November 1980, pp. 1371-1375.

# PART V
# PROCESSING SCIENCE AND TECHNOLOGY

V-A INITIAL SAILPLANE PROJECT: RP-1

V-B SECOND SAILPLANE PROJECT: RP-2

## V-A INITIAL SAILPLANE PROJECT: THE RP-1

Senior Investigators: F. P. Bundy
R. J. Diefendorf
H. Hagerup
H. Scarton

### 1. Status

Recognizing that the resins in composite materials can change properties somewhat with aging and exposure to temperature/moisture cycles, the wing/fuselage ensemble structure of the RP-1 glider has been static tested about once a year since its initial fabrication in '79-'80. This initial series of tests consisted of simple vertical bending, and the last of this series was done on August 5, 1981. That test consisted of simple bending using a distributed load up to a maximum of 590 pounds per wing, which corresponds to a little over 4 g's for average pilot weight.

Some changes were made in the wing beam "carry-through" structure of the RP-2 glider, in the summer of 1982, with a eye to making it stronger and more fail-proof. In subsequent tests of the RP-1 glider, the wing-fuselage assembly was subjected not only to simple vertical bending, as in previous years but, in addition, to a bending-torsion test with fore-aft bending components, which would simulate the stresses in a high speed pull-out. It was in this mode that the RP-2 wing beam carry-through failed (see Section V-B of the 43rd Semiannual Progress Report, dated December 1982).

In the simple bending tests, the fuselage was held in a horizontal position and the weights were laid directly over the wing beam. In the bending/torsion tests, the fuselage was positioned on a ten degree slant (nose low, tail high, inverted) and the weights placed on a line fourteen centimeters aft of the wing beam. Thus, both torsion and fore-aft bending were induced, in addition to vertical bending. These two static tests were survived very successfully.

Following the static tests, in July of 1982, winch-launched flight tests were carried out to evaluate the influence of aerodynamic fairings installed earlier that year, on sink rate and glide slope. The effect was to lower the minimum sink rate to about 200 FPM (from 250 FPM in the unfaired configuration) and to increase the optimum glide slope from about 10 or 11:1 to 14:1.

Tests have been conducted on structural elements of two different kinds, typical of those used on the RP-1 and hidden from view, in the falls of '81 and '82. Five of each kind were tested each year. It appears that degradation with time is well within the spread in strength due to fabrication or materials quality.

## 2. Progress During Report Period and Plans for Upcoming Period

With the achievement during the summer of 1982 of sustained thermal soaring of the RP-1 on two separate occasions, the first all-composite glider built under this program has been set aside. Some additional flights may be undertaken in the future for demonstration purposes, to stimulate student interest in the program, to maintain an experienced flight crew, to test ideas for further aerodynamic refinement and for their influence on structural life. In addition, the program of yearly structural proof-tests and structural subassembly tests will be continued, for the purpose of securing information on possible long-term degradation of the structure. The emphasis of the work, however, has shifted to the second aircraft, the RP-2.

## V-B SECOND SAILPLANE PROJECT: THE RP-2

Senior Investigatiors: F. P. Bundy
R. J. Diefendorf
H. Hagerup
H. Scarton

### 1. Status

The bending-torsion failure and secondary damage experienced during the static test in the fall of 1981 necessitated structural redesign of the center wing-connection and extensive development of advanced composite material repair techniques on our part. Subsequently, the center wing-connection was partly rebuilt, and the two damaged outboard portions of the wings were completely rebuilt. This involved developing a splicing technique in which autoclave-cured primary structures (i.e., spar caps and splice material) were joined by cold bonding. The fuselage framework and carry-through structure were also modified, both to provide an improved load-path and to accommodate the somewhat larger redesigned wing-connection. The former modification included spreading the pins which transfer wing root rib loads to the fuselage; the greater distance between them reduces the magnitude of torsion and fore-aft bending induced forces.

### 2. Progress During Report Period

The rebuilt outboard portions of the wings were joined with the undamaged inboard portions, and wing skins to cover the area of these repairs were installed and skin splices applied. Aileron and flap connections, linkages and control rods were installed. Modifications were made to the root ribs, as necessitated by the new shear-pin locations and changes in the carry-through structure generally. Rebuilding of the center wing-connection was completed, including fabrication and installation of the heavy U-channels which are now an important part of the design. Final adjustments were made to the fuselage framework, the wings were connected to each other and to the fuselage, and the repaired airframe was ready for structural proof-tests at the end of the reporting period.

Meanwhile, a wind tunnel model of the RP-2 fuselage, including stub wings, was prepared, for the purpose of verifying that there are no special problems of aerodynamic interaction at the wing-fuselage intersection. The model is ready for wind tunnel testing at this writing.

In addition to their becoming familiar with advanced composite design and fabrication techniques, and working on the RP-2 airframe, participants in the Sailplane Project also do some original work on the following:

a) fabrication technique and structural properties of tube connections;

b) fabrication technique and structural properties of double wall tubes with honeycomb between the walls;

c) fabrication of I-beam with sinusoidal web and

d) design and fabrication of a new concept for a variable geometry wing-airfoil section.

## 3. Plans for Upcoming Period

The completed RP-2 airframe will be subjected to structural proof-tests later this spring. Non-structural detail work on the wings will be completed during the summer and fall. The wind tunnel test on wing-fuselage interaction will also be performed in late spring, provided that the wind tunnel test results are positive, fabrication of the female molds for the fuselage will start immediately. The fuselage shell will be laid up in early fall, and the final detail work on the entire aircraft will have begun by the end of the next reporting period.

## 4. Current Publications or Presentations by Professors Bundy and Scarton on this Subject

"Rensselaer's 'home-built' RP-2", F. P. Bundy with S. J. Winckler.

To be published in Soaring, June 1983.

"Acoustic Emission Proof Testing of Composite Sailplanes", H. A. Scarton.

To be presented at the First International Symposium on Acoustic Emission from Reinforced Plastics, CARP, San Francisco, CA, July 19-21, 1983.

# PART VI
# TECHNICAL INTERCHANGE

## INTRODUCTION

Technical meetings, on- and off-campus, provide important opportunities for interchange of technical information. Because of the large number of composites meetings, a central catalog with all upcoming meetings is being maintained and distributed periodically. In this way we help to assure that a Rensselaer faculty/staff member can participate in important meetings. The calendar for this reporting period is shown in Table VI-1. Meetings attended by RPI composites program faculty/staff/students during the reporting period are shown in Table VI-2. Some meetings particularly relevant to composites, held on-campus with special speakers, are listed in Table VI-3. A list of composite-related visits to relevant organizations by RPI faculty/staff/students, with the purpose of each visit outlined, is presented in Table VI-4.

For the last several years, as the diversity of the research conducted within this program has increased, once-a-week luncheon programs have been held to insure information transfer among the faculty and graduate students involved (listed in Part VII - Personnel of this report). These meetings are held continuously when classes are in session and are known as "Brown Bag Lunches"(BBL's), since attendees bring their own. Each BBL is an opportunity for graduate students and faculty to present briefly plans for,

TABLE VI-1

CALENDAR OF COMPOSITES-RELATED MEETINGS

(September 30, 1982 through April 30, 1983)

| | |
|---|---|
| 1982 | |
| 10/4-7 | Symposium on Advanced Trends in Structural and Solid Mechanics, Washington, D.C. Sponsored by George Washington University and NASA Langley. |
| 10/5-7 | 8th Annual Mechanics of Composites Review, Dayton, OH. Sponsored by W.P.A.F.B. |
| 10/7-8 | High Performance Composites, CFC 8, Toronto, Canada. Sponsored by the Canadian Commission for Research on the Strength and Fracture of Materials. |
| 10/17-21 | 14th Annual Tri-Service Manufacturing Technology Conference, Phoenix, AZ. Sponsored by the Air Force and DOD. |
| 10/25-27 | The Plastics ABC's: Polymer Alloys, Blends and Composites, Bal Harbour, FL. Sponsored by SPE and NATEC. |
| 10/25-28 | 4th International Conference on Composite Materials (ICCM-IV), Tokyo, Japan. Sponsored by AIME and the Japanese Society for Composite Materials. |
| 11/1-4 | Japanese Carbon Conference, Toyohashi, Japan. |
| 11/17 | 2nd Chautauqua Conference on Productivity in Engineering and Design, The CAD Revolution, Kiawal Island, SC. |
| 12/15-17 | International Conference on Biaxial/Multiaxial Fatigue, San Francisco, CA. Sponsored by ASTM. |
| 12/15-17 | Indian Carbon Conference, New Delhi, India. |
| 12/20-22 | Silver Jubilee Meeting: Recent Advances in Materials Research, Bombay, India. |
| 1983 | |
| 1/10-12 | 21st Aerospace Sciences Meeting, Las Vegas, NV. Sponsored by AIAA. |
| 1/11-13 | Composites in Manufacturing II Conference and Exhibits, Anaheim, CA. Sponsored by SME. |

TABLE VI-1 continued

1983

| | |
|---|---|
| 1/16-20 | 7th Annual Conference on Composites and Advanced Materials, Cocoa Beach, FL. |
| 1/17-20 | Gordon Conference on Composite Materials, Santa Barbara, CA. |
| 1/21 | Society for Advancement of Material and Process Engineering (SAMPE) Meeting on Composites, San Jose, CA. |
| 1/24-27 | 6th Conference on Fibrous Composites in Structural Design, New Orleans, LA. Sponsored by the Army, Navy, Air Force, FAA and NASA. |
| 2/7-11 | 38th Annual Conference, Houston, TX. Sponsored by the Society of Plastics Industry. |
| 3/18 | Applied Mechanics Colloquia, University College, Swansea, U.K. |
| 3/21-25 | Meeting of the High Polymer Division of the American Physical Society, Los Angeles, CA. |
| 3/23-25 | National Composite Structures Specialists Meeting, Philadelphia, PA. Sponsored by AHS. |
| 3/28 | American Society of Metals Symposium, Utica, NY. |
| 4/10-15 | 56th Panel Meeting/Specialists Meetings, Structures and Materials Panel of AGARD, London, U.K. Sponsored by NATO. |
| 4/12-14 | Fiber Producers Symposium and Exhibition, Greenville, SC. |
| 4/12-14 | 28th National Symposium, Anaheim, CA. Sponsored by SAMPE. |
| 4/20-22 | Symposium on Computer-Aided Geometry ModelING, Hampton, VA. Sponsored by NASA Langley. |
| 4/20-22 | National and International Meeting on Composite Materials, Milan, Italy. Sponsored by AMME. |

TABLE VI-2

COMPOSITES-RELATED TECHNICAL MEETINGS ATTENDED OFF-CAMPUS

(September 30, 1982 through April 30, 1983)

1982

10/4-7 Symposium on Advanced Trends in Structural and Solid Mechanics (Prof. Loewy and Grad. Student F. Luban-Tobing), Washington, D.C.

Professor Loewy chaired session on Composite Materials and Structures.

F. Lumban-Tobing presented the paper: "Finite Element Modeling of Moisture Effects in Graphite/Epoxy Composites".

10/4-7 8th Annual Mechanics of Composites Review (Prof. Goetschel), Dayton, OH.

10/25-28 4th International Conference on Composite Materials (ICCM-IV) (Prof. Diefendorf), Tokyo, Japan.

Professor Diefendorf chaired a session and presented the paper, "Residual Stress in High Modulus Carbon Fibers".

Professor Hoff presented the paper*, "Stress Concentrations in Cylindrically Orthotropic Plates with Radial Variation of the Compliances" (Co-authored with C. Muser).

11/1-4 Japanese Carbon Conference (Prof. Diefendorf), Toyohashi, Japan.

Professor Diefendorf presented the lectures:

"Mesophase Formation in Polynuclear Aromatic Compounds"
"Mesophase Formation from Fractions of a Mesophase Pitch"
"Molecular Weight and Molecular Weight Distributions in Pitch"
"The Chemical Vapor Deposition of Carbon on Graphite Surfaces"

*Work supported by the subject grant.

TABLE VI-2 continued

1982

11/17 2nd Chautauqua Conference on Productivity in Engineering and Design, The CAD Revolution (Prof. Shephard), Kiawal, SC.

Professor Shephard presented the paper, "The Effective Use of Finite Element Methods in Engineering Design".

12/15-17 International Conference on Biaxial/Multiaxial Fatigue (Prof. Krempl), San Francisco, CA.

Professor Krempl presented the paper, "Biaxial In-Phase and Out-of-Phase Behavior of Graphite-Epoxy Tubes".

12/15-17 Indian Carbon Conference (Prof. Diefendorf), New Delhi, India.

Professor Diefendorf presented two papers and a plenary lecture as follows:

"Transverse Thermal Expansion of Carbon Fiber/Epoxy Matrix Composites"
"Residual Stresses in Carbon Fibers"
"Mesophase Pitches"

12/20-22 Silver Jubilee Meeting: Recent Advances in Materials Research (Prof. Diefendorf), Bombay, India.

Professor Diefendorf chaired a session and presented the paper, "Carbon Fibers, Present Properties and Future Applications".

1983

1/17-20 Gordon Conference on Composite Materials (Profs. Diefendorf and Sternstein), Santa Barbara, CA.

1/21 Society for Advancement of Material and Process Engineering (SAMPE) Meeting on Composites (Prof. Diefendorf), San Jose, CA.

Professor Diefendorf presented the Keynote Lecture, "RP-X Composite Sailplanes".

3/18 Applied Mechanics Colloquia, University College (Prof. Shephard), Swansea, U.K.

Professor Shephard presented the paper, "Developments in Mesh Generation and Adaptive Techniques".

TABLE VI-2 continued

1983

3/21-25 Meeting of the High Polymer Division of the American Physical Society (Prof. Sternstein), Los Angeles, CA.

Professor Sternstein presented the paper, "Characterization of High Performance Composites".

3/23-25 AHS National Composite Structures Specialists Meeting (Profs. Diefendorf, Goetschel and Loewy, and Mr. Paedelt), Philadelphia, PA.

Professor Loewy chaired session, "VI: Analysis II".

3/28 American Society of Metals Symposium (Prof. Diefendorf), Utica, NY.

Professor Diefendorf presented, "Principles of Composite Materials".

4/10-15 56th Panel Meeting/Specialists Meetings, Structures and Materials Panel of AGARD (Prof. Loewy), London, U.K.

4/12-14 Fiber Producers Symposium and Exhibition (Prof. Diefendorf), Greenville, SC.

Professor Diefendorf presented the Invited Speech, "A Comparison of High Modulus Fibers".

TABLE VI-3

COMPOSITES-RELATED MEETINGS/TALKS HELD AT RPI

(September 30, 1982 through April 30, 1983)

| Topic | Date | Speaker(s) |
|---|---|---|
| | 1982 | |
| Computer Aided Mechanism | 10/12 | Arthur G. Erdman<br>Professor, University of Minnesota |
| Some Considerations of Structural Reliability with Respect to Risk Analysis of Large Technological Systems | 10/18 | G. I. Schuëller<br>Institut für Mechanik<br>Universität Innsbruck<br>Austria |
| | 1983 | |
| Design, Manufacturing and Testing of High Speed Rotating Graphite/Epoxy Shafts | 1/26 | Olivier A. Bauchau<br>St. Gobain Recherche<br>Paris, France |
| Biaxial Fatigue of Graphite/Epoxy $[\pm 45]_s$ Tubes | 2/3 | Tyan-Min Niu<br>Doctoral thesis dissertation<br>Department of Mechanical Engineering, Aeronautical Engineering and Mechanics |
| Structural Analysis of Jet Engine Combuster Liners | 3/1 | Kevin P. Walker<br>Habbitt Karlsson and Sorensen, Inc. |
| Recent Trends in the Computer-Aided Control of Material Processing Methods | 4/8 | Daeyong Lee<br>General Electric Corporate Research and Development<br>Schenectady, New York |
| Commemorative Symposium: Rensselaer Salutes 200 Years of Manned Flight | 4/5 | |
| daVinci's VTOL Comes of Age | | Robert Zincone<br>Senior, Vice President for Engineering<br>Sikorsky Div., UTC |
| A/C Development in the Skunk Works | | Ben Rich<br>Vice President and General Manager<br>Lockheed California |

TABLE VI-3 continued

| Topic | Date | Speaker(s) |
|---|---|---|
| | 1983 | |
| Twenty-Five Years on "This New Ocean" | | John F. Yardley<br>President<br>McDonnell Douglas Astronautics |
| The Year of the Shuttle: Fifth Annual Hemke Lecture | | Col. Robert Overmeyer<br>STS-5 Pilot<br>NASA Astronaut |
| The Effect of Stress Relaxation on the Tearing of Elastomers | 4/12 | R. S. Rivlin<br>Lehigh University |
| Fibrous Skins | 4/26 | S. Wainwright<br>Duke University |

TABLE VI-4

COMPOSITES-RELATED VISITS TO RELEVANT ORGANIZATIONS

by RPI Faculty/Staff/Students

(September 30, 1982 through April 30, 1983)

| Visited | Date | By | Purpose |
|---|---|---|---|
| | 1982 | | |
| Techniche Hochochules, Darmstat and Braunschweig Federal Republic of Germany | 10/18, 20 and 21 | M. V. Paedelt | Discussed operations of "Akaflieg" groups on these campuses |
| Toray, Ind. Shiga, Japan | 10/26 | Prof. R. J. Diefendorf | Plant visit to one of the largest manufacturers of carbon fibers |
| NASA Lewis Research Center Cleveland, OH | 11/19 | Prof. R. J. Diefendorf | Participated in SiC Semiconductor Workshop |
| Air Force Institute of Technology, Dayton, OH | 12/28 | Prof. E. J. Brunelle | Gave invited lecture: New Research Areas in Composite Structures |
| | 1983 | | |
| Sikorsky Division, United Technologies Corp, Stratford, CT | 1/27 | Profs. R. J. Diefendorf and D. Goetschel | Made plant tours and discussed potential composite research projects |
| NASA Langley Research Center Hampton, VA | 1/31-2/4 | Prof. M. S. Shephard | Attended workshop on finite element modeling and presented talk: "Finite Element Mesh Generating Techniques and the Interface of Finite Elements and Geometric Modeling" |
| University of Michigan Ann Arbor, MI | 3/14 | Prof. S. S. Sternstein | Presented talk: "Characterization of Composites and Neat Resins" |

problems encountered in and recent results from their individual projects. These sessions also are occasions for brief administrative reports, usually on the part of one of the Co-Principal Investigators, and for brief reports on what transpired at off-campus meetings attended by one of the participants (as listed in Tables VI-2 and VI-4 of this report). Visitors from off campus, who are at RPI during a BBL day are often invited to "sit in". A calendar of internal, oral progress reports as they were given during the last reporting period at BBL's is listed in Table VI-5.

TABLE VI-5

COMPOSITE MATERIALS AND STRUCTURES PROGRAM

BROWN BAG LUNCH (BBL) SCHEDULE

(September 30, 1982 through April 30, 1983)

| Date | Topic | Responsible Faculty |
|---|---|---|
| 1982 | | |
| 10/1 | Administrative Report | R. Loewy |
| | Computer-Aided Design and Analysis | M. Shephard |
| | Resin Matrix Research | J. Diefendorf |
| 10/8 | Administrative Report | J. Diefendorf |
| | Generic Structural Components | D. Goetschel |
| | Fatigue Studies Research | E. Krempl |
| 10/15 | Administrative Report | J. Diefendorf |
| | Fabrication Technology Experiments | F. Bundy<br>H. Hagerup<br>V. Paedelt |
| | Report on Mechanics of Composites Review | D. Goetschel |
| 10/22 | Administrative Report | R. Loewy |
| | Matrix Characterization and Environtal Effects | S. Sternstein |
| | Computer-Aided Design and Analysis | M. Shephard |
| 10/29 | Administrative Report | R. Loewy |
| | Generic Structural Components | D. Goetschel |
| | Advanced Analytical Methods | E. Brunelle |
| 11/5 | Administrative Report | J. Diefendorf |
| | Fabrication Technology Experiments | F. Bundy<br>H. Hagerup<br>V. Paedelt |
| | Fatigue Studies Research | E. Krempl |
| 1983 | | |
| 1/28 | Administrative Report | R. Loewy |
| | Report on Gordon Conference | J. Diefendorf |

TABLE VI-5 continued

| Date | Topic | Responsible Faculty |
|---|---|---|
| 1983 | | |
| 2/4 | Matrix Characterization of Environmental Effects | S. Sternstein |
| | Fabrication Technology Experiments | F. Bundy<br>H. Hagerup<br>V. Paedelt |
| 2/11 | Generic Structural Components | D. Goetschel |
| | Computer-Aided Design and Analysis | M. Shephard |
| 2/18 | Resin-Fiber Interface Research | J. Diefendorf |
| | Composites Fatigue Research | E. Krempl |
| 2/25 | Administrative Report | R. Loewy |
| | Pin-Loaded Holes in Composite Plates | W. Kim |
| | Computer-Aided Design and Analysis | M. Shephard |
| 3/4 | Matrix Characterization and Environmental Effects | S. Sternstein |
| | Fabrication Technology Experiments | F. Bundy<br>H. Hagerup<br>V. Paedelt |
| 3/11 | Generic Structural Components | D. Goetschel |
| | Advanced Analytical Methods | E. Brunelle |
| 3/25 | Report on Vertol Research | E. Krempl<br>W. Kim |
| | Resin-Fiber Interface Research | J. Diefendorf |
| 4/1 | Administrative Report | S. Wiberley |
| | Composites Fatigue Research | E. Krempl |
| | Computer-Aided Design and Analysis | M. Shephard |
| 4/8 | Matrix Characterization and Environmental Effects | S. Sternstein |
| | Fabrication Technology Experiments | F. Bundy<br>H. Hagerup<br>V. Paedelt |

TABLE VI-5 continued

| Date | Topic | Responsible Faculty |
|---|---|---|
| 1983 | | |
| 4/15 | Administrative Report | J. Diefendorf |
| | Generic Structural Components | D. Goetschel |
| | Free Edge Failures of Laminates | S. Sham |
| 4/22 | Report on AGARD Meeting | R. Loewy |
| | Resin-Fiber Interface Research | J. Diefendorf |
| 4/29 | Administrative Report | R. Loewy |
| | Composites Fatigue Research | E. Krempl |
| | Computer-Aided Design and Analysis | M. Shephard |

# PART VII

# PERSONNEL

# AUTHOR INDEX

# PERSONNEL

## Co-Principal Investigators

| | |
|---|---|
| Ansell, George S., Ph.D. | Dean, School of Engineering |
| Loewy, Robert G., Ph.D. | Institute Professor |
| Wiberley, Stephen E., Ph.D. | Professor of Chemistry |

## Senior Investigators

| | |
|---|---|
| Brunelle, E. J., Jr., Sc.D. (Aeroelastic and structural design and analysis, applied mechanics of composite structures)* | Associate Professor of Aeronautical Engineering |
| Bundy, F. P., Ph.D. (Physical chemistry and structures testing)* | Research Professor of Materials Engineering |
| Diefendorf[i], R. J., Ph.D. (Fabrication, resin matrix, fiber behavior, interfaces)* | Professor of Materials Engineering |
| Feeser[i]. L. J., Ph.D. (Computer applications and graphics, computer-aided design, optimization)* | Professor of Civil Engineering |
| Goetschel, D. B., Ph.D. (Structural analysis design and testing)* | Assistant Professor of Mechanical Engineering |
| Hagerup, H. J., Ph.D. (Aerodynamics, configuration, pilot accomodation, flight testing)* | Associate Professor of Aeronautical Engineering |
| Krempl, E., Dr.Ing. (Fatigue studies, failure criteria)* | Professor of Mechanics and Director of Cyclic Strain Laboratory |
| Scarton, H., Ph.D. (Acoustic emission NDE)* | Associate Professor of Mechanical Engineering and Mechanics |

---

*Fields of Speciality

[i] Member of Budget Committee together with Co-Principal Investigators

Senior Investigators

| | |
|---|---|
| Shephard, M. S., Ph.D. (Computer graphics, finite element methods)* | Associate Director, Center for Interactive Computer Graphics and Assistant Professor of Civil Engineering |
| Sternstein[i], S. S., Ph.D. (Failure analysis, matrix behavior, moisture effects)* | William Weightman Walker Professor of Polymer Engineering |

Research Staff

Manager & Master Technician, Composites Laboratory

Paedelt, Volker

Research Associate

Kim, Wonsub, Ph.D.

Graduate Assistants

Anderson, Stephen, B.S.
Baxter, Scott, B.S.
Bertolazzi, Andrew, B.S.
Burd, Gary, B.S.
Cackett, Mathew, B.S.
DeMint, Thomas, B.S.
Father, Philip, B.S.
Helmer, James, B.S.
Hu, Tsay-hsin, M.S.
Liu, Shiann-hsiung, M.S.
Lumban-Tobing, Frida, M.S.
Niederer, Melvin, B.S.
Sing, Sachchida, B.Tech.
Srinivasan, Krishna, B.S.
Uzoh, Cyprian, B.S.
Yehia, Nabil, M.S.
Yang, Philip, M.S.
Yurgartis, Steven, M.S.

Undergraduate Assistants - Seniors

Casabella, Susan
Cerro, Eric
Chin, Hong
Chiusano, Michael
Delzer, Francis
Kloiber, James
Kolotylo, Michael
Lafreniere, Suzanne
Malusa, Stephen
Olsen, Kenneth

---

*Fields of Speciality

[i]Member of Budget Committee together with Co-Principal Investigators

Undergraduate Assistants - Seniors (continued)

Porter, James
Rizika, Ann
Taflin, David
Toomey, John
Welch, Kevin

Undergraduate Assistants - Juniors

Bacich, Linda
Blasioli, Lou
Bortfeldt, Paul
Dunlap, Robert
Dyer, Richard
Griffiths, Kay
Guintoli, Michael
Halicki, Paul
Jun, Wan Ki
Keavney, Thomas
Kilfeather, James
Lopez, Matthew
Martin, Randall
Robertson, Scott
Tomlin, Rogers
Vatis, Thomas
White, Eric
Younes, Mona

Undergraduate Assistants - Sophomores

Bigelow, Margaret
Hart, Laurence
Norton, Philip
Schiller, Paul
Sodell, Lorin

# AUTHOR INDEX

**End of Document**